Improving Estimates of Structural Seismic Motion

By

Dimitris Hadjiharitou

Diploma in Civil Engineering
National Technical University of Athens, July 2012

Submitted to the Department of Civil and Environmental Engineering in Partial Fulfillment of the Requirements for the Degree of

Master of Engineering in Civil and Environmental Engineering
At the
Massachusetts Institute of Technology

June 2013

Signature of Author: _____
Department of Civil and Environmental Engineering
May 17th, 2013

Certified by: _____
Jerome J. Connor
Professor of Civil and Environmental Engineering
Thesis Supervisor

Certified by: _____
Rory Clune
Massachusetts Institute of Technology
Thesis Reader

Accepted by: _____
Heidi Nepf
Chair, Departmental Committee for Graduate Students

Improving Estimates of Structural Seismic Motion

By

Dimtiris Hadjiharitou

Submitted to the Department of Civil and Environmental Engineering on May 17, 2013 in Partial Fulfillment of the Requirements for the Degree of Master of Engineering in Civil and Environmental Engineering

ABSTRACT

A critical field in civil engineering is the evaluation of structural damage after severe earthquakes. Seismic events are taken into serious consideration in areas of the world such as California and countries adjacent to the Mediterranean. After these events, structural engineers are called to evaluate structural damage and to enhance the structure's future capabilities and serviceability. Due to the large number of structures and the significant time needed to evaluate the potential damage in each structure, other methods for structural behavior observation were needed. One of those has been established in the late 1950's and had to do with the implementation of electronic monitoring devices in structures. This dissertation evaluates the placement of today's motion sensing instruments and proposes an algorithm that proposes optimized instrumentation schemes in buildings.

The dissertation starts with a presentation and critique of today's instrumentation techniques and suggests how they could be optimized or refined to get a better approximation of the structure's behavior. Furthermore, optimization schemes provided by the literature are presented.

In addition, the author proposes an algorithm that estimates and proposes instrumentation schemes of buildings. The proposed instrumentation schemes take into consideration all three dimensions. The algorithm is described by a flow chart and mathematical equations and is implemented in MATLAB.

To check the validity of the algorithm, case studies are conducted. These case studies are based on finite element models of buildings that were hit by the Northridge earthquake and were instrumented during that period. Actual recorded accelerations from the base of the structures have been used to conduct the case studies.

Finally, the results of these case studies are presented. The results present the exact positions of the sensors in order to get better approximation of the structure's behavior in a cost effective manner. In addition, an evaluation is conducted for the estimation of the behavior of the algorithm on different earthquake data.

Thesis Supervisor: Jerome J. Connor
Title: Professor of Civil and Environmental Engineering

Acknowledgements

Among all the people that supported me through all these years of my educational development, I would like to thank the ones that contributed more to this thesis.

First of all, I would like to thank my advisor Professor Jerome Connor for his inspirational work and help. Furthermore, I would like to thank my thesis reader PhD candidate Rory Clune, for all his insights, comments and patience through the development of this thesis.

In addition, I would like to thank Dr. Farzad Naeim for providing me the CSMIP-3DV software, and Dr. Moh Huang and Dr. Tony Shakal for their help. Also, my heartfelt gratitude goes to Professor Charis Gantes of the National Technical University of Athens for his support, advice and friendship during the past two years.

I would like to acknowledge the help and support from all of my friends at MIT, Cyprus and the rest of the world. Especially, I would like to thank Deborah Alexandra Vacs Renwick for proofreading this thesis.

Εν τέλει, θα ήθελα μέσα από τα βάθη της καρδιάς μου να ευχαριστήσω τους γονείς μου, Μαρία και Χαράλαμπο, οι οποίοι μου χάρισαν τα δώρα της ζωής και της γνώσης. Ελπίζω αυτά τα δώρα να μπορέσω και εγώ να τα χαρίσω στα παιδιά μου. Επίσης, θα ήθελα να ευχαριστήσω τον αδερφό μου Νουφρή για την συμπαράσταση και αγάπη του.

Table of Contents

1 Introduction

This chapter serves as an introduction to the thesis and explains the origins of the problem. The chapter starts with a brief description of the nature of earthquakes and the effect they have on civil structures, by considering fundamental equations of motion. In addition, past significant earthquakes are mentioned to show the importance of this phenomenon. Furthermore, general instrumentation techniques are mentioned to provide a general idea of the current practices and limitations. Finally, in the last two sections the author states the problem the thesis addresses.

1.1 Earthquakes

1.1.1 Where do they come from?

The commonly-accepted understanding of earthquakes might lead to a definition such as: "An earthquake is the result of a sudden release of energy in the Earth's crust that creates seismic waves". This definition is ambiguous and does not really explain what an earthquake is. Actually an earthquake is a sudden release of energy, but where does that energy come from?

Earthquakes occur near tectonic faults. A fault is a fracture on the earth's crust where the two planes of fracture can move relatively to each other. The faults vary in length from some centimeters to some hundreds of kilometers. An earthquake is caused when there is a sudden slip on the fault. Due to the momentum of the relative displacement, stress is created between the two planes of the fault. This stress builds up until it overcomes the stress resistance or strength of the fault. Once the stress level exceeds the strength of the fault, the fault slips suddenly. Therefore, energy is released in the form of waves that travel through the subsurface (rock or soil). These waves shake the subsurface and cause us to feel the earthquake (Bolt, 2001).

1.1.2 How do they affect civil structures?

During a seismic event, the subsurface - because of the propagation of the waves - is shaking. Due to this movement at the base of each structure, a reaction due to inertia forces is created on the structure (Bolt, 2001). For better understanding, Figure 1-1 shows a representation of a building as a multi degree of freedom system (MDOF) with lumped masses at each floor slab.

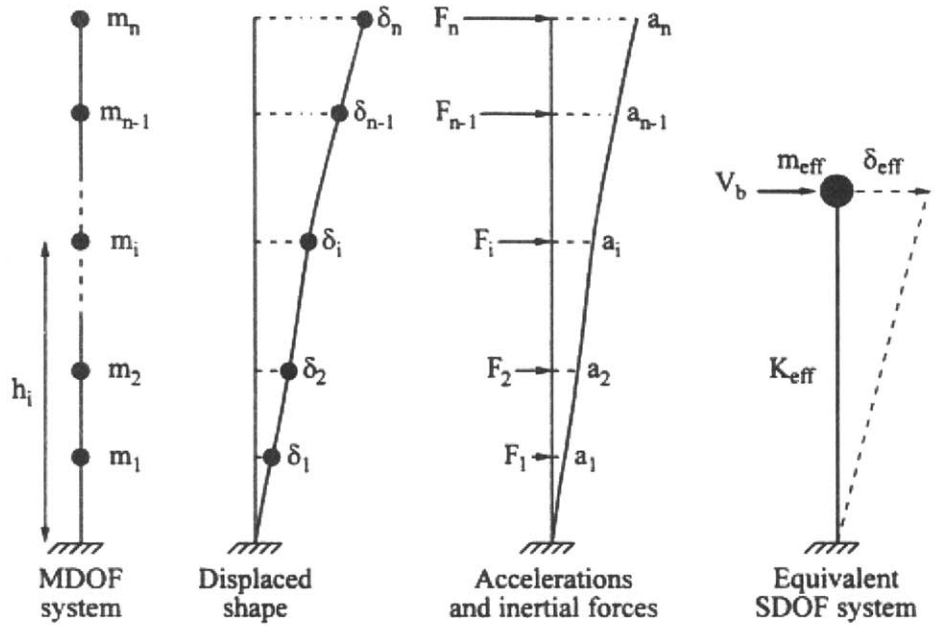

Figure 1-1: Multi degree of freedom system (Chopra, 1995)

The movement of the base causes the lumped masses (shown with the letter *m* in Figure 1-1) to move as well, but because of inertia the lumped masses resist this movement. This resistance produces forces at the level of the lumped masses proportional to the acceleration and mass magnitude at that level. These forces are represented in Figure 1-1 by the "F" labeled arrows. This simple representation shows how buildings are affected during a seismic event (Anderson, 2001).

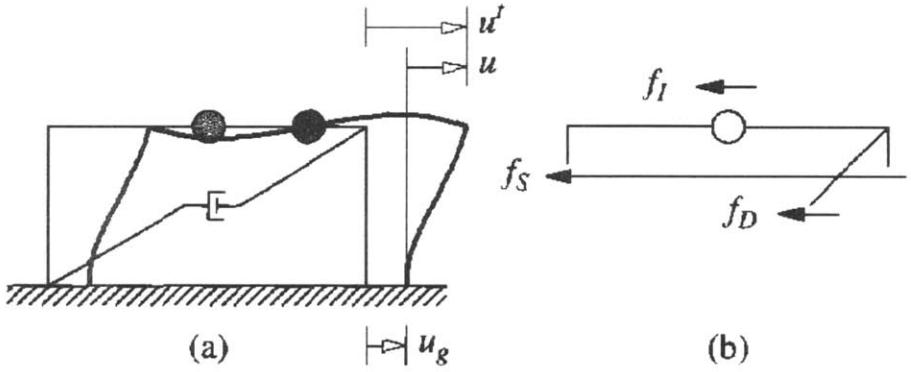

Figure 1-2: Single degree of freedom model under earth movement (Chopra, 1995)

To better understand a seismic event, consider the following single degree of freedom model as described in Figure 1-2. In this figure the displacement at the plane where the lumped mass is, consists of the following two parameters:

$$u^t(t) = u(t) + u_g(t) \tag{1.1}$$

Where u_g is the ground displacement, u^t is the absolute displacement of the mass and u the relative displacement between the mass and the ground. u_g, u^t and u are functions of

time. The above movement causes inertia forces to act on the structure. The inertia forces are shown in Figure 1-2 (b). The equation of the dynamic equilibrium is:

$$f_I + f_D + f_S = 0 \tag{1.2}$$

Where f_I, is the inertia force related to the acceleration $\ddot{u}_g$; f_D is the force related to the system's damping and, f_S is the force related to the system's stiffness. The latter two forces are produced due to the relative motion, u. The inertia force is correlated to the acceleration $\ddot{u}^t$ by:

$$f_I = m\ddot{u}^t \tag{1.3}$$

Therefore, the substitution of equation (1.3) to equation (1.2) provides:

$$m\ddot{u} + c\dot{u} + ku = -m\ddot{u}_g(t) \tag{1.4}$$

The above equation describes the motion of a single degree of freedom system subjected to ground acceleration $\ddot{u}_g(t)$. The above concept can be easily expanded for a multi-degree of freedom model as described in Figure 1-1. The methodology for this will not be further expanded on as it is outside the scope of this thesis. Nevertheless, the statement of the aforementioned methodology is intended to introduce the reader to the basics of structural dynamics. These equations show that to fully describe the motion of the building under a seismic excitation three parameters are needed; acceleration, velocity and displacement at each time step, t. The last statement shows why instrumentation in buildings is needed to estimate a building's motion. The placement of sensors can calculate the above parameters at preselected time intervals and estimate a building's total behavior.

Furthermore, earthquake shaking can produce severe motion displacements in a structure, especially if a structure's fundamental period and the period of the excitation coincide (Chopra, 1995). This phenomenon is called resonance and its results are usually catastrophic for the structure.

In addition, the displacement and accelerations of the structure affect both structural and non-structural elements. Subsequently, buildings engineers and designers have introduced factors for measuring the lateral displacement on each floor of a building. Among these factors are the overall drift of a structure Δ_{TOP}, the inter-story drift $\Delta_i - \Delta_{i-1}$, the overall drift index Δ_{TOP}/H and the inter-story drift index $(\Delta_i - \Delta_{i-1})/h_i$. A graphical representation of these factors is shown in Figure 1-3 (Naeim, 2001).

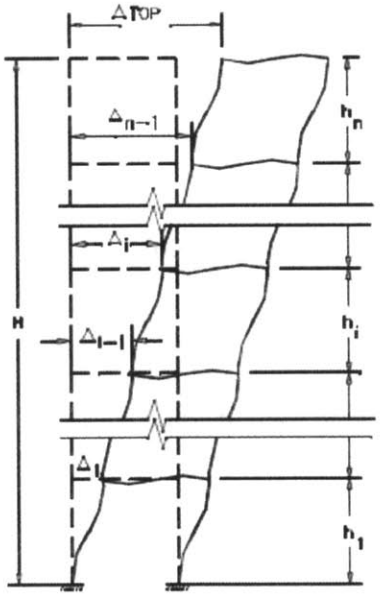

Figure 1-3: Definition of a drift (Naeim, 2001)

The above parameters of design (overall drift of a structure Δ_{TOP}, the inter-story drift $\Delta_i - \Delta_{i-1}$, the overall drift index Δ_{TOP}/H and the inter-story drift index $(\Delta_i - \Delta_{i-1})/h_i)$ are important, as stated by Naeim, considering the three following perspectives: 1. Structural stability, 2. Architectural integrity (e.g. geometry of the building stays as designed) and potential damage to various non-structural components and 3. Human comfort during, and after, a seismic event. Therefore in building codes and also in a large number of publications, tolerances for residual deformation of structures are proposed. For example McCormick et al (McCormick et al., 2008) state in their publication that after a close scrutiny of the results from past earthquakes in Japan, the safety inter-story drift value must be under 0.01 rad for both reinforced concrete and steel buildings. Also the permissible residual deformation for non-structural elements can be maximum 0.005 rad (McCormick et al., 2008).

Acceleration affects mostly the non-structural systems and the human comfort during an earthquake. Examples of acceleration sensitive systems are suspended ceilings, heating-ventilation-air-conditioning systems, elevators, file cabinets, bookshelves, emergency power generation systems and water pumps. As stated by Reinoso and Miranda (Reinoso and Miranda, 2005), tall buildings are more affected by non-structural damage. Reasons for this phenomenon are:

1. The significant economic investment concentrated in one building,
2. The high percentage (almost 75%) of the construction cost that represents non-structural components (this also true for any building according to Kircher et al (Kircher et al., 1997)); and
3. The affect in functionality of large portions of the building due to non-structural damage.

The above parameters such as inter-story drift and acceleration show their correlation with structural and non-structural damage. Buildings with values of inter-story drift or acceleration above the aforementioned limits may become inappropriate for use after a seismic event. Therefore, instrumentation of buildings is a methodology that records and transmits information relative to drift and acceleration (i.e. acceleration, velocities and displacements). The knowledge of this information may lead engineers to accurately represent and calculate a building's behavior and estimate possible damage on the building structural elements or monitor the building behavior after the seismic event. Hence, buildings need efficient instrumentation schemes that will accurately estimate their motion during and after a seismic event.

1.1.3 Past earthquakes around the globe

The purpose of this section is to introduce to the reader the significant effect of earthquakes on structures. Most importantly, the section references the number of human life casualties after seismic events to show how a lack of understanding of the structural effects of earthquakes can lead to human loses. This lack of understanding might be mitigated by introducing efficient motion recording instrumentation schemes on structures.

1.1.3.1 The Northridge earthquake, CA, USA, 1994

The Northridge earthquake was one of the most catastrophic earthquakes in the history of California. It happened on the 17th of January 1994 and had a magnitude of 6.7. The

result was approximately 60 deaths, 7,000 injured, 20,000 homeless and more than 40,000 buildings damaged. Areas affected by the event were the counties of Los Angeles, Ventura, Northridge and more. The cost of the damage was estimated between 13 and 20 billion US dollars (USD). The maximum acceleration was recorded at Tarzana, about 7 km south of the epicenter and had the value of 1.8g. Figures 1-4 to 1-6 show damages in structures by the Northridge Earthquake ("Significant Earthquakes of the World," 1994).

Figure 1-4: Building collapsed after the Northridge earthquake

Figure 1-5: Buckling of longitudinal reinforcement bars possibly due to inadequate transverse reinforcement, Northridge 1994

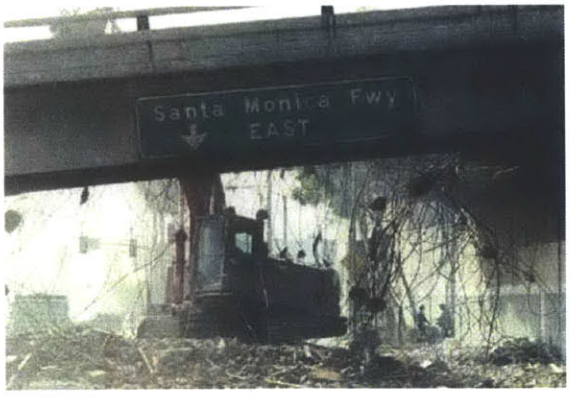

Figure 1-6: General view of the disaster, Northridge 1994

1.1.3.2 Christchurch, New Zealand, 2011

On the 22nd of February 2011, at noon, the city of Christchurch in New Zealand experienced a major earthquake. The magnitude of the earthquake was 6.3 and the number of the casualties was 185 deaths. This earthquake was the costliest in New Zealand's history since the damage was estimated at 15 billion New Zealand Dollars. In Figures 1-7 to 1-9 damages from the Christchurch earthquake are shown. In particular, Figure 1-7 and Figure 1-8 show possible flaws in the design of the structures. In addition, Figure 1-9 shows the significant effect that soil-structure interaction should have in our design parameters and models (McSaveney, 2012).

Figure 1-7: Collapsed Building, Christchurch 2011

Figure 1-8: Destructed structure, Christchurch 2011

Figure 1-9: Soil liquefaction, Christchurch 2011

1.1.3.3 The Kobe Earthquake, 1995

The Kobe earthquake, named after the city of Kobe in Japan, occurred on January the 17th 1995 and had a magnitude of 6.8. This earthquake was one of the most catastrophic in the history of Japan with over 6,400 lives lost. The cost of the damage at the time was 100 billion USD. The following figures (Figure 1-10 to 1-12) show some of the damages due to Kobe earthquake (Johansson, 2000).

Figure 1-10: Collapsed aerial highway, Kobe 1995

Figure 1-11: Collapsed bridge deck, Kobe 1995

Figure 1-12: Damaged exterior columns, Kobe 1995

The figures shown above (Figure 1-4 to Figure 1-12) show the post seismic event catastrophes. The author cannot state whether the damage on the structures in the figures is correlated directly with excessive inter-story drift or acceleration or any other possible damage correlated parameter (e.g. not proper construction methods). Therefore, strong arguments in favor of instrumentation regarding the damage shown in the figures above cannot be derived. Nevertheless, instrumentation of structures can lead to the estimation of the behavior of structures with the use of algorithms (Beck, 1978) and may predict potential damage in real time, for example with the use of inter-story drift exceedance values (Naeim, 2001)

1.2 Strong Motion Instrumentation of Buildings

1.2.1 Purpose of Instrumentation

Since the beginning of building design, engineers have tried to measure and model the effects of a seismic event on buildings' design and construction process. This procedure has led to the establishment of several building design and construction codes where loads generated by earthquakes are taken into consideration with the use of simplified assumptions. Modern building codes try to overcome the ambiguity of a seismic event regarding time of occurrence, epicenter, intensity, frequency of the waves, and unique response of every structure by categorizing the above parameters. Categories include building categories (i.e. low-rise, mid-rise, high-rise), structural system categories (i.e. braced frames, moment connection frames), sub-structure soil category and peak ground acceleration spectrum for several locations. For example the current building codes state the most significant effects on buildings arise from excitation of their first mode. This assumption, although it has been followed with significant success over the past 50 and more years, is not always true due to the complexity of the behavior of a structure, the materials used in a structure, and excitation parameters (e.g. the duration of the excitation). According to Naeim, the 2^{nd} and 3^{rd} mode contributed more to the overall response of the buildings under the code name LAOFFI 52, LAOFFI 54, SHERMAN 13 and NHHOTEL 20 during the Northridge earthquake. The aforementioned code names refer to instrumented buildings in the report conducted by Naiem (Naeim, 1998). Furthermore, Naeim states that the building codes methodology for the calculation of a building's period estimate a smaller period than the initial and fundamental period derived from the data extracted from the instrumented buildings during the Northridge earthquake. Hence, the measurement of the response of buildings during seismic events can provide direct information on the behavior of the building and verification of the designing assumptions.

In conclusion, from buildings instrumentation, engineers and designers possess information regarding (Celebi, 2001):

1. Possible reconstruction of a building's response for comparison with the response gained from mathematical, finite element or laboratory models.
2. Possible explanation of the reasons behind damage of a building.

The information needed can be evaluated with the calculation of buildings' periods, damping ratios, base shears, and story drifts from the data collected by accelerographs (Huang and Shakal, 2002). In particular, M. Celebi in his publication (Celebi, 2001) clarifies the significance of the information derived from a well instrumented building. He states that: "... a well-instrumented building should provide useful information to:

1. Check the appropriateness of the dynamic model in the elastic range;
2. Determine the importance of nonlinear behavior on the overall and local response of the structure;
3. Follow the spreading nonlinear behavior throughout the structure as the response increases and determine the effect of this nonlinear behavior on the frequency and damping;
4. Correlate damage with inelastic behavior;
5. Determine the ground-motion parameters that correlate well with building response damage;
6. Make recommendations eventually to improve seismic codes;
7. Facilitate decisions to retrofit/strengthen the structural system; and
8. Develop new techniques for measurement and analyses to meet need of the user community and to validate performance of new applications in design and construction methods."

1.2.2 Code and current practice regarding instrumentation

The first US motion sensors were installed in California in the summer of 1932 and following the successful measurement of the of the 1933 Long Beach earthquake more and more structures are instrumented under the supervision of state or national programs as the California Strong Motion Instrumentation Program (CSMIP) and the National Strong Motion Project (NSMP).

In the US, the code that addresses the problem of instrumentation is UBC-1997 (and prior editions). The aforementioned code recommends the placement of minimum three accelerometers in buildings over six stories and a square footage over 60,000 square feet, and in every building over 10 stories. The previous recommendations apply for seismic zones 3 and 4. Seismic zones 3 and 4 refer to peak ground accelerations of 0.3g and 0.4g respectively ("Uniform Building Code Volume 2 - 1997," 1997). In Figure 1-13 (a) the UBC-1997 proposed scheme is depicted.

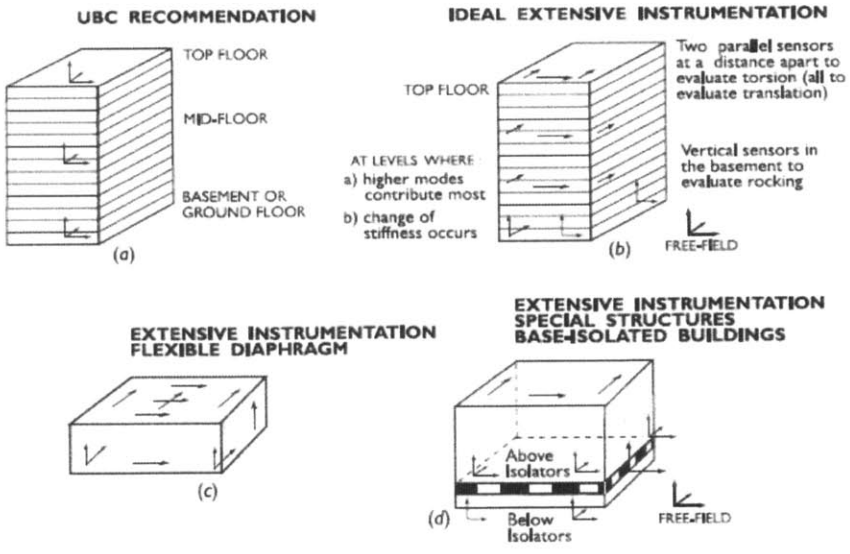

Figure 1-13: Instrumentation Schemes (Celebi, 2001)

The UBC-1997 instrumentation scheme does not provide sufficient data to verify the model of instrumented buildings (Celebi, 2001). Therefore, Celebi (Celebi, 2002, 2001) established a scheme that provides enough data to reproduce the response of a structure. This scheme is called *ideal extensive instrumentation* and it is shown in Figure 1-13 (b). The schemes shown in Figure 1-13 (c) and Figure 1-13 (d) represent proposals for instrumentation for flexible floor slabs (floor diaphragms) and base-isolated buildings.

In addition, Huang and Shakal (Huang and Shakal, 2002), from the California Strong Motion Instrumentation Program (CSMIP) created 6 models of instrumentation that take into account the least amount of information needed to be extracted and the cost of the placement. The schemes of the models proposed are shown in Figure 1-14. The models are:

a. Base or reference free field tri-axial sensor, Figure 1-14 (a)
b. Sensor at the base and roof of the structure, Figure 1-14 (b)
c. Base, roof and a free-field sensor, Figure 1-14 (c)
d. Base, middle floor and roof (UBC-1997), Figure 1-14 (d)
e. Multi-level lateral motion and roof only torsion, Figure 1-14 (e)
f. Multi-level lateral and torsional motions, Figure 1-14 (f)

See chapter 2 for a detailed explanation of the above schemes.

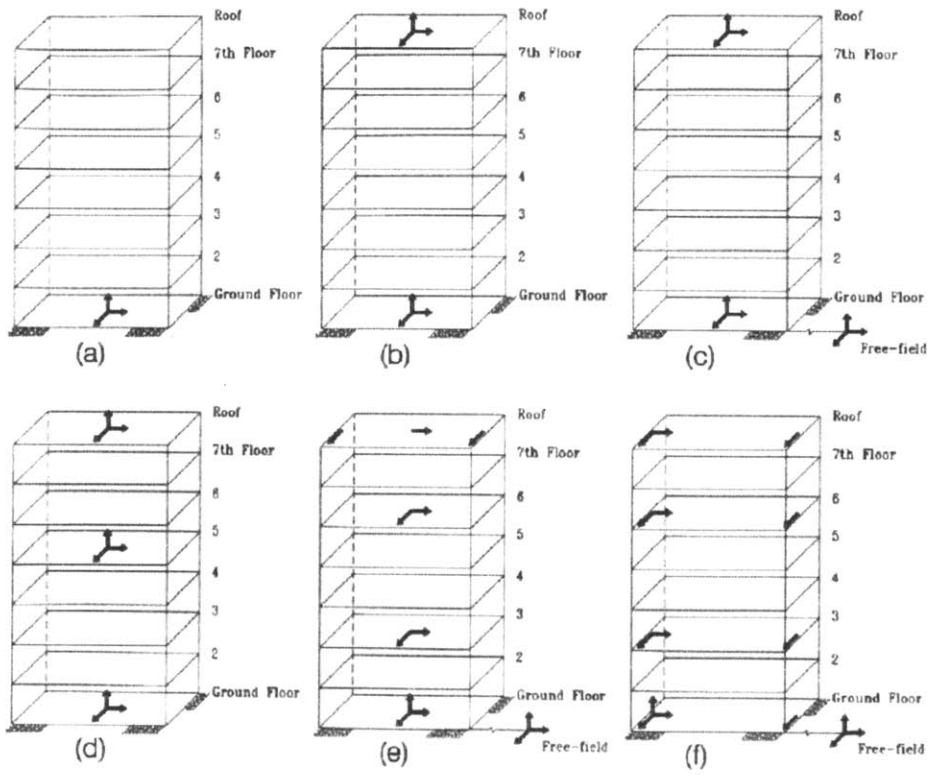

Figure 1-14: Models for Building Instrumentation (Huang and Shakal, 2002)

1.2.3 Types of Sensors Used

The types of sensors used in building instrumentation are accelerometers, seismometers, displacement sensors and GPS sensors. The accelerometer is a sensor that measures the acceleration and produces records that are called accelerographs. These sensors measure the acceleration at certain points in "g" units; where "g" is the vertical acceleration of gravity. The seismometer, which has high precision and is the most commonly used sensor, measures the velocity of a point on the ground as it moves during a seismic event. The displacement sensor records the relative displacement between two points. Finally, during the last decade GPS guided sensors have been used to enhance the general instrumentation procedures.

In recent years, improvements have been made towards wireless instrumentation of buildings. The purpose of improvement is to minimize the cost of instrumentation and maintenance, and to transmit more accurate data over larger distances during and after seismic events. Particularly, the cost of instrumentation is a significant obstacle towards instrumentation. The California Department of Transportation (Caltran) instrumented approximately 60 of the state's 22,000 bridges and has estimated a cost of 300,000 USD per toll bridge for an installation of 60 accelerometers. A quick calculation shows that 6.6 billion USD are needed for the instrumentation of all of California's bridges. Obviously the amount of money needed may restrain the implementation of instrumentation technologies. A significant amount of this cost is the cost related to maintenance and anti-weather-hazards protection of wires: a cost estimated at the price of 10 USD per linear foot (Huang and Shakal, 2002). Therefore, the use of Wireless Modular Monitoring Systems (WiMMS) is considered to be the future of instrumentation (Lynch et al., 2001). Some of the advantages of using WiMMS is the absence of wires, the functional independence of the individual sensing units and the possibility of rendering applications for damage detection in real time. Figure 1-15 shows the instrumentation scheme proposed by Lynch using the WiMMS technology. The figure shows clearly that the removal of the wires needed for instrumentation, reduces the complexity of the placement. A WiMMS sensor is shown in Figure 1-16

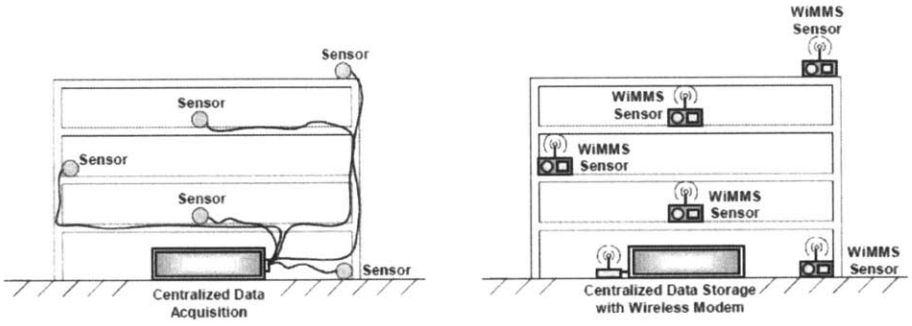

Figure 1-15: From a Cable based system to a Wireless based system (Lynch et al., 2001)

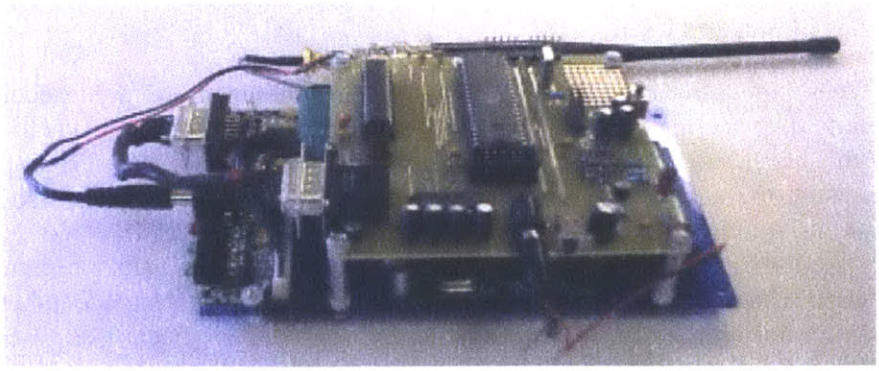

Figure 1-16: An ADXL210 wireless accelerometer (Lynch et al., 2001)

In addition to wireless sensors some researchers such as Kim and Feng (Kim and Feng, 2006) propose the use of fiber optic accelerometers. These accelerometers take advantage of the use of fiber optic cables and their capabilities for adequate instrumentation. Fiber optic sensors share the merits of immunity to electromagnetic noise and electric shock and have the ability to measure both low and high amplitude vibrations with high precision, without pre-setting a gain level.

1.2.4 Limitations of instrumentation

Instrumentation of buildings and structures can provide the structural engineer, company or organization, which designed or occupies a structure, with information regarding the behavior of the building under severe or everyday environmental hazards. This information might be used for verification of the assumptions the design of the structure was based on. In addition, instrumentation might assist the engineers to calculate changes in the structural properties of a building. Nevertheless, beside the potential benefits of instrumentation, buildings, new or existing, have not been instrumented. A reason that might explain the lack of instrumentation in buildings is the insufficient information provided by the building codes. Codes do not give clear answers regarding where and what type of sensors to implement. Dr. Farzad Naeim in his book "The Seismic Design Handbook" (Naeim, 1989) states that the codes specify that the minimum instrumentation for a structure is to place tri-channel accelerometers at the base, mid-height and roof of the building. If an extensive instrumentation is needed then a large number (on the order of 10 to 30) should be placed along the plan and elevation of a structure. This ambiguity makes it difficult for the practicing structural engineer who wants to know the response of the buildings she/he designed. It is proper to mention that 95% of the buildings are low-rise that usually are not instrumented.

Furthermore, the complexity of instrumentation, wireless or not, leads to unnecessary costs and raises the prices of buildings. Strong motion instrumentation sensors, as every high technology system, often need maintenance. Maintenance of hi-tech systems comes with a price to pay. Therefore, the owners of the buildings are trying to cut-down "unnecessary" costs. According to Celebi (Celebi, 2002), the hardware and the installation cost vary between $30-60K. This cost depends though on the number of channels used. Specifically, for the instrumentation of federal buildings, Celebi approximates the cost for an instrumentation scheme similar to the one in Figure 1-13(b) to a value of $50K. This price includes also a free field tri-axial station near the site of the building (Celebi, 2002). Moreover, the aforementioned prices represent the value of the currency at the time when

the publication was written (2001). Huang and Shakal estimate the instrumentation cost to a value of $3,300 per channel (i.e. for a tri-axial accelerometer the cost is almost $11,000) (Huang and Shakal, 2002). Into the total cost, the cost of maintenance should be taken into consideration. The maintenance of sensors should take place at least once a year and includes procedures such as calibration, inspection for electronic malfunctions and measurement of threshold of the triggering system. The use of new data transmitting technologies through the World Wide Web has extra hardware costs and monthly subscription fees (Celebi, 2002). Maintenance cost is estimated to $500 per year for the scheme shown in Figure 1-14(a). For the other schemes the maintenance cost is almost proportional (not always though) to the number of sensors (Huang and Shakal, 2002).

In addition, there is a psychological factor intervening in the procedure for strong motion instrumentation. Owners of real estate often believe that the application of instruments for motion sensing will make their property unattractive for leasing because they believe that a monitored building is one with flaws. They are also afraid of potential future litigation if the building does not perform as designed despite monitoring (Celebi, 2001).

Another limitation is the fact that most of the civil/structural engineers do not have a clear path on how to interpret the data provided by the sensors. These data are usually confusing text files filled with numbers and need constant interpretation into a Civil engineer's logic results such as inter-story drifts and displacements. Therefore a need for real-time interpretation software is needed for translating these data from a machine's language to an engineer's language. Additionally, the instrumentation programs proposed by the codes (UBC-1997) aim to monitor the structure than to analyze it. Hence, the provided data by the code scheme are not sufficient for the scientific and engineering purposes of the instrumentation (Celebi, 2002).

1.3 Problem Statement

The problem that the author addresses is the fact that although instrumentation schemes exist(Celebi, 2002; Chopra, 1995); the schemes are not optimized to capture the motion of a building during a seismic event. Therefore, an algorithm is needed to propose the exact number and placement scheme of the sensing instruments.

The problem of instrumentation could be addressed by making a back-analysis to the question that motivated the author to write this thesis. The question is: "After an earthquake can we predict possible flaws in the structure immediately and inform the occupants for the necessity of an immediate evacuation through telecommunication systems?" Let's assume that the technology to monitor structures by wireless means is available (Lynch et al., 2001). Are there instruments that measure motion data? Yes, there are (accelerometers, strain-gauges, and GPS connected systems) (Celebi, 2001). Is there a procedure to estimate damage through motion data? Yes, there is (calculation of inter-story drifts and comparison with maximum allowances) (Naeim, 1989). Considering that these questions have already been answered, one major question that remains to be explored is the optimization of placing sensing instruments. This is a large and complex question that will not be fully answered in this work alone.

Therefore, due to the lack of optimization some instruments might be redundant and cause the overall cost (purchase, installation and maintenance) to be a deterrent factor for instrumentation. Hence, the owners (private or public) avoid instrumentation of buildings which leads to lack of monitoring. By this practice, estimation of buildings' behavior after a seismic event cannot be fully captured; a result that leads to unsatisfactory validation of the current building codes and possibly threatens human life due to the lack of immediate

structural and non-structural damage calculation. The latter is caused by the extended time that engineers' crews need to inspect and estimate damage on site.

In summary, the unclear placement scheme might lead to unnecessary use of motion sensors and increase the cost of instrumentation. As a result, the owners avoid instrumentation of their buildings. Furthermore, most of the instrumentation schemes suggested in present codes and practices are based on a linear elastic behavior of structures. Hence, the codes do not provide sufficient explanation with regard to potential inelastic behavior of the structures (Rojahn and Matthiesen, 1977).

1.4 Purpose of this Thesis

The purpose of this thesis is to estimate the necessary sensor positions to sufficiently instrument a building. The thesis will try to overcome one of the aforementioned limitations of the strong motion instrumentation which is the ambiguous and arbitrary placement of sensors in a building with the result of increased cost and lack of monitoring of the structure in the years of service. The author provides an optimized scheme of instrumentation, through an optimization algorithm that uses information from time history analyses of finite element models of previous instrumented buildings.

Initially, a seismic event that occurred in the past and affected buildings that were instrumented at the time of the event are selected. This event is the 1994 Northridge Earthquake. Data regarding the motion of instrumented buildings, as well as the geometric and mechanical parameters of the structural members will be found. The structures are re-designed in software with finite element analysis capabilities (i.e. SAP2000). The models have the purpose of being as realistic as possible. These models are then excited by a simulation of the 1994 Northridge Earthquake. Data for this excitation can be found in the accelerograms provided by the accelerometers at the base of each building. Motion information of the buildings is extracted through the software analysis. The data regarding the motion are implemented in an algorithm the author produced for optimization of the placement of the sensors. The proposed optimized schemes are then compared to the actual schemes on the buildings. Furthermore, a discussion regarding cost and optimization error is held with the help of appropriate plots.

1.5 Chapter Summary

This chapter introduced earthquake generation and how the effects of a seismic motion is applied and calculated on buildings. Furthermore, a list of past earthquakes was mentioned with particular reference on their devastating results. The chapter continued with a short introduction of the general purpose of instrumentation and ended with the problem stated by the author and the purpose of the dissertation.

2 Current instrumentation schemes

The purpose of this chapter is to introduce the reader to current building instrumentation practices. The chapter starts with the presentation of a method for the estimation of motion of a building through data recorded from instruments on buildings. Furthermore, this chapter mentions the current instrumentation schemes proposed by the current building codes or state organizations. In addition, the theoretical background behind the current instrumentation schemes is stated. The chapter concludes with a short discussion about the current methodology.

2.1 How the current procedures evaluate the motion of the structure

2.1.1 Introduction

The purpose of instrumentation is to track the motion of the structure which is applied. To successfully estimate the dynamic characteristics, and particularly the motion of a structure, several methods have been proposed (e.g modal identification, identification using discrete time-filters). The methods are called *system identification*. Generally, *system identification* method includes three major steps (Safak, 2001):

i. Establishment of a mathematical model for the structure.
ii. Calculation of the model parameters from the recorded data.
iii. Comparison and evaluation of the model's response to the response calculated from the recorded data.

Specifically, there are generally two approaches to identify model parameters, the prediction-error approach and the maximum likelihood, or Bayesian identification. The prediction-error approach determines the model's parameters by minimizing the difference between the mathematical model of the structure and the model calculated from the recorded data. The Bayesian identification works by maximizing the probability that the mathematical model parameters will match the recorded model (Safak, 2001). In the next paragraph, the most popular form of system identification is presented.

2.1.2 Modal Identification

In this section a system identification form is introduced. This form uses the prediction-error approach. The form is called modal identification and was introduced by Beck (Beck, 1978). Modal identification is based on the estimation of the modal parameters of a building (or structure in general) by taking into account the vibration records (Safak, 2001).

Consider a multi-degrees-of-freedom (n) system imposed to seismic loads. The relative displacement $y_i(t)$ of node i can be written as a superposition of n nodal parameters:

$$y_i(t) = \sum_{j=1}^{n} x_{ij}(t) \quad \text{Eq. 2.1}$$

The parameter $x_{ij}(t)$ represents the amplitude of the *j*'th modal response at node *i*. The equation of motion is:

$$\ddot{x}_{ij}(t) + 2\xi_j\omega_j\dot{x}_{ij}(t) + \omega_j^2 x_{ij}(t) = -p_{ij}\ddot{x}_g(t) \quad \text{Eq. 2.2}$$

In the equation above, ω_j and ξ_j are the modal frequency and damping ratio of the j'th mode, p_{ij} is the participation factor of the *j*'th mode at node *i*, and $\ddot{x}_g$ is the ground acceleration. $\ddot{x}_{ij}(t)$ and $\dot{x}_{ij}(t)$ are respectively the acceleration and velocity of the *j*'th modal response at node *i*. The unknowns of the *j*'th mode that this method requires to be calculated are represented by θ:

$$\theta_j = [\omega_j, \xi_j, p_{ij}, \dot{x}_{ij}(0), x_{ij}(0)] \quad \text{Eq. 2.3}$$

The use of the above notation leads to:

$$\ddot{x}_{ij}(t) = F_j(\theta_j) \quad \text{Eq. 2.4}$$

Where $F_j(\theta_j)$ is a nonlinear function of θ_j. The next step is to calculate F for all the modes and substitute in equation 2.1:

$$\ddot{y}_i(t) = \sum_{j=1}^{n} F_j(\theta_j) \quad \text{Eq. 2.5}$$

Finally, θ_j is determined by minimizing the difference between the recorded and calculated accelerations at node *i*. The acceleration provided by the recorded data is denoted by $\ddot{y}_{ri}(t)$, and the difference is:

$$J = \int_{t=0}^{t_d} [\ddot{y}_{ri}(t) - \ddot{y}_i(t)]^2 dt \quad \text{Eq. 2.6}$$

t_d states the duration of earthquake. The parameter *J* requires numerical minimization due to its non-linear nature. The minimization occurs by using iterative optimization algorithms (Beck, 1978). The procedure above can be extended from a single-input and single-output, to multi-input and multi-output scheme (Werner et al., 1987).

The above system identification form is a methodology that can be used to estimate the dynamic characteristics of a building after a seismic event. The above methodology uses data recorded by sensors placed in a building. Therefore, it connects physical instrumentation with mathematical algorithms. A similar approach has been created by the author and it is explained in the next chapters.

2.2 Code specifications regarding instrumentation

This section introduces the specifications provided by current codes, and specifically by the Uniform Building Code of 1997 (from now on referred as UBC 1997). UBC-1997 is considered as the most used code in the United States (Celebi, 2001) and provides the engineer with a short description on the type of building that needs instrumentation and where the measurement units would be placed.

2.2.1 General

UBC-1997 recommends that every building over six stories height with a floor area of 60,000 square feet or more, and every building over 10 stories, without considering any area restrictions, should be instrumented with no less than 3 accelerometers. The

accelerometers must be interconnected for timing issues ("Uniform Building Code Volume 2 - 1997," 1997).

2.2.2 Location

UBC-1997 provides to the engineer very general guidelines on where the accelerometers should be placed. The accelerometers, based on UBC-1997 instructions, should be positioned in the basement, middle, and near the top of the building. In addition, the code states that the location of the sensor should be clear for access and maintenance constantly and with a sign stating "Maintain clear access to this instrument" placed near the sensor ("Uniform Building Code Volume 2 - 1997," 1997).

2.2.3 Maintenance

Maintenance and service of the instruments are responsibility of the building owner and subjected for approval by the building's official. The building's official has the authority to request data produced by the instruments from the building owner ("Uniform Building Code Volume 2 - 1997," 1997).

2.2.4 Instrumentation of existing buildings

Jurisdiction authorities have the right to select the structures that require instrumentation and where the instruments should be placed. The owners of the structures must provide appropriate space for installing the accelerometers. The recorded data are property of the jurisdiction authorities and can be requested by the public on request("Uniform Building Code Volume 2 - 1997," 1997).

2.2.5 Comments

The above description of the UBC-1997 instrumentation scheme shows that the code proposed instrumentation practices does not provide extensive detail in a complex scientific field such as strong motion instrumentation. Therefore, the UBC-1997 instrumentation scheme does not provide sufficient data for the extraction of useful information regarding a building's behavior during or after a seismic event (Celebi, 2001). To overcome this obstacle Celebi (Celebi, 2001) introduced to the scientific community an instrumentation scheme which provides enough data to estimate the behavior of building. The scheme is called *ideal extensive instrumentation.*

2.3 CSMIP Instrumentation Models

Prior to the 1971 San Fernando earthquake in California, the dominant instrumentation scheme was the one proposed by the Uniform Building Code as it was described in the previous subchapter (note: the instrumentation scheme proposed by UBC-1997 is the same as the prior editions). After the San Fernando earthquake, there was a desire for greater and more accurate instrumentation to prevent the kind of damages seen in that earthquake. Therefore models were developed by the California Strong Motion Instrumentation Program (referred as CSMIP from now on) (Huang and Shakal, 2002) based on the theory proposed by Rojahn and Matthiesen (1997). The models that follow provide a description

of each instrumentation scheme. The titles used for the models are the same used in the publications provided by CSMIP.

2.3.1 Model 1: Base or Reference Free-Field Only

Model 1 is the basic instrumentation scheme and it is shown in Figure 2-1(a). This scheme includes only a tri-axial instrument. This instrument should be placed at the base of the building or in the area around of the building. The recorded date from this scheme provides information concerning the building base motion or the ground shaking around the building. The actual response of the building is not measured; therefore building parameters such as the period cannot be measured (Huang and Shakal, 2002).

2.3.2 Model 2: Base and Roof

Model 2 is shown in Figure 2-1(b). The difference with the previous model is the placement of an additional tri-axial instrument on the roof of the building. This model provides information about the input at the base and the response at the roof. Modal periods and damping can be estimated for the first few modes. Mode shapes are not possible to be derived by this scheme (Huang and Shakal, 2002).

2.3.3 Model 3: Reference/Free Field, Base and Roof

Model 3 (Figure 2-1 (c)) recommends the placement of 3 tri-axial instruments, one at the base, one at the top and one outside the building (free-field instrument). This instrumentation scheme provides similar information with the previous one (Model 2) but with some extra information on the soil-structure interaction. Potential rocking of shear walls cannot be recorded (Huang and Shakal, 2002).

2.3.4 Model 4: Base, Mid-height, and Roof

Model 4 is depicted in Figure 2-1 (d). This instrumentation scheme is the one proposed by the code (UBC-1997 Chapter 16 Appendix). The information gathered from this model is the same as Model 2, but with more data for estimation of the first 2 modes shapes. Torsional motion of the floor slab is not measured. Since a free-field instrument does not exist soil-structure interaction cannot be assessed (Huang and Shakal, 2002).

2.3.5 Model 5: Multi-Level Lateral Motion, Roof-Only Torsion

Model 5 is shown in Figure 2-1 (e). This instrumentation scheme usually includes 12 channels for data recording, placed on 3 or more levels of the building. Data records from this scheme include translational movement of the base, translational and torsional movement of the roof, and if a free-field instrument exists, soil-structure interaction can be measured too. Torsional movement on other levels cannot be measured due to only two sensors are place on those floors. With this scheme lateral mode shapes can be calculated. Torsional mode shapes cannot (Huang and Shakal, 2002).

2.3.6 Model 6: Multi-Level Lateral and Torsional Motion

Model 6 is described in Figure 2-1 (f). This model usually includes more than 12 channels for data recording placed strategically in more than 3 levels of the building. This scheme provides the same information as Model 5, but with additional information on the torsional mode shapes. In addition, torsional movement of the base and soil-structure interaction can be measured. If rocking of shear walls or flexible floor diaphragm behavior is needed to be measured, additional instruments can be placed at the base of the shear walls or at the middle of floor slabs respectively. Regarding cost Model 6 is approximately six times more expensive than Model 1 (Huang and Shakal, 2002).

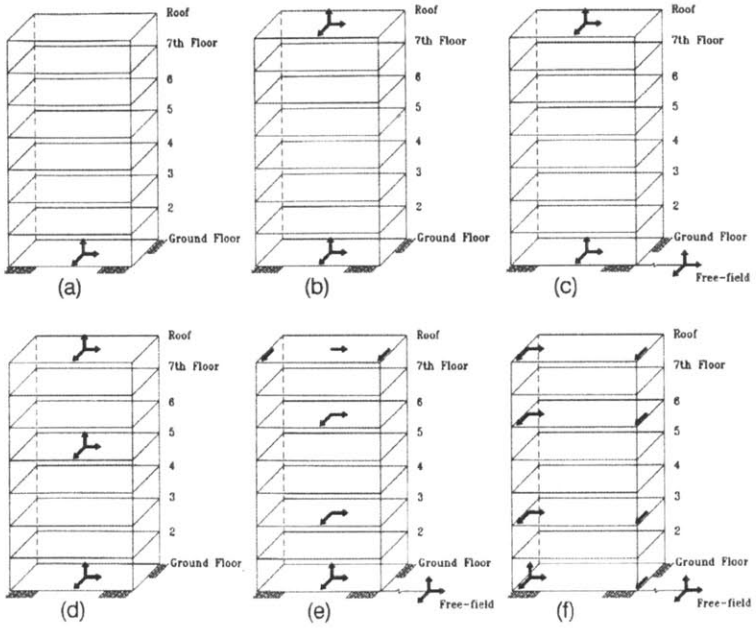

Figure 2-1: Instrumentation schemes proposed by CSMIP (Huang and Shakal, 2002)

2.3.7 Comments

The CSMIP instrumentation schemes obviously provide more details, compared to the UBC-1997 instrumentation scheme, on which floors should be instrumented and where on the floor slabs the sensors should be placed. CSMIP proposals also mention the type of movement each instrumentation model captures. Nevertheless, the above instrumentation schemes are not automated procedures that use mathematical algorithms to suggest the spatial coordinates of each sensor. In addition, the schemes do not provide the exact location of each sensor on a floor slab. This implies that a sensor's horizontal coordinates do not affect the estimation of the motion. Therefore, the author questions the effectiveness of these schemes on complex or out-of-the-ordinary buildings.

2.4 Theoretical background of UBC-1997 and CSMIP instrumentation schemes

In this subchapter, the theoretical background of the instrumentation schemes proposed by UBC-1997 and CSMIP is stated. Most of the theory was developed by Christopher Rojahn and Ralph Matthiesen (Rojahn and Matthiesen, 1977). On the concept provided by

Rojahn and Matthiesen, Huang and Shakal (Huang and Shakal, 2002) developed the instrumentation schemes for CSMIP, as shown in the previous section.

2.4.1 Need for instrumentation

Buildings when excited at their base have 2 sets of movement, one concurring with the ground motion and one relative to it. If buildings were infinitely rigid their movement would match the ground movement and the forces occurred on a building would be the multiplication of the mass of each floor times the ground acceleration. It is clear that a rigid building does not need any instrumentation on the floors above the ground. But this is not the case in real buildings. In reality buildings due to their structural and soil flexibility, have relative motion to the ground. This motion is the one that instruments aim to record (Rojahn and Matthiesen, 1977). The relative motion of the building is in direct relation to the stiffness, mass and damping properties if the building and its surrounding soil. In addition, parameters such as the amplitude, frequency and duration of the absolute ground motion affect the relative motion of the structure. Strong motion instrumentation's objective is the calculation of the above parameters (Huang and Shakal, 2002).

2.4.2 Modeling assumptions and explanation

The assumptions behind the Rojahn's and Matthiesen's proposed instrumentation techniques are the following:

1. Masses of the building are lumped at each floor level.
2. Masses move horizontally
3. Floors are rigid in their own plane.
4. Buildings behave in the linear elastic range.

The assumption that masses move horizontally is based on the fact that vertical response is independent from the horizontal and also due to the direct correlation between horizontal movement and structural damage (Rojahn and Matthiesen, 1977). Therefore, a building's response can be described by three degrees of freedom per floor; two horizontal translations and one rotation. In total, the degrees of freedom required to fully analyze a building based on this assumption are 3 times N; where N is the number of floor slabs (Rojahn and Matthiesen, 1977).

A building's response based on the aforementioned assumption, is generally based on the mode shapes produced by the solution of the Eigenvalue problem (Anderson, 2001).

$$([K] - \omega^2[M])[\Phi] = [0] \qquad \text{Eq. 2.7}$$

Whereas K is the stiffness matrix, M the mass matrix and Φ the mode shapes for each frequency ω.

Generally, buildings respond predominantly in their first 4 modes. Mode shapes derived from analytical and experimental data are shown in Figure 2-2. The response between the mode shapes can be coupled or uncoupled. The independence of mode shapes depends on the buildings characteristics, such as the building stiffness and mass distribution. For example, buildings with a rectangular shaped plan where the stiffness in one direction is significantly different than the other probably have an uncoupled response.

Buildings symmetrical in plan with similar stiffness characteristics in both directions most likely have coupled behavior (Rojahn and Matthiesen, 1977).

The aforementioned analysis is based on the assumption of in-plane rigid floors. Flexible floor slabs have more complex analysis scheme. However, due to the fact that floor slabs usually behave as infinitely stiff systems in their in-plane bending, as well as the minimal potential effects that non-rigid slabs have on a building's response, assumption number 3 is mostly valid (Rojahn and Matthiesen, 1977). Instruments that measure the vertical movement of the slab might be needed if flexible slab behavior occurs. The most appropriate position to set instruments that measure vertical displacements is in the middle of a slab, away from vertical elements (Rojahn and Matthiesen, 1977).

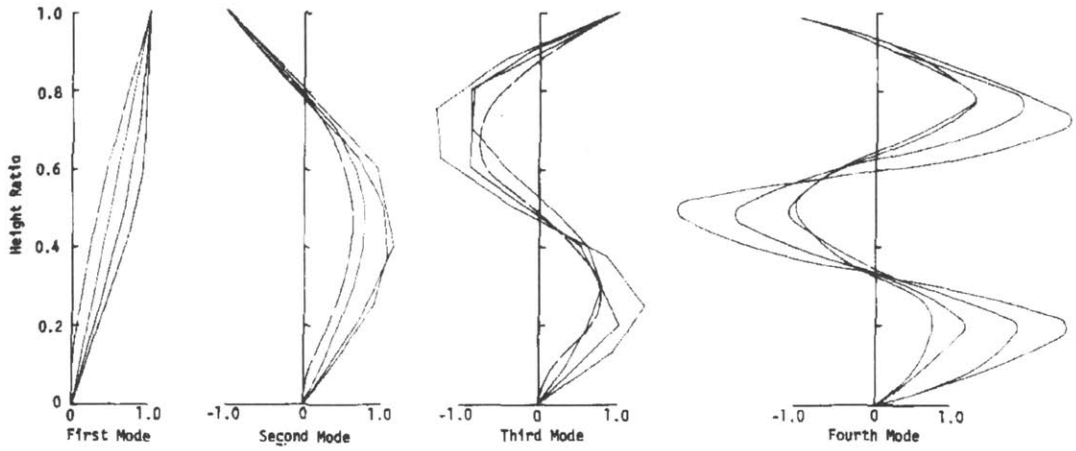

Figure 2-2: Experimental and analytical mode shapes of buildings (Rojahn and Matthiesen, 1977)

In addition, instrumentation schemes are based on linear elastic behavior of structures. Although structures can behave in a nonlinear and inelastic way under a high-amplitude motion with long-duration, researchers believe that instrumentation procedures based on linear elastic theory can represent sufficiently any potential nonlinear and inelastic response. The aforementioned statement is based on the methodology of representing nonlinear response with a sequence of successively changing linear models (Clough and Penzien, 1964). Furthermore, that data derived from buildings after the San Fernando earthquake showed that property changes due to nonlinear behavior do not affect considerably the mode shapes (Rojahn and Matthiesen, 1977).

2.4.3 Recommendations and Guidelines

A common accelerometer consists of 3 orthogonal accelerometers. Due to this fact, the placement of a single accelerometer on a floor slab does not provide sufficient information regarding the motion of the slab. Therefore it is recommended that minimum three accelerometers are placed in every floor slab needed to be instrumented (Rojahn and Matthiesen, 1977).

Accelerometers should be placed at least on the base floor and the roof of the potential instrumented structure. The number of sensors and scheme that these floors should be instrumented is related to the foundations type and conditions, building size,

architectural layout, structural system, structure's dynamic characteristics and location of seismic joints (Rojahn and Matthiesen, 1977).

The base accelerometers have the objective to measure the input motion due to a seismic event. Guidelines suggest placing two horizontal and one vertical accelerometer on the foundation floor near the center of the plan. This is the minimum recommended instrumentation. The horizontal accelerometers should be parallel to the floor plans transverse and longitudinal direction. Buildings with large floor slabs should be instrumented with two more accelerometers, placed on the furthest sides of the slab. These accelerometers measure potential torsional movement of the slab. Furthermore, if rocking motion is expected, additional vertical accelerometers are needed to record the rocking. Also, changing foundation and soil conditions might require the use of more accelerometers to sufficiently record the soil-structure interaction (Rojahn and Matthiesen, 1977).

On floors above the ground level the expected motion is mostly horizontal. Therefore, the instrumentation is mostly sufficient with the use of horizontal accelerometers placed in strategic positions. Generally vertical accelerometers are considered to be unnecessary for floors above the ground. Nevertheless, if significant vertical motion is expected then vertical accelerometers might be needed. As stated in a previous paragraph the roof should be instrumented as a minimum. The instruments should consist of two horizontal accelerometers placed at the center of the slab and one accelerometer placed at the far-out side of the roof. The sensors at the center measure the horizontal displacement and the third one measures potential torsional movement. If other motions are expected such as vertical movement of a potential non rigid slab, placement of additional sensors is highly recommended (Rojahn and Matthiesen, 1977).

Floors between the roof slab and the basement slab also need instrumentation. The number of levels that require instrumentation is directly related with the following parameters: structural framing system, number of stories, architectural configuration and building's dynamic characteristics. Instrumentation of floors in between is necessary in order to increase the accuracy of the recorded motion. The accuracy of the model that represents a building's response is proportional to the number of instrumented floors. Guidelines recommend at least the instrumentation of two floors between the roof and the basement for buildings over six stories high, and at least one instrumented floor for buildings with less than six stories. Stories selected for instrumentation should not match with nodal points at any of the 4 predominant mode shapes. As shown in Figure 2-2 the most appropriate position for sensor placement is about 25%, 40% and 70% of the height of the building starting from the base floor. Furthermore, stiffness discontinuities are crucial in sensor placement due to their direct influence on mode shapes. Hence, a more thorough investigation of the structural system of the building is needed (Rojahn and Matthiesen, 1977).

Furthermore, Rojahn and Matthiesen (Rojahn and Matthiesen, 1977) proposed schemes for particular types of buildings based on their theory. The proposed schemes are shown in Appendix V.

2.5 Conclusions-Remarks

This chapter summarized instrumentation guidelines as provided in the codes (UBC-1997) and state programs (California Strong Motion Instrumentation Program – CSMIP), theoretical background regarding the proposed instrumentation schemes and a methodology on how to measure motion from recorded data.

The most common instrumentation scheme is the one provided by UBC-1997. This scheme provides the owner a quick determination in a potential period lengthening in the fundamental translational modes of vibration (Huang and Shakal, 2002).

The instrumentation schemes provided by CSMIP provide more details regarding the reasons of implementing them. As a minimum, CSMIP suggests an instrumentation scheme similar to Model 6. Implementation of this model will provide to the owner sufficient information regarding translational and torsional mode shapes. In addition, data from this model will provide information useful for the verification of a structure's mathematical model.

Rojahn and Matthiesen theory and suggestions provide a general view and validation on where sensors should be placed. Their theory is based on experimental and analytical models. Furthermore, the assumptions behind their theory is also based on their engineering experience (Rojahn and Matthiesen, 1977).

The modal identification form (Beck, 1978) provides a clear and straightforward mathematical procedure for the calculation of a building's response from motion sensing instruments.

The information regarding instrumentation schemes provided by the above researchers might be sufficient for the estimation of the motion of a building from recorded data. Nevertheless, the author believes that a more deterministic procedure, with the use of computer algorithms, could be produced in order to directly find the most cost effective and accurate motion prediction scheme.

The author believes that the UBC-1997 and CSMIP instrumentation schemes have limitations with respect to a building's motion estimation. These limitations derive from the fact that the schemes do not propose the exact positions and number of the required sensors. These limitations might lead to insufficient data recordings that lead to insufficient motion estimation. In addition, to overcome possible insufficiencies more sensors might be placed. The latter may lead to increased instrumentation costs, compared to an optimized instrumentation scheme. The author's work address the ambiguity regarding the sensors coordinates with the establishment of a computer algorithm that proposes the exact number and coordinates of the motion capturing instruments.

2.6 Chapter Summary

This chapter stated the current practices regarding building instrumentation schemes and the theoretical background behind the current practices. The chapter starts with Modal Identification, which is a system identification form, introduced by Beck in 1978, and estimates the motion of a building from recorded data from sensors placed in buildings. Furthermore, the current specifications provided by UBC 1997 and the California Strong Motion Instrumentation Program are mentioned. These specifications include figures and parameters taken into consideration before a building is instrumented. Finally, part of the theoretical background behind the current instrumentation provisions is stated. The theoretical background statement is based on the publication Christopher Rojahn and Ralph Matthiesen published in 1977.

The next chapter introduces the methodology and data the author uses to overcome the limitations of the UBC-1997 and CSMIP instrumentation schemes. The author's proposal starts with the procedures followed in order to create a sufficient database for the algorithm implementation. Furthermore, an extensive description of the algorithm is stated.

3 Optimization of Placement – Tracking the motion

This chapter states a method based on the theory described in previous chapters in order to optimize the placement of the sensors in buildings. The method uses results produced by time-history analyses of finite element models that represent existing instrumented buildings. The time history analyses are based on data from instrumented buildings recorded after the Northridge Earthquake in 1994. The results from the time history analyses are implemented into a program produced in MATLAB. The code implemented with the necessary mathematical background produces the results which are shown in Chapter 4.

3.1 Introduction

After the review of the current instrumentation techniques and schemes provided by codes (UBC-1997) or CSMIP in Chapter 2, the author believes that the methods of instrumentation are not precise enough in order to mitigate instrumentation cost and optimize motion estimation. As mentioned in previous chapters, the instrumentation schemes proposed by UBC-1997 and CSMIP do not provide to the building engineers the exact spatial coordinates of the sensors. This might lead to under estimation of a building's motion and possibly increased the overall cost of the building's design.

Therefore, this thesis proposes a method to estimate the most efficient instrumentation scheme. Efficient instrumentation scheme is the one that provides to the owner of a building the ability to estimate accurately the motion of the building during a seismic event and provides a low cost for implementation.

In order to evaluate efficient instrumentation schemes structures that were instrumented during a major seismic event were needed. Since USGS started implementing sensors in structures more often after the 1971 San Fernando earthquake, the author searched for structures that were instrumented during a major seismic event after 1971. As it was explained in chapter 1 a major seismic event in the United States was the Northridge Earthquake in 1994 (Huang and Shakal, 2002). The literature search regarding instrumented buildings during the Northridge earthquake came across to a publication by Dr. Farzad Naeim related to the problem this dissertation is addresses. The publication is called "Performance of 20 extensively instrumented buildings during the 1994 Northridge Earthquake" (Naeim, 1998). In this publication Dr. Naeim states his inspection through 20 instrumented buildings in the area of Northridge Earthquake's range and estimated the behavior of the structures from data extracted by the implemented accelerometers. Dr. Naeim used the data from the accelerometers to produce a software called CSMIP-3DV in order to graphically reproduce the motion of each building. Furthermore, the software (CSMIP-3DV) has an extensive database with information about several other buildings and earthquakes. This dissertation takes into consideration 3 buildings mentioned in the aforementioned publication or modeled in CSMIP-3DV and the input data at the base of these buildings, as they were recorder by the sensors placed at the base of the buildings, to run time-history analyses in finite element software.

The buildings executed in the finite element software represent existing buildings in the state of California. Nevertheless, due to legal restrictions imposed in gathering the actual

geometric, material and construction data of the buildings, the finite models do not describe accurately the behavior of the existing structures. The latter statement is part of the limitations of the further proposed methodology. The data used for the buildings' representation with finite elements were gathered from descriptions in publications (Naeim, 1998) and from the CSMIP-3DV's database. In addition, basic engineering has been used to validate the results of the models. The buildings are described thoroughly in the next section.

As mentioned before, the finite element models went through a time history analysis using the recorded data from the sensors placed on the existing buildings. The finite element software calculated the displacements (1 vertical and 2 horizontal) at each joint of the building. The program coded by the author, takes the data from the finite element program and proposes where sensors should be placed in order to satisfy the cost and motion sensing efficiency requirements described previously. The program proposes exact 3D coordinates of the instrumentation schemes.

With the use of the above buildings as case studies and a mathematical sequence through MATLAB the author checks the validity of the current instrumentation schemes proposed by codes and organizations and proposes procedures for instrumentation.

3.2 Description of the Buildings Used

In this subchapter description of each building can be found. The description is related to the geometry, materials and cross sections used in the analyses models and their correlation with the real buildings. The following subchapters are named after the names of the buildings as used in this dissertation's analyses and in the publication by Farzad Naeim, "Performance of 20 extensively instrumented buildings during the 1994 Northridge Earthquake". The same nomenclature is used in CSMIP-3DV. The names are: Office 14 El Segundo, Hospital 5 San Bernardino and Parking 6 Los Angeles. Each name consists of three parameters. The first one describes the purpose of the building (e.g. Office: Office Building), the second states the number of floors and the third the location.

To check the validity of the finite element models, load combinations were imposed. The purpose of the imposed static analysis was to check for excessive displacements and members' forces. Under the load combination of 1.2D+1.6L (D:Dead load; L:Live load) the maximum calculated vertical displacement was 0.03ft or less, which is negligible considering all the uncertainties implemented in the models. Also the maximum member forces were under the elastic limit.

Wherever the description of the real building states ductile moment resisting steel frames, ductility on the finite model was not imposed. Ductility has not been imposed due to the lack of information regarding the existing buildings' properties. Furthermore, the literature states that a building's non-linear response can be adequately estimated by a "sequence of successively changing linear models" (Rojahn and Matthiesen, 1977). Hence, a linear behavior of a structure can be a useful tool for the estimation of the actual building's behavior.

3.2.1 Office 14 El Segundo

This building represents an office building located in El Segundo, CA. It has 14 floors above the ground. The existing building is a steel structure with concrete slabs. The gravity system constitutes of steel I shaped columns and concrete slabs with metal deck 7.25 inches thick in total. The lateral system is defined by chevron type braced frames at the cores of the building and ductile moment resisting steel frames at the perimeter. Due to the

unavailability of real data and drawings from the real building, the finite element model constitutes of:

1. W24X370 A992 steel cross section for the columns.
2. W30X170 A992 steel cross section for the girders.
3. W18X143 A992 steel cross section for the beams.
4. 7.5in thick 4000 psi concrete slabs.
5. HSS14X0.375 A992 for the chevron type braced frames.

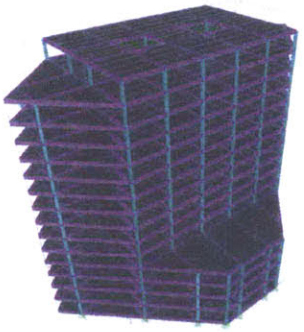

Figure 3-1: Office 14 El Segundo Perspective View

Figure 3-1 shows the modeled building in the finite element software (SAP2000). Each color represents a structural element with different purpose (e.g. pink are the girders, light blue are the columns).

Figure 3-2 shows the value of the period in seconds for each of the first 10 modes. The results derived from an eigenvector modal analysis with the use of the finite element software. The first mode has a period of 1.88 seconds, followed by the second mode with 1.875 seconds. This shows the close correlation between the first two modes. The first mode is a torsional one. The second mode has movement of the building along the East-West axis. The third mode has a period of 1.73 seconds with a building's motion along the North-South axis with a slight torsion.

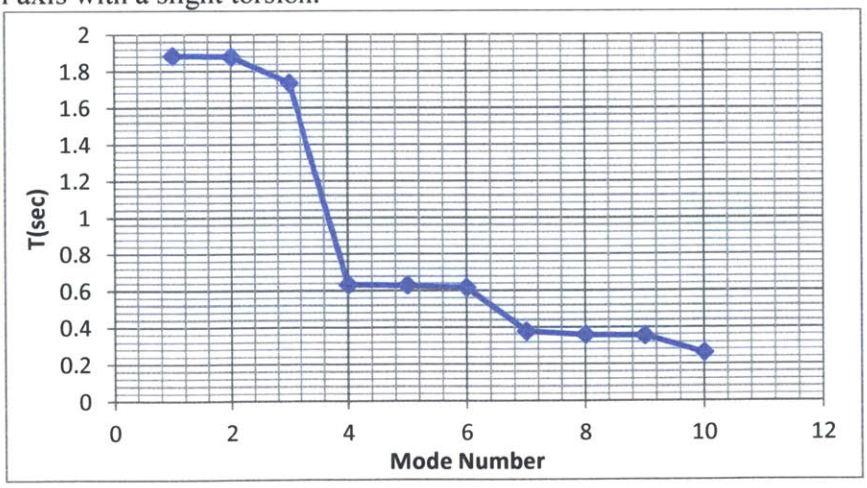

Figure 3-2: Periods of the first 10 modes (Office 14 El Segundo)

Regarding instrumentation, the existing building is instrumented with 16 sensors placed along the height of the structure. More information regarding the instrumentation of the existing building can be found in Appendix I.

3.2.2 Hospital 5 San Bernardino

This building represents a Hospital in San Bernardino with 5 stories. The building is a steel frame building with concrete slabs and ductile moment resisting steel frames in both directions. The finite element model of the building constitutes of:

1. W18X131 A992 steel cross section for the columns of the lateral framed system.
2. W30X173 A992 steel cross section for the girders.
3. W24X76 A992 steel cross section for the beams.
4. 6in thick 4000 psi concrete slabs.

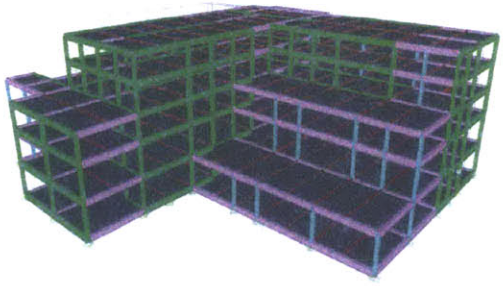

Figure 3-3: Hospital 5 San Bernardino Perspective View

Figure 3-3 shows the model of the building in the finite element software. The green colored elements represent moment resisting frames. These frames are the lateral resisting system of the building.

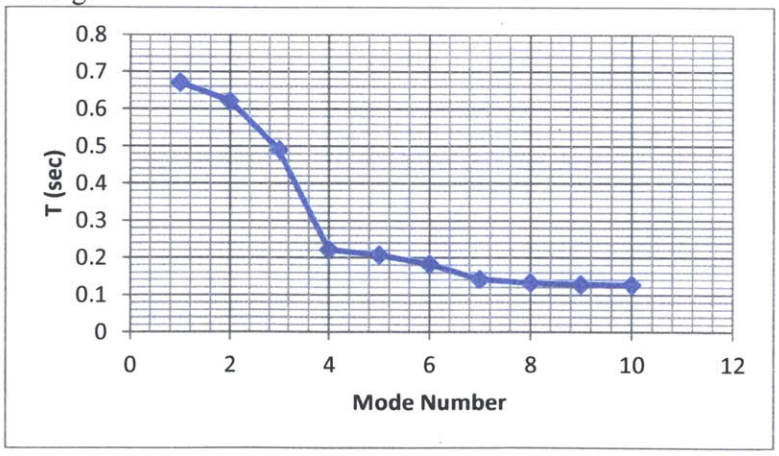

Figure 3-4: Periods of the first 10 modes (Hospital 5 San Bernardino)

Figure 3-4 shows the value of the periods for each mode. The values were calculated by the finite element program using a modal analysis. The first period is approximately 0.67 seconds and has a movement along the East-West axis. The second mode has a period of 0.62 seconds and has a movement along with the North-South axis with a slight torsion due to the irregular shape. The third period has a period of 0.5 seconds and is purely torsional.

Regarding instrumentation, the existing building is instrumented with 12 sensors placed along the height of the structure as shown in Appendix I.

3.2.3 Parking 6 Los Angeles

This building represents a parking structure with 6 stories located in the area of Los Angeles. The building is a concrete frame structure with shear walls for its lateral system. The finite element model constitutes of:

1. 25cmX50cm 4000 psi reinforced concrete girders (25cm is the width and 50cm the height of the girder.
2. 50cmX50cm 4000 psi reinforced concrete columns.
3. Six 14in thick, 32ft 6in long shear walls in the North-South direction.
4. Two 16in thick, 72ft long shear walls in the East-West Direction.

No reductions in the area and stiffness of the elements have been imposed on the model. Concrete is assumed to behave within the elastic region keeping the whole cross sectional area of the beams and columns effective.

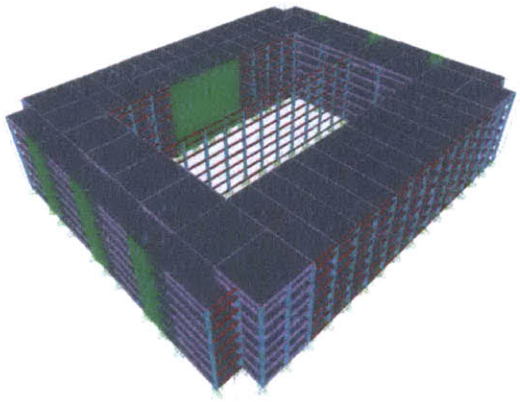

Figure 3-5: Parking 6 Los Angeles Perspective View

Figure 3-5 shows the finite element model of the building described in this section. The green color indicates the shear walls in both directions. These shear walls represent the main lateral resisting system of the building.

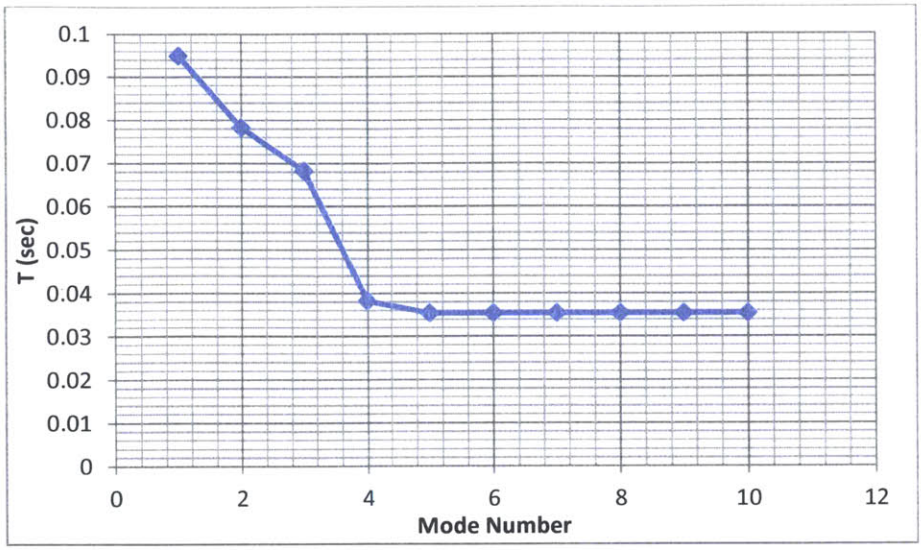

Figure 3-6: Periods of the first 10 modes (Parking 6 Los Angeles)

Figure 3-6 depicts the value of period in seconds for each mode. The first mode has a period of approximately 0.11 seconds and is described by a rocking movement along the East-West axis with the addition of a slight torsion. The second mode has a period of 0.10 and has purely lateral movement along the North-South axis. The third mode has a period of 0.085 seconds and has similar behavior as the first mode, but with more torsion. As it is shown by the modal analysis the structure is quite stiff. This probably has to do with the long shear walls that constitute the lateral resisting system of the building. Modes above the third are local modes and have almost the same period. This will probably lead to an instantaneous excitation of several high order modes.

Regarding instrumentation, the existing building has 14 sensors placed along its height. Details can be found in Appendix I.

3.3 Steps of analysis

This section describes how results are extracted from the finite element model in order to be used in MATLAB for the calculation of optimal instrumentation schemes. The information extracted from SAP2000 refers to the maximum and minimum displacements and rotations of the joints or nodes of the finite element model. In this thesis a joint and a node have the same properties and refer to the end points of the finite elements.

As it was mentioned in previous chapters, the analyses are based on results derived from time history analyses. In order to proceed with a time history analysis a numerical step-by-step representation of the excitation (earthquake) is needed. In this dissertation the Northridge earthquake is taken into account. Therefore, every finite element model executed in this dissertation has been excited by the Northridge earthquake as it was recorded by sensors placed at the base of the actual buildings. These data have been retrieved by the database of the CSMIP-3DV program, produced by Naiem. The database categorizes the data with respect to the channel they were retrieved from. Channels represent the directions where the sensors recorded data. For example an orthogonal tri-axial sensor has three channels that record data with respect to three orthogonal axes (i.e. X Y and Z). Particularly, for:

1. Office 14 El Segundo data from channel 5 and from channels 3 and 4 were used for excitation along North-South and East-West axis respectively. The acceleration imposed on the structure in either North-West or East-West direction was divided into 15001 steps equally spaced at 0.01 seconds.
2. Hospital 5 San Bernardino data from channel 2 and from channel 3 and 4 were used for excitation along North-South and East-West axis respectively. The acceleration imposed on the structure in either North-West or East-West direction was divided into 10001 steps equally spaced at 0.01 seconds.
3. Parking 6 Los Angeles date from channel 3 and 4 and from channel 2 were used for excitation along North-South and East-West axis respectively. The acceleration imposed on the structure in either North-West or East-West direction was divided into 6001 steps equally spaced at 0.01 seconds.

Where data from 2 channels were available along an axis, the time history analysis used the average of the data values in that direction. This of course can be used only when the recorded data have the same total duration and time intervals. The data provided by the sensors have units of cm/sec^2. The graphical representation of the excitation can be found in Appendix II.

After running the structures through a time history analysis in North-South and East-West directions, the information regarding the displacements of each node at the structure was extracted. To reduce computational power, only the maximum and minimum rotations and displacements along global X and global Y axis of each joint have been taken into account. The displacement data and the coordinates of each joint were exported in spreadsheets for further analysis using the program written in MATLAB.

3.4 Data processing – information extraction

The following section provides the methodology and mathematical background of the program the author created in MATLAB for the optimization of the placement of sensors. The MATLAB code is shown in Appendix VII.

3.4.1 Description of the Algorithm - Flow Chart

This section contains a description of the algorithm and methodology used to propose optimal instrumentation schemes. The description is depicted as a flow chart in Figure 3-7. Each step of the methodology is assigned with a small letter in an orange circle. All the step names mentioned in the description refer to Figure 3-7. The data processing starts with the implementation of an earthquake (the Northridge earthquake in this case) to the model through a time history analysis. This step is shown in "a". Through the time history analysis the horizontal displacements of each joint on the structure are calculated, as shown in step "b". The displacements u and v refer to maximum displacement along the horizontal X and Y axis respectively. The information extracted by the time history analysis is saved in Table 1, as shown in "c". Using the displacements of each joint from Table 1 the displacement of the reference point is calculated, as shown in "d". The reference point in this methodology is the geometric center of each floor slab. In step "e" the maximum and minimum displacements along the horizontal global X and Y axis of the geometric center are saved in Table 2. Furthermore, the rotation of the geometric center of each floor is saved in Table 2.

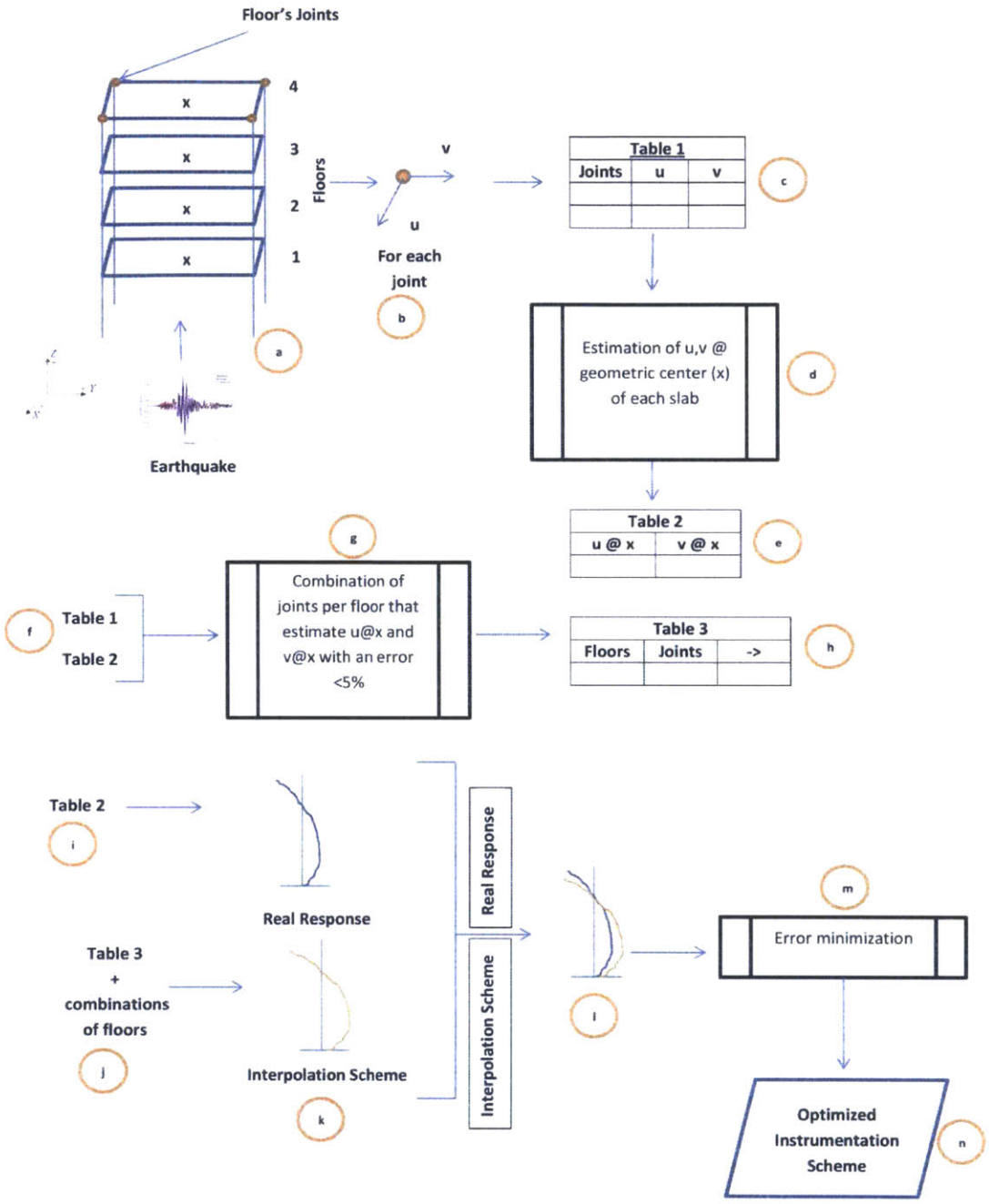

Figure 3-7: Algorithm's Flow Chart

At steps "f" and "g" the methodology uses the data in Table 1 and Table 2 to estimate which combination of joints on each floor estimates the displacements and rotation of the geometric center with a difference of 5%. The difference of 5% is with respect to floor slab's motion calculation when all the joints of the slab are instrumented. At step "h", the labels of the number of joints that satisfy the previous criteria are saved in Table 3. To summarize, the algorithm until step "h" has the exact motion of each floor slab as

displacements with respect to the geometric center of each slab saved in Table 2. Moreover, Table 3 possesses which joints should be instrumented on every floor in order to provide estimation under 5% of the displacements with respect to the geometric center as saved in Table 2.

Furthermore, using Tables 2 and 3 from step "i" and "j" the responses of the model are calculated at step "k". The algorithm calculates two forms of responses. The first one is called *Real Response* and it is calculated with the use of the data from Table 2. The second form is called *Interpolation Scheme*. This form is calculated by taking all the possible combinations of instrumented floors. The algorithm considers always that the ground floor and the roof are always instrumented. An example of a possible instrumentation combination for a 10-storey building is ground floor, 3rd floor, 8th floor and the roof. The displacements of the floor that are not instrumented are calculated using a cubic spline interpolation. By comparing all the possible floors' instrumentation scheme combinations with the real response, as shown in "l", the scheme with the least cost and the least amount of error is selected, as shown in "m". Finally, the algorithm proposes one instrumentation scheme for excitation of the model along the North-South direction and one for excitation along the East-West direction.

3.4.2 Geometric Center

Since the displacements and rotations were calculated in a finite element program for each joint on each floor, a point of reference should be found in order to calculate the motion of each floor slab. Taking into consideration that the inertia forces from a time history analysis are applied to the center of mass of each floor slab, and that the appropriate point on the floor slab to calculate the displacements of the slab is the center of stiffness (Chopra, 1995), a more general point should be found to represent the total movement of the floor slab. This reference point should overcome parameters (e.g. the cross section of the girders and columns of building) that correlate with the mass and stiffness of the structure. Hence, the geometric center of the floor slab has been selected. The geometric center of each floor slab does not take into account any mass or stiffness parameters. It is calculated based on the coordinates of the joints that constitute the floor slab. This point has also been selected for the production of CSIMP-3DV software (Naeim et al., 2004). As mentioned in the previous chapter, the coordinates of each joint on each floor has been extracted from the finite element program. The geometric center of each slab can be calculated as follows:

$$X_{c,i} = \frac{1}{n}\sum_{j=1}^{n} X_{ij} \qquad \text{Eq. 3.1}$$

$$Y_{c,i} = \frac{1}{n}\sum_{j=1}^{n} Y_{ij} \qquad \text{Eq. 3.2}$$

Where:
i: the number of the floor,
j: the number of joint on floor i,
n: the total number of joints on floor i,
$X_{c,i}, Y_{c,i}$: The coordinates of the geometric center of floor i.

When the coordinates of each floor are calculated they are assigned in matrix with all the necessary information for each floor. The information includes the number of joints per floor, the horizontal coordinates of the geometric center of each floor and the vertical coordinate (height) of each floor.

$$[FloorInfo] = [Number\ of\ joints;\ X_c;\ Y_c;\ Z_c] \qquad \text{Eq. 3.3}$$

3.4.3 Calculation of the displacement of the geometric center

To proceed with the analysis the horizontal displacement of each floor slab at its geometric center should be calculated. The following equations show how the rotation and horizontal displacements of each floor slab are calculated.

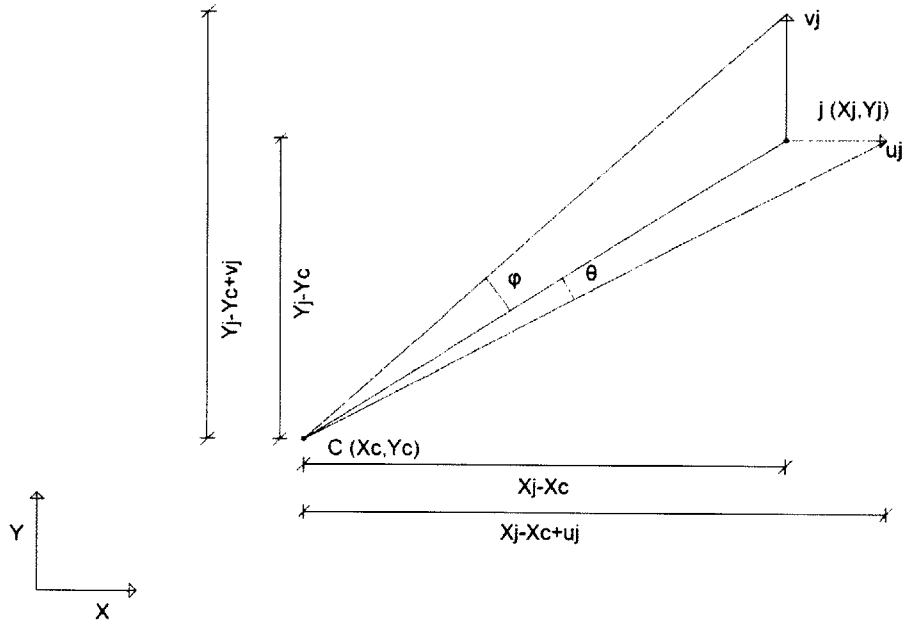

Figure 3-8: Rotation calculation scheme

The figure above shows the rotation of the geometric center C due to horizontal and vertical displacement u and v respectively of an arbitrary joint j.

$$\theta_{ij} = \tan^{-1}\left(\frac{X_{ij}-X_{c,i}+u_{ij}}{Y_{ij}-Y_{c,i}}\right) - \tan^{-1}\left(\frac{X_{ij}-X_{c,i}}{Y_{ij}-Y_{c,i}}\right) \qquad \text{Eq. 3.4}$$

$$\varphi_{ij} = \tan^{-1}\left(\frac{Y_{ij}-Y_{c,i}+v_{ij}}{X_{ij}-X_{c,i}}\right) - \tan^{-1}\left(\frac{Y_{ij}-Y_{c,i}}{X_{ij}-X_{c,i}}\right) \qquad \text{Eq. 3.5}$$

$$\omega_{c,i} = \frac{1}{n}\sum_{j=1}^{n}(\varphi_{ij} - \theta_{ij}) \qquad \text{Eq. 3.6}$$

Eq. 3.4 to Eq. 3.6 refer to the calculation of the rotation on floor i due to movement of joint j. Eq. 3.4 and Eq. 3.5 calculate the rotation angle of the geometric center due to a

displacement of a joint along the axes on the plane of the slab. θ_{ij} and φ_{ij} are shown in Figure 3-8. Where ω is the rotation of the geometric center of the slab of the floor *i*. As it is shown in Eq. 3.6 the rotation at the geometric center is considered as the mean of all the rotations of the geometric center due to displacement of the joints on each floor. The horizontal displacements of the geometric center derive as follows:

$$\begin{pmatrix} u_{c,ij} \\ v_{c,ij} \end{pmatrix} = \begin{bmatrix} u_{ij} & Y_{c,i} - Y_{ij} \\ v_{ij} & -(X_{c,i} - X_{ij}) \end{bmatrix} \begin{pmatrix} 1 \\ \omega_{c,i} \end{pmatrix} \quad \text{Eq. 3.7}$$

$$\begin{pmatrix} u_{c,i} \\ v_{c,i} \end{pmatrix} = \frac{1}{n} \sum_{j=1}^{n} \begin{pmatrix} u_{c,ij} \\ v_{c,ij} \end{pmatrix} \quad \text{Eq. 3.8}$$

Where:

$u_{c,ij}$: The horizontal displacement along the global X axis of the geometric center *c*, of the floor slab *i*, due to translation of joint *j*.

$v_{c,ij}$: The horizontal displacement along the global Y axis of the geometric center *c*, of the floor slab *i*, due to translation of joint *j*.

u_{ij}: The horizontal displacement along the global X axis of joint *j*, on floor slab *i*.

v_{ij}: The horizontal displacement along the global Y axis of joint *j*, on floor slab *i*.

$\omega_{c,i}$: The rotation angle at the geometric center of floor *i*.

$X_{c,i}$: The coordinate of the geometric center of floor *i* along the global X axis.

$Y_{c,i}$: The coordinate of the geometric center of floor *i* along the global Y axis.

X_{ij}: The coordinate of the joint *j* of floor *i* along the global X axis.

Y_{ij}: The coordinate of the joint *j* of floor *i* along the global Y axis.

The above equations provide the horizontal displacements at the geometric center of floor *i* as it is calculated by the horizontal displacements of the joints on floor *i* ($u_{c,i}$, $v_{c,i}$). The displacements of the geometric center of each floor slab are saved in a matrix.

3.4.4 Floor's joints combinations

Since the displacement of each floor's geometric center has been calculated, the next step finds how many and which joints on each floor provide a close estimation of the floor's geometric center displacements. Since the general scheme of this dissertation is optimization, an arbitrary selection of joints would not be appropriate. Therefore, all the possible combinations of joints on each floor have been taken into account. Each of the combinations is used to calculate the displacement at the geometric center on the examined floor slab. The analysis in the end, selects the first combination that has the least amount of joints and estimates the displacement of the geometric center of the examined floor with a difference less than 5% on both horizontal directions (global X and Y). The equations describing the procedure are the following:

$$[j^p] = \left[\binom{n_i}{1,2,3,\dots\dots n_i}\right] \quad \text{Eq. 3.9}$$

Eq. 3.9 creates a matrix with all the possible combinations of joints on each floor. Eq. 3.10 to Eq. 3.14 estimates the rotation and horizontal displacements at the geometric center considering the displacements of the proposed combination of joints. The

explanation of the parameters is the same as in subchapter 3.4.3, but with the additions of the superscript p which states the proposed joints.

$$\theta_{ij}^{p} = \tan^{-1}\left(\frac{X_{ij}^{p} - X_{c,i} + u_{ij}^{p}}{Y_{ij}^{p} - Y_{c,i}}\right) - \tan^{-1}\left(\frac{X_{ij}^{p} - X_{c,i}}{Y_{ij}^{p} - Y_{c,i}}\right) \quad \text{Eq. 3.10}$$

$$\varphi_{ij}^{p} = \tan^{-1}\left(\frac{X_{ij}^{p} - X_{c,i} + u_{ij}^{p}}{Y_{ij}^{p} - Y_{c,i}}\right) - \tan^{-1}\left(\frac{X_{ij}^{p} - X_{c,i}}{Y_{ij}^{p} - Y_{c,i}}\right) \quad \text{Eq. 3.11}$$

$$\omega_{c,i}^{p} = \frac{1}{n^{p}} \sum_{j=1}^{n^{p}} (\varphi_{ij}^{p} - \theta_{ij}^{p}) \quad \text{Eq. 3.12}$$

$$\begin{pmatrix} u_{c,ij}^{p} \\ v_{c,ij}^{p} \end{pmatrix} = \begin{bmatrix} u_{ij}^{p} & Y_{c,i} - Y_{ij}^{p} \\ v_{ij}^{p} & -(X_{c,i} - X_{ij}^{p}) \end{bmatrix} \begin{pmatrix} 1 \\ \omega_{c,i}^{p} \end{pmatrix} \quad \text{Eq. 3.13}$$

$$\begin{pmatrix} u_{c,i}^{p} \\ v_{c,i}^{p} \end{pmatrix} = \frac{1}{n^{p}} \sum_{j=1}^{n^{p}} \begin{pmatrix} u_{c,ij}^{p} \\ v_{c,ij}^{p} \end{pmatrix} \quad \text{Eq. 3.14}$$

$$e_{u,i}^{p} = \frac{\left|u_{c,i} - u_{c,i}^{p}\right|}{|u_{c,i}|} < 5\% \quad \text{Eq. 3.15}$$

$$e_{v,i}^{p} = \frac{\left|v_{c,i} - v_{c,i}^{p}\right|}{|v_{c,i}|} < 5\% \quad \text{Eq. 3.16}$$

Eq. 3.15 and Eq. 3.16 show the convergence of the displacement estimation of the geometric center of floor i using the displacement from the proposed combination. The value 5% has been selected to make the algorithm faster and to reduce the number of joints selected. The last has to do with cost feasibility. $e_{u,i}^{p}$ and $e_{v,i}^{p}$ refer to the displacement convergence values of joint i along the X and Y axis respectively. Joint i is part of the proposed combination of joints.

3.4.5 Estimating the global motion of the building

The previous subchapter shows the procedure to find which joints are the most appropriate to estimate the motion of the floor slab. By using these data, the next step is to estimate the global motion of the building along its height; i.e. find which combination of floors should be selected in order to estimate better the global response of the building. The algorithm produced by the author assumes that at least the base and roof of every potential instrumented building should always be instrumented (Huang and Shakal, 2002). The estimation of the building lateral motion is calculated by using the built-in cubic spline interpolation function of MATLAB. Cubic spline interpolation is used also in CSMIP-3DV (Naeim et al., 2004). To estimate which instrumentation scheme is the most appropriate, the least square method is used to compare all the possible combinations of floor instrumentation, as it is proposed by the literature (Safak, 2001).

The equation is the following:

$$LS_f(k) = \sum_{k=1}^{n_f} (U_c - U_f)^2 \qquad \text{Eq. 3.17}$$

Where:
LS_f: The least square value.
U_c: The displacements of the geometric center of each floor.
U_f: The estimation of displacements of the geometric center using the proposed floor instrumentation scheme.
n_f: The total number of combinations.

3.4.6 Dummy Variable and Final Selection

Obviously, the least square method provides as the best result the one that will have all the floors of the building instrumented. Although this is true, it is not optimal since the cost of instrumentation is significant and proportional to the number of sensors. Therefore, a dummy variable has been introduced in order to consider the best instrumentation scheme along the height, considering motion estimation and cost. The equation of the dummy variable is:

$$R = 3000 * n_f + LS_f(k) \qquad \text{Eq. 3.18}$$

The number 3000 represents the cost in USD of each sensor needed by the proposed scheme. The number 3000 has been taken into account considering publications regarding the cost of each sensor installed (Celebi, 2002). Due to the way the algorithm is designed, the instrumentation schemes proposed have different value of $LS_f(k)$ for the same number of required sensors. This leads the algorithm to propose for a specific cost value (e.g. 20,000 USD) different instrumentation schemes. Therefore, the algorithm did not consider the $LS_f(k)$ parameter for the instrumentation scheme proposal. To overcome this inefficiency the $LS_f(k)$ was added in the R variable.

By ordering the proposed floor instrumentation schemes in an ascending order based on the R value of each scheme, the program produces results that show which floors and where should be instrumented.

3.5 Assumptions and Limitations of the analysis

This section states the assumptions and limitations of the previous mathematical methodology. Some of the assumptions are based on researchers' work (Rojahn and Matthiesen, 1977).

3.5.1 Assumptions

1. The buildings behave in the linear elastic region. Structures may deform extensively in the inelastic region in order to dissipate large amounts of energy. Since the algorithm proposals are based on the displacements of elements, this assumption might affect the results of the algorithm since none of the potential inelastic displacements are considered.

2. Floor slabs are infinitely rigid diaphragms. This assumption restrains the movement of the joints assigned on each slab along the horizontal X and Y axes. The representation of floor slabs as rigid diaphragms is a common practice and it is used by engineers in practice; it is not always accurate though since slabs can have out of their plane displacements. Due to this assumption the algorithm does not proposes schemes for the estimation of motion of flexible slabs.
3. The models used for the analysis do not exactly represent the actual buildings stricken by the Northridge earthquake. This assumption reduces the validity of the comparison between instrumentation schemes of the existing buildings and the schemes proposed by the algorithm.
4. Soil-structure interaction is not taken into account. All the columns are fully fixed. Therefore, potential displacements due to soft subsurface or foundations failure are not considered. An algorithm that takes into account the soil-structure interaction might propose different instrumentation schemes than the ones the current algorithm proposes.
5. Calculating the displacement with respect to the geometric center of each slab is a sufficient method to estimate the real motion of the slab. As mentioned in previous sections the forces applied on structures due to seismic motion are applied to the center of mass of each slab. In addition, the calculation of the displacements of the joints assigned on each slab requires the estimation of the stiffness center of each floor. The use of the geometric center as a point of reference overcomes the need for calculation of the stiffness or mass center. If an algorithm uses one of the latter points as point of reference for the motion of each slab it might proposes different instrumentation schemes.
6. The maximum and minimum horizontal displacement along the X and Y axis happen at the same time. A joint on a slab does not necessarily have its maximum displacement along the X axis at the same point in time with its maximum displacement along the Y axis. Therefore, the implementation in the algorithm of the values of the displacement envelope for each joint might provide the algorithm with improper data. Hence, the instrumentation schemes might not estimate the motion of a building realistically.
7. The 5% convergence is sufficient for estimating the motion of the geometric center. This percentage is added to the algorithm to increase its calculation speed. A different percentage, for example 1%, might mitigate the error of the proposed instrumentation scheme, but in the same time increase the cost of the proposed schemes.
8. Cubic spline interpolation is the best way to describe the lateral motion of a building. This interpolation scheme was used based on the work of other researchers (Naeim et al., 2004). An algorithm with a different interpolation scheme may propose different schemes regarding cost and error values.
9. The roof and base of each building are always instrumented. This assumption is based on the literature (Huang and Shakal, 2002). An algorithm that does not imposes the necessity of the roof and base's instrumentation might produces different results. The difference is due to the interpolation scheme selected. If the roof and the base of a building are not always instrumented then the interpolation points change, hence, the instrumentation scheme changes.
10. The R parameter as described in Eq. 3.18 is an appropriate efficiency's comparison factor between instrumentation schemes. This assumption is quite critical since the results of the algorithm are based directly on it. A change of this parameter provides different results and therefore conclusions.

3.5.2 Limitations

1. The code might not work for inelastic behavior of the structure.
2. Soil-structure interaction is not taken into consideration.
3. The code uses the format extracted information that the finite element program used for the analyses provides.
4. The program does not take into account vertical movement of the floors.
5. Flexible floor slabs are not taken into consideration.

The above limitations and assumptions were used as a base for the preparation of the program in MATLAB. Some of them, such as the one regarding soil-structure interaction might be tackled by changing the code.

3.6 Comparison of the algorithm and current instrumentation procedures

As mentioned in previous sections, the algorithm proposes instrumentation schemes that use cubic spline interpolation to estimate the motion of each floor slab. In addition, the instrumentation schemes state clearly which floors should be instrumented and where on the floor should the sensors be placed. Furthermore, the algorithm can be implemented into a structural analysis software and propose instrumentation schemes after every modification of the structure.

On the contrary the UBC-1997 and CSMIP do not provide information regarding the exact position of the proposed sensors. Furthermore, the current procedures are not applicable to every structure. In chapter 2 the current instrumentation models are stated in Figure 2-1. From the comparison of the instrumentation in the aforementioned figures and the capabilities of the algorithm it is clear that the algorithm can be implemented in every building and propose to the engineer precise locations for sensor placement. The main advantage of the algorithm is that it provides the exact sensor placement coordinates, in a relative short period of time.

Nevertheless, the algorithm is a mathematical procedure that is based on specific assumptions and has several limitations. Therefore, the current procedures, especially CSMIP's procedures, can be used to validate qualitatively the schemes proposed by the algorithm.

3.7 Chapter Summary

This chapter starts with the presentation of the methodology the author uses in this dissertation. A description of the buildings' finite element representations is given. The models used in this dissertation are three in number and have the following code names: Office 14 El Segundo, Hospital 5 San Bernardino and Parking 6 Los Angeles. Furthermore, the steps of the analyses are stated. The chapter ends by stating the algorithm used for the calculation of the results in the Chapter 4 with mathematical equations in the order the algorithm uses them. The assumptions and limitations of the algorithm are also mentioned. Finally a comparison between the algorithm and the current instrumentation procedures is stated.

4 Results

The following chapter presents the results from the analyses described in the previous chapter. The results are plotted in two forms. The first one shows the displacements' envelope of the structure and which floors should be instrumented. The second shows where the sensors should be placed on the slab in order to effectively capture the motion. Furthermore, a comparison between the proposed schemes considering cost is showed with the help of plots.

4.1 Validation of motion calculation

In this section the results from the previous analyses are presented. The subchapter is organized in three sections. Each section describes one of the models analyzed in the previous chapter.

The graphs in the following subchapter are divided into two categories. One category describes the actual response of the building along its height and proposes which floors should be instrumented for better approximation of motion. The second category shows the plan views of the floors that need instrumentation. One plot per category is shown in this chapter. The rest of the plots can be found in Appendix III.

The graphs of the first category are called displacement envelopes, since they represent the maximum displacement calculated on the building. The horizontal axis states the displacement in centimeters (cm). The vertical axis states the Floor number. The blue line represents the building's response calculated when every joint of each floor is instrumented. Therefore, it can be said that the blue line represents the *Real Response* of the building calculated with respect to geometric center of each slab of the building. The plots' legend refers to the blue line as the *Real Response*. The red dashed line represents the estimation of the full motion of the building by instrumenting the floors indicated by black circles. The red dashed line derives from a cubic spline interpolation of the points shown in black circles. The plots' legend refers to the red dashed line as *Interpolation* and the black circles as *Instrumented Floors*.

The graphs of the second category show the floor plan of the proposed instrumented floors. These graphs do not include ground floor's instrumentation due to the assumption of a fully fixed base. Hence, the instrumentation scheme of the ground floor does not affect the results since the displacement of the ground floor is always zero. On these graphs each joint of the floor is represented with a blue dot. Although the joints are not connected with lines, the reader can clearly observe the general geometry of the floor plan. The horizontal axis states the X axis coordinate of the joints in meters (m). The vertical axis states the Y axis coordinate of the joints in meters (m). The proposed sensor coordinates are shown with a green circle and the word "Sensor" placed to the left of each circle. In addition, arrows are added at the position of the sensor to show in which direction the sensors should record data. Furthermore, the geometric center of the floor plan (and point of reference of the analysis) is shown with a red 'x' mark.

4.1.1 Office 14 El Segundo

This model was excited into two directions, along the North-South axis and along the East-West axis. The data retrieved from the finite element program were used to calculate the maximum displacement on the model. The displacement is shown in the figure below and the figures in Appendix III.

Figure 4-1 shows the displacement envelope for the excitation stated in the subtitle. Figure 4-2 shows the proposed instrumentation scheme of the 4th floor.

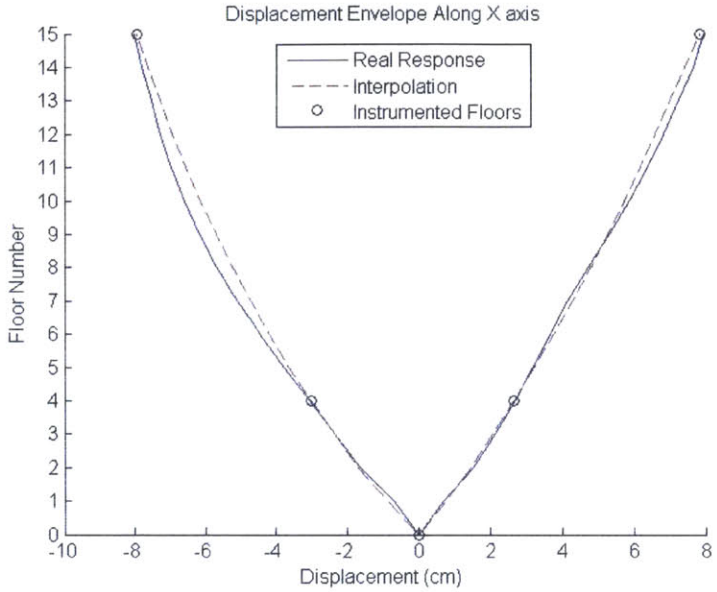

Figure 4-1: Excitation along the N-S direction

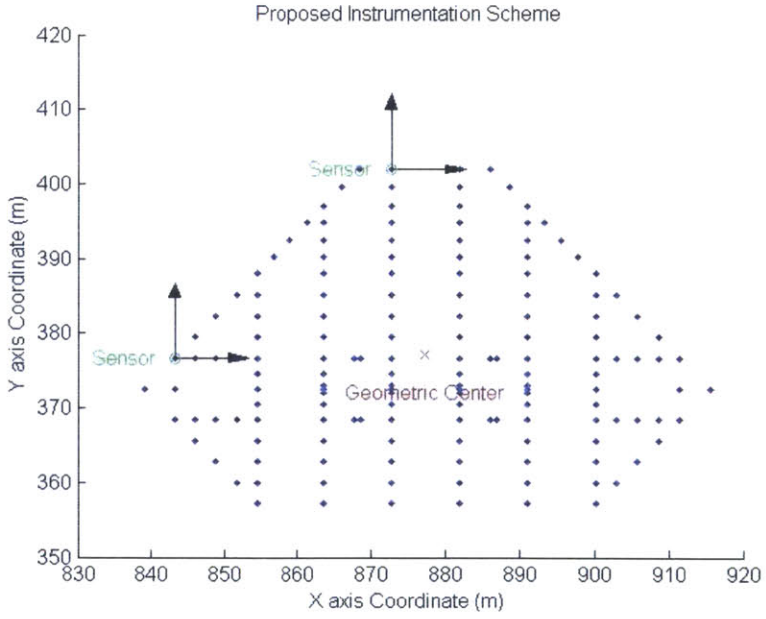

Figure 4-2: 4th floor - N-S excitation

As it is shown by the figures above and the figures in Appendix III the overall proposed instrumentation scheme includes the base floor, 2nd floor, 6th floor and the roof. The instrumentation of these floors according to the floors' instrumentation schemes described in Figure 4-2 and the figures in Appendix III, the estimation of motion is close to the motion of the full instrumented building.

The excitation of the building in the North-South direction shows that the displacements envelope affects the response in both directions X and Y of the plan of the building. This might have to do with the fact that the first three mode shapes of the building are close to each other as shown in Figure 3-2. For excitation at the East-West direction the building displacements envelope shows that the response of the building in the X direction is much smaller than in the Y. This might mean that the second mode of the building is dominant in this excitation direction.

The floor instrumentation scheme for the roof of this building is quite different for the two directions of excitation. The North-South excitation requires only two sensors to track the motion. The East-West excitation's scheme requires 4 sensors, and only one of them is the same with the ones proposed by the North-South Excitation's scheme.

4.1.2 Hospital 5 San Bernardino

This model was excited into two directions; along the North-South axis and along the East-West axis. The data retrieved from the finite element program were used to calculate the maximum displacements of the model. The displacements are shown in Figure 4-3 and the figures in Appendix III.

Figure 4-3 shows the displacements envelope for the excitation stated in the subtitle. Figure 4-4 shows the proposed sensors' placement scheme for the 2nd floor.

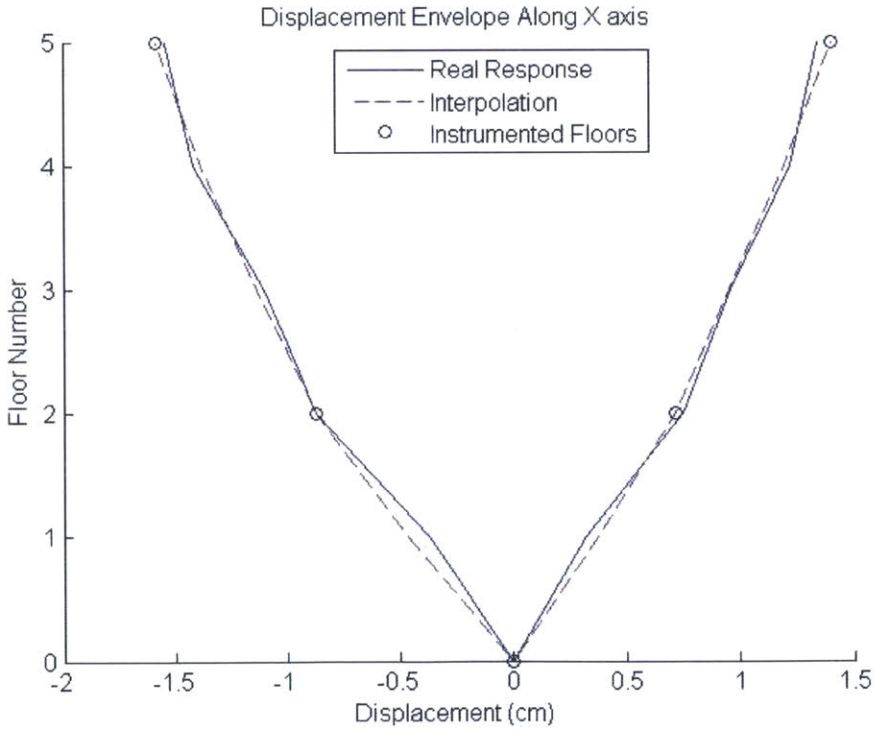

Figure 4-3: Excitation along the N-S direction

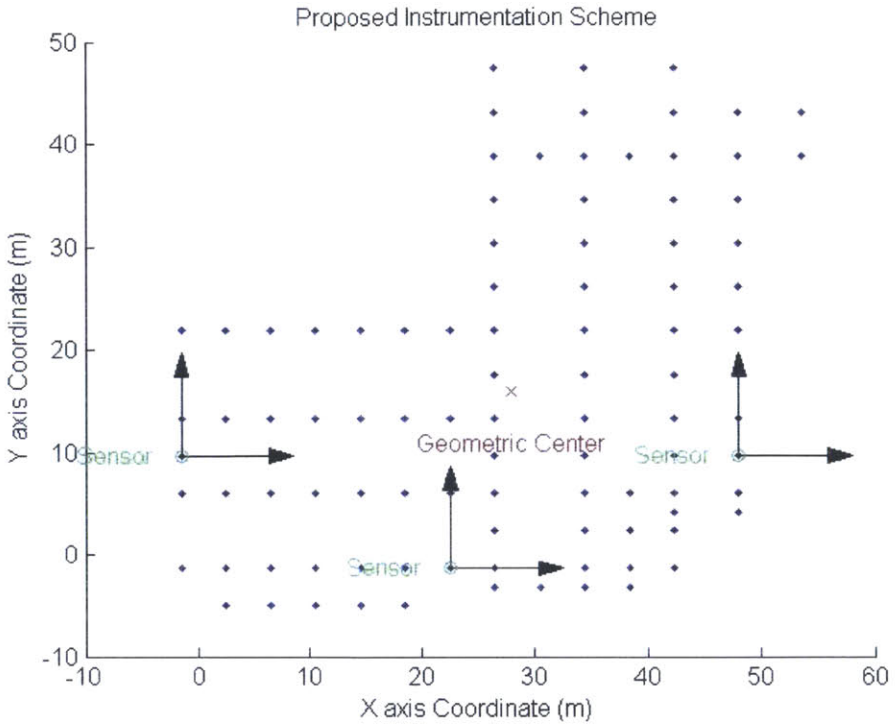

Figure 4-4: 2nd floor's plan view for N-S excitation

As it is shown by Figure 4-3 and the figures in Appendix III the overall proposed instrumentation scheme includes the base floor, the 2nd floor and the roof. The instrumentation of these floors, according to the floors' sensor placement schemes, estimates the motion of the model with the accuracy indicated in Figure 4-3 and the figures in Appendix III.

The excitation of the model in the North-South direction shows that the displacement envelope affects the response mainly in the X direction of the building. This might be caused by the excitation of mainly the 2nd and 3rd mode. For excitation at the East-West direction the model's response is mainly in the Y direction which means that the first mode is dominant during this behavior.

The floor instrumentation scheme for the roof of this building model is quite reasonable for the East –West excitation due to the fact that the lateral motion of the model is mainly in the Y direction. The proposed scheme for the North-South excitation has to do probably with the modes that constitute the overall behavior of the building. Since the 2nd and 3rd mode are probably the ones excited during North-South excitation and since these modes have torsional behavior, the proposed scheme seems reasonable. The scheme for the 2nd floor follows similar explanation as for the roof's instrumentation.

4.1.3 Parking 6 Los Angeles

This model was excited into two directions; along the North-South axis and along the East-West axis. The data retrieved from the finite element program were used to calculate the maximum displacements of the model. The displacements are shown in Figure 4-5 and the figures in Appendix III.

Figure 4-5 shows the displacements' envelope for the excitation stated in the subtitle. Figure 4-6 shows the proposed sensors' placement scheme for the 3rd floor.

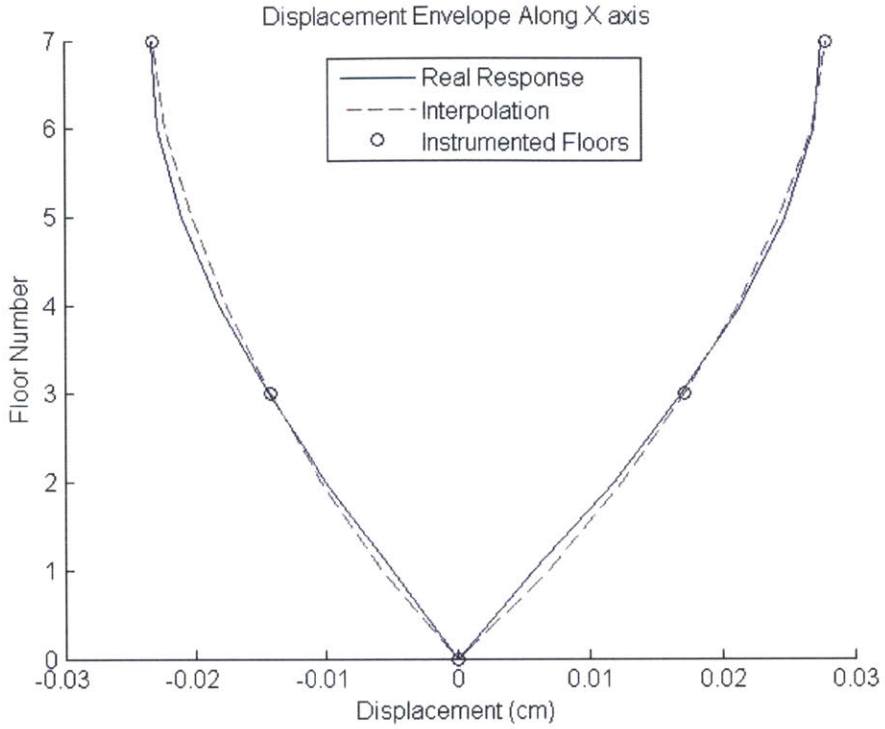

Figure 4-5: Excitation along the E-W direction

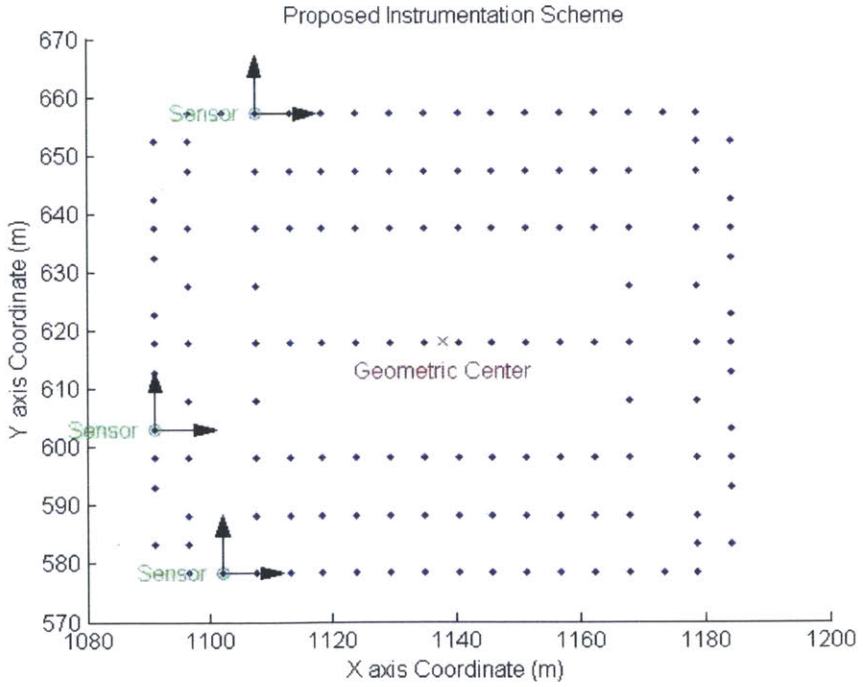

Figure 4-6: 3rd floor's plan view for E-W excitation

As it is shown in Figure 4-5 and the figures in Appendix III, the overall proposed instrumentation scheme includes the base floor, 2nd floor, 3rd floor and the roof. The instrumentation of these floors estimate the behavior of the building depicted in the plots. Generally the figures show that the building has increased stiffness. This can be derived from the fact that the displacement values are significantly small. A reasonable explanation is the large shear walls incorporated in this building.

The displacements envelopes show that the behavior of the building follows the excitation direction. This can be derived from the fact that the graph referring to the axis perpendicular to the excitation axis has very small values of displacement.

The floor instrumentation for the East-West excitation is the same for the roof and 3rd floor. The reason behind this might be that the excitation in this direction affects only the translational modes.

4.2 Comparison between proposed schemes

This section contains a comparison between the proposed instrumentation schemes and the instrumentation schemes of the existing buildings. Information regarding the instrumentation schemes of the existing buildings can be found in Appendix II. In addition, the proposed instrumentation schemes and the types of models used are compared. By proposed instrumentation scheme (or proposed scheme) the author describes the scheme that the algorithm proposes. By current instrumentation scheme (or current scheme) the author describes the instrumentation scheme of the existing buildings; these schemes can be found in Appendix II.

4.2.1 Office 14 El Segundo

The comparison between the respective figure from Appendix II referring to this building with Figure 4-1 and the respective figures of Appendix III indicates that, the number of floors proposed from the algorithm matches the number of floors that are currently instrumented. The current instrumented floors are the ground floor, 3rd floor, 8th floor and the roof. The proposed scheme includes the ground floor and the roof, but counter proposes the instrumentation of the 2nd and 6th floor. Considering the height of each floor as a percentage of the total building's height, the proposed scheme suggests instrumentation at 14.7% and 40.4% of the total building height. The current instrumentation scheme sets the sensors at the 21.1% and 53% of the total height. These results compared to the suggestions of the bibliography (Rojahn and Matthiesen, 1977) (25%,40% and 70%) for possible antinodes, provide similar values. Anti-nodes are points along the height of the building that never have zero displacement in modal analysis. Especially the proposed instrumentation scheme, hits the 40% suggestion by an offset of 0.4%. Although the literature provides suggestions on which floors should be instrumented to avoid nodal (zero displacement) nodes, the proposed instrumentation scheme shows other floors might be more appropriate for instrumentation.

Regarding the sensors' placement scheme on floors, the current instrumentation scheme has, for horizontal movement, 3 channels for the 3rd floor, 2 channels for the 8th floor and 3 channels for the roof. The proposed scheme requires 6 channels for the 2nd and 6th floor and 10 channels for the roof. The current instrumentation scheme is based on literature's suggestions that 6 channels per floor are capable to record the motion of the floor. Since the proposed instrumentation scheme calculates the position of the sensors considering the movement of the slab under a time history analysis, it can be assumed that the proposed instrumentation scheme might be more accurate.

4.2.2 Hospital 5 San Bernardino

The current instrumentation scheme for this building seems that it follows UBC-1997 suggestions ("Uniform Building Code Volume 2 - 1997," 1997); three instrumented floors, ground level, roof and a floor in the middle of the height. This scheme also derives from the algorithm written by the author. Figure 4-3 shows that the optimal floor instrumentation scheme is the one that includes the base floor, the 2nd floor and the roof for both excited directions.

The current instrumentation scheme has 3 channels on the base floor, 4 channels on the 2nd floor and 4 channels on the roof. The algorithm proposes 8 channels for the roof and 10 for the 2nd floor. The difference between the schemes might be explained by potential torsional motion that the algorithm detects during the time history analysis. Hence, it proposes more channels for better motion prediction.

4.2.3 Parking 6 Los Angeles

The instrumentation scheme implemented in this building constitutes by sensors on the base, 3rd floor and the roof. The algorithm proposes that the 2nd and 3rd floor should be instrumented in order to get better results regarding motion prediction.

Regarding the placement on the floor the current instrumentation scheme has 3 channels for the base floor, 3 channels for the 3rd floor and 4 channels on the roof. On the contrary, the proposed instrumentation scheme suggests 6 channels for the 2nd floor, 6 channels for the 3rd floor and 12 channels for the roof.

The difference between the proposed instrumentation scheme and the existing instrumentation might be explained by the torsional behavior of the 1st and 3rd mode of the model. Due to this behavior more floors need to be instrumented to adequately capture the motion.

4.2.4 Comparison between the models

The models of the analysis can be divided in three categories regarding the height, floor plan and main structural material. Office 14 El Segundo is a tall building, with pretty much normal floor plan shape and it is made out of steel. Hospital 5 San Bernardino is a short building made of steel with a floor plan similar to the Greek letter "Γ". Parking 6 Los Angeles is short in height, with a normal plan view and considered a concrete made building.

Office 14 El Segundo due to its height requires 2 floors between the roof and the base to be instrumented. Its difference from the rest buildings is that the height difference between the middle instrumented floors is larger.

The difference in the floor plan does not affect significantly the floor placement scheme since all the proposed schemes require sensors close to the perimeter and the geometric center of the building. The last observation does not agree with the parking structure since there are not any joints near the geometric center of the building.

The material of the buildings does not seem to affect the proposed instrumentation schemes. Since the analyses are based on the assumption of linear response of the elements the last observation is reasonable. Furthermore, a parameter that might affect the proposed schemes is the type of lateral resistance system.

4.2.5 Comparison between CSMIP-3DV and algorithm's proposed schemes

This section compares quantitatively the information extracted by CSMIP-3DV and the algorithm's proposes schemes. CSMIP-3DV is a software produced by Naeim and uses data recorded during the Northridge earthquake (and several other earthquakes) by the existing sensors in order to estimate the response of the buildings. In theory, the response indicated by CSMIP-3DV corresponds to the *actual behavior* of the building under a seismic excitation.

In addition, this section shows quantitatively the difference between the response produced by SAP2000 and the response produced by the interpolation of the proposed instrumented floors. All the information related to this section can be found in Appendix VI in the form of tables. Detailed explanation on how the tables are formed and shown is also stated in Appendix VI. Therefore, a description of the tables is not given in this section.

A general conclusion that can be derived by the tables in Appendix VI is that the finite element representations of the buildings do not represent the actual buildings, at least in the matter of lateral displacements under Northridge earthquake. The large differences in displacement were expected since the finite element models were modeled without any actual data from the buildings' blueprints. Due to the lack of blueprints the models (as described in Chapter 3) have structural elements' cross sections, material properties and loads that correspond to the author's engineering perception. Due to the large differences a quantitative comparison between the algorithm's optimization schemes' response and the CSMIP-3DV's response cannot take place.

Although a comparison between the CSMIP-3DV and the proposed instrumentation scheme is not valid; the tables show small and potentially acceptable differences between the SAP2000 response and the response produced by the proposed algorithm instrumentation schemes. The percentages of difference shown in the lower right corner of the tables are in most case in acceptable levels. Particularly, for the floors that the algorithm proposes for instrumentation (highlighted in yellow) the percentage of difference is 5% or lower. The latter observation shows that the equations that describe the algorithm (as shown in Chapter 3) function appropriately in MATLAB. Furthermore, the use of a cubic spline interpolation for the estimation of the response of the floors that are not instrumented indicates small differences. Hence, it could be said that a cubic spline interpolation is an appropriate method to describe a building's lateral displacement response. Equally important is the fact that the small percentages of difference between the algorithm's proposed instrumentation scheme and SAP2000 indicate that the algorithm works appropriately with SAP2000 (and possibly with other finite element software).

4.3 Optimized Instrumentation Schemes vs. Cost

This section contains a comparison of the efficiency of the algorithm towards the prediction of the models' motion under several earthquakes. The term efficiency correlates the accuracy of the motion prediction and the cost of instrumentation. The term accuracy describes the difference between the motion of a model predicted by an instrumentation scheme and the motion predicted by a fully instrumented model. Larger values of accuracy mean that the proposed schemes estimate better the motion. Smaller values of accuracy estimate the motion of the building in a worse way. The accuracy is represented in Figure 4-7 to Figure 4-12 with the factor *log(1/LSE)*.A fully instrumented model is the model that the displacements of the geometric center of each slab are calculated with the use of the

displacements of every joint on the floor. This model represents the benchmark for comparison with all the possible instrumented schemes.

To calculate the effectiveness of the algorithm on different earthquakes, the models stated in Chapter 3 have been imposed to time history analyses along their North-South and East-West axes. The time history analyses have been based on acceleration data retrieved from past earthquakes. The earthquakes considered are the following:

1. Imperial Valley, 1979.
2. Landers, 1992.
3. Loma Prieta, 1989.
4. Mammoth Lakes, 1983.
5. Mt. Lewis, 1986.
6. Northern California, 1975.
7. San Fernando, 1971.
8. Northridge, 1994.

The time history analyses provided the required by the algorithm input data, as described in Chapter 3. The algorithm uses the data to calculate instrumentation schemes based on its embedded mathematical equations. The algorithm calculates all the possible instrumentation schemes of floors. Each instrumentation scheme is assigned with an "accuracy" parameter and cost value. The accuracy parameter is described at the beginning of this section. The cost value is directly correlated to the number of sensors each instrumentation scheme requires. To estimate the effectiveness of the algorithm the results are plotted in Figure 4-7 to Figure 4-12.

The aforementioned figures indicate the lower values of LSE of all the possible instrumentation schemes with respect to each earthquake. The proposed schemes are plotted in the following figures as markers of different shape and color. Each shape and color represents a different earthquake. Details are shown in the legend of each figure. In addition, each data series of each earthquake is fitted with a trend line that has the largest R^2 factor. All the trend lines are polynomials.

Figure 4-7 and Figure 4-8 show the results of the Office 14 El Segundo model for excitation along the North-South and East-West direction respectively. Figure 4-7 shows that trend lines of the data start from lower values of accuracy for smaller cost. By increasing the cost of instrumentation (i.e. move along the horizontal axis) the accuracy of the schemes has higher values. The latter statement makes sense since the cost is directly correlated with the number of sensors. Therefore, schemes with more sensors predict more accurate the motion of a building. Nevertheless, it seems that the accuracy reaches a certain peak value for most of the earthquakes applied on the model. After the peak the accuracy remains approximately constant or it decreases slightly. For example, the Northridge's trend line increases until the cost value of approximately 60,000 USD. After that value the proposed schemes, although they have more sensors, estimate the motion of the model less accurate. In a similar way, Figure 4-8 shows that the accuracy increases with cost. The difference with Figure 4-7 is that the trend lines in Figure 4-8 increase their accuracy with a small increase of cost. A clear peak value cannot be derived. The accuracy of the instrumentation schemes remains approximately constant along the horizontal axis. Only the Northern California's instrumentation schemes increase their accuracy with the increase of cost.

Figure 4-9 and Figure 4-10 show the results of the Hospital 5 San Bernardino model for excitation along the North-South and East-West direction respectively. Figure 4-9 show more fluctuations of the accuracy compared to Figure 4-7 and Figure 4-8 as the cost

increases. The accuracy of the schemes proposed for Imperial Valley, Loma Prieta and Northridge are approximately constant along the entire horizontal axis. The data regarding the rest earthquakes show fluctuations in their accuracy along the horizontal axis. The most significant fluctuations are those of the Landers's data. Figure 4-10 indicates that the accuracy of the data of most earthquakes considered in the analyses is constant along the horizontal axis. Close observation reveals a slight increase of the accuracy as the cost of the instrumentation increases. The San Fernando and Northern California earthquakes do not follow the previous description. The data collected from these earthquakes increase their accuracy by increasing the cost.

Figure 4-11 and Figure 4-12 show the results of the Parking 6 Los Angeles model for excitation along the North-South and East-West direction respectively. Figure 4-11 shows that most of the instrumentation schemes increase their accuracy with increased cost. Nevertheless, the accuracy increment is not significant and it can be said that the accuracy remains constant along the horizontal axis. The Imperial Valley's data do not follow the previous observation since its trend line increases with cost. Figure 4-12 indicates that the accuracy of the data of most earthquakes used in the analyses remains constant, although a slight increase can be observed. As it is shown in Figure 4-12 the trend lines for Loma Prieta and San Fernando earthquakes show significant differences with respect to the other earthquakes' trend lines.

In general, Figure 4-7 to Figure 4-12 show that the algorithm can be used in earthquakes different than Northridge. The Northridge earthquake has been the base for the algorithm's design. The range of accuracy between different earthquakes as it is shown in Figure 4-7 to Figure 4-12 stays in the same order of magnitude. Therefore, the algorithm proposes instrumentation schemes that have almost the same accuracy for different earthquakes. The latter statement validates the use of the algorithm in earthquakes different than the Northridge.

Furthermore, Figure 4-7 to Figure 4-12 show that the increase cost and therefore the number of sensors, does not provide more accurate estimation of a buildings response. Even if most of the trend lines in the figures show an increase in the accuracy along the horizontal axis, the increase remains approximately constant after a certain cost value.

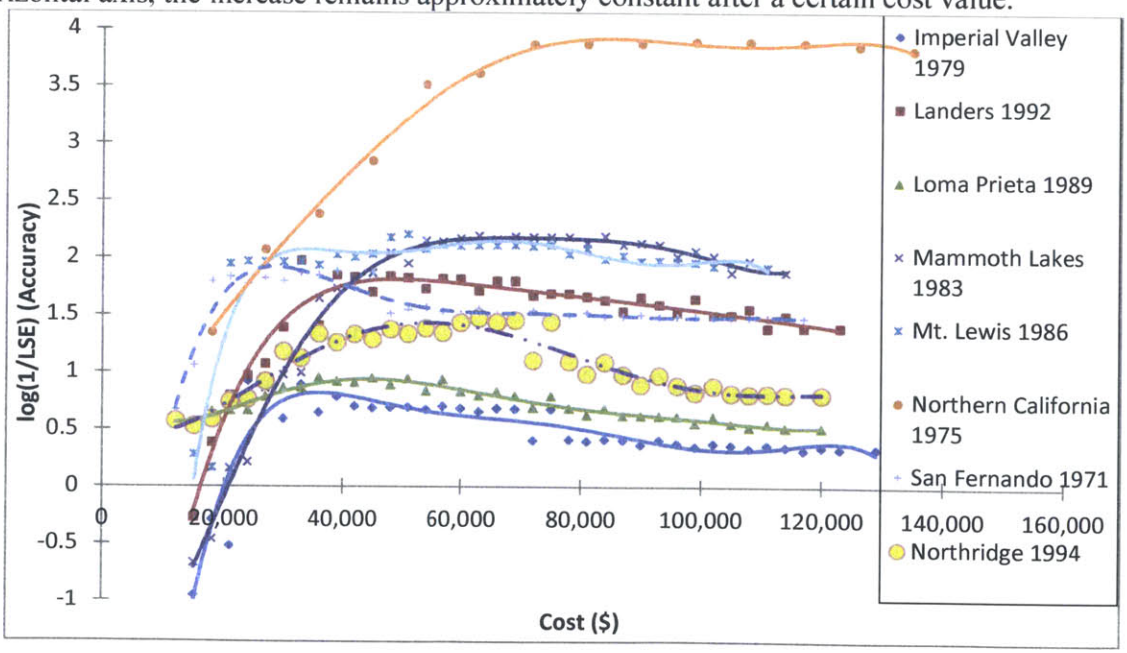

Figure 4-7: Accuracy vs. Cost - Office 14 El Segundo - NS Direction

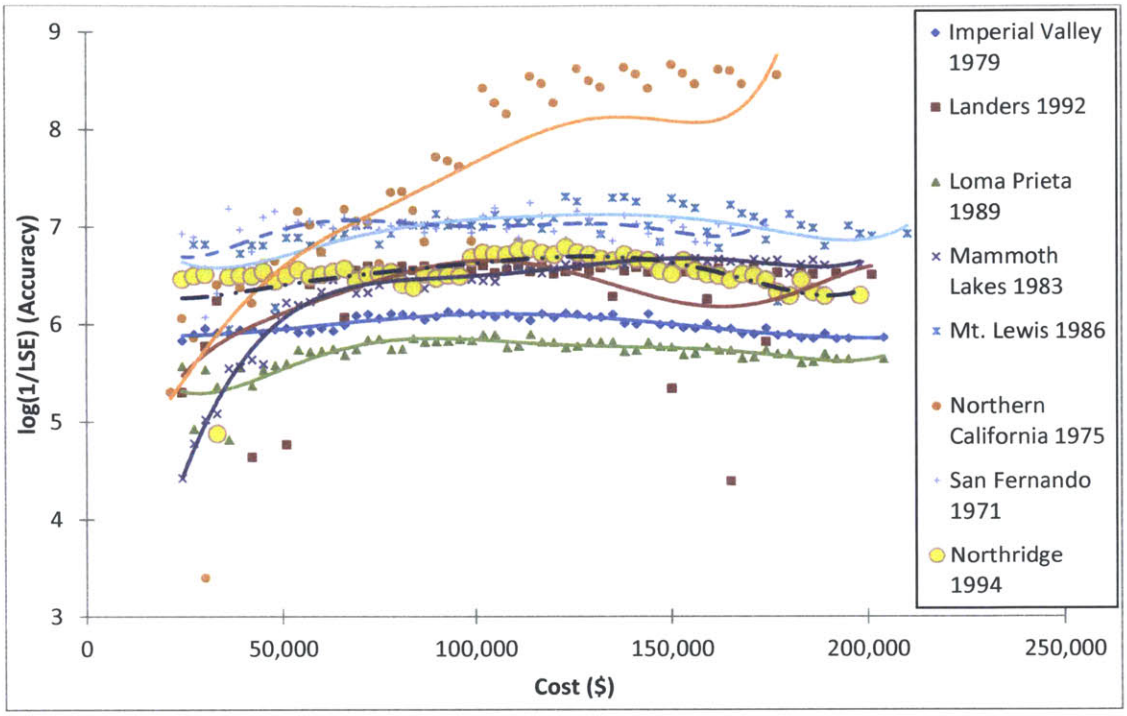

Figure 4-8: Accuracy vs. Cost - Office 14 El Segundo - EW Direction

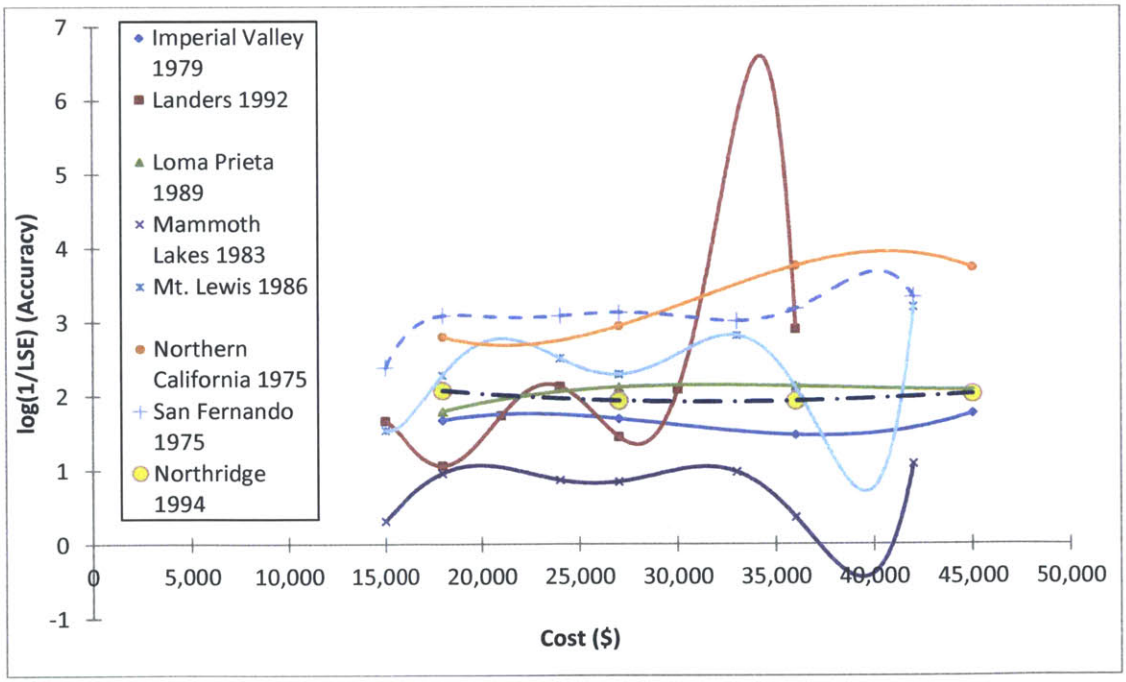

Figure 4-9: Accuracy vs. Cost - Hospital 5 San Bernardino - NS Direction

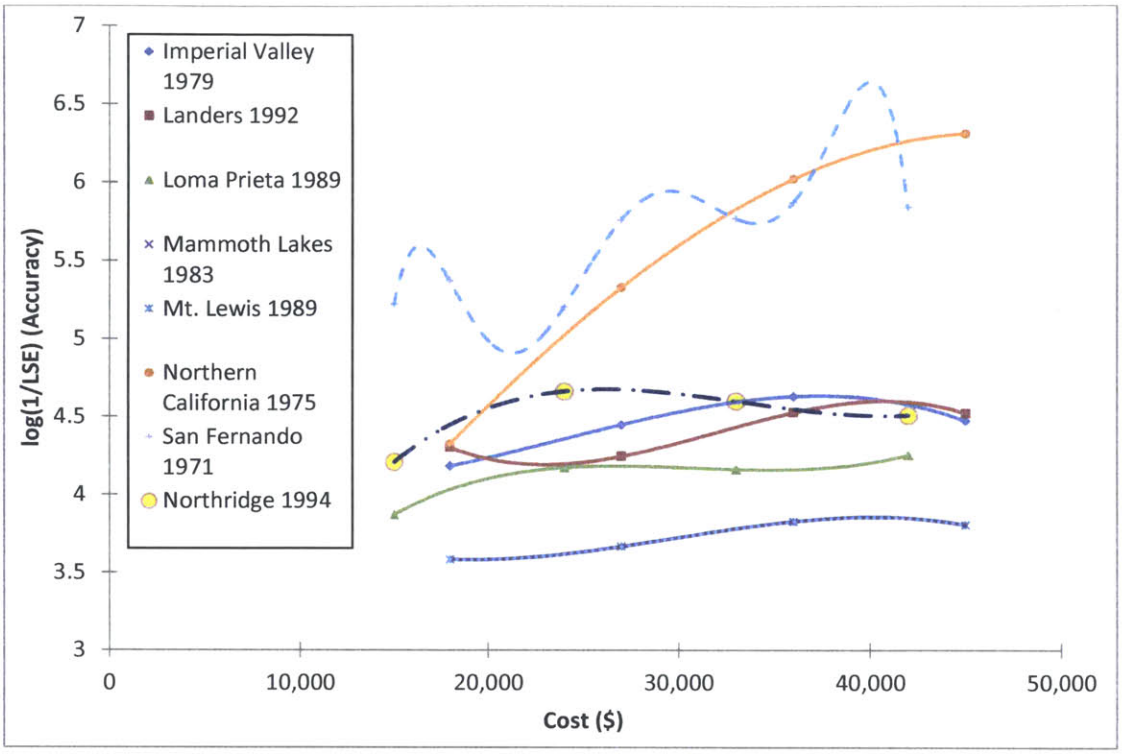

Figure 4-10: Accuracy vs. Cost - Hospital 5 San Bernardino - EW Direction

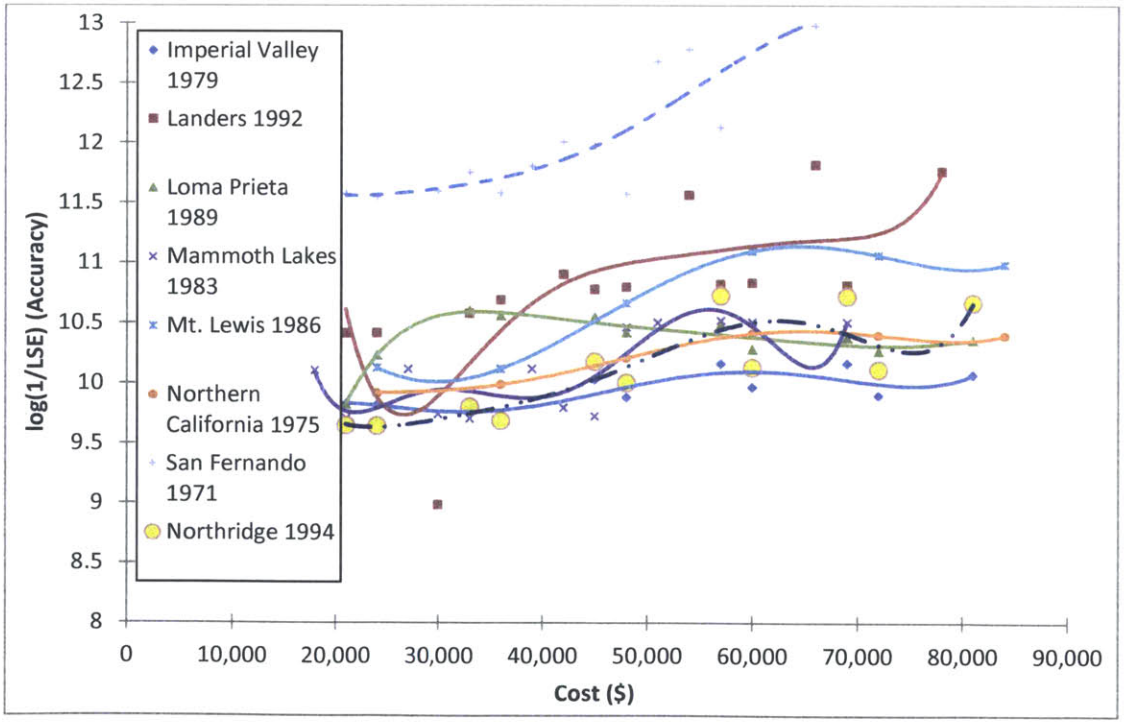

Figure 4-11: Accuracy vs. Cost - Parking 6 Los Angeles - NS Direction

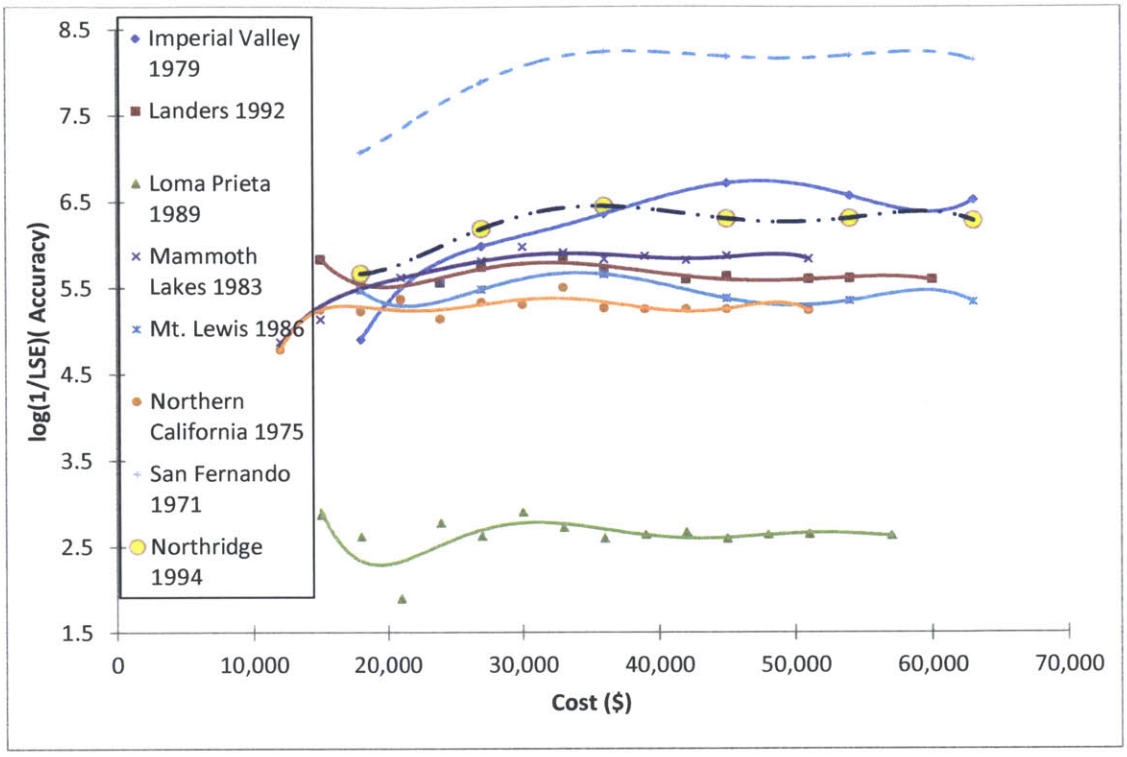

Figure 4-12: Accuracy vs. Cost - Parking 6 Los Angeles - EW Direction

4.4 Chapter Summary

This chapter shows the results of the analysis mentioned in Chapter 3. The results derived from the implementation of the author's algorithm with the use of MATLAB. The form of the results is in figures that show where sensors should be implemented along the height of a building and along the plane of the instrumented floor. Each instrumentation scheme is compared with the one shown in Appendix I. The proposed schemes clearly show that only 3 floors in a building should at least be instrumented in order to estimate the motion under a seismic event using cubic spline interpolation. In addition, figures were plotted that show a correlation between the motion estimation accuracy and the cost of instrumentation. The aforementioned plots might be a useful tool for building engineers with limitations towards the instrumentation budget.

5 Conclusions

This chapter starts with a summary of the dissertation and continues with the statement of the conclusions. In addition, limitations and further investigation proposals are mentioned.

5.1 Summary

This dissertation started with a discussion on the generation of earthquakes and how engineers account their effect on structures. Examples and equations are shown that describe the motion and effect of earthquakes using mathematics. In addition, examples and the aftermath of latter seismic events are stated. The introduction concludes with a short description of the general attributes and purpose of instrumentation in buildings.

The second chapter states the current procedures of instrumentation proposed by the current building codes or by state organizations (CSMIP). Furthermore, the theoretical background behind the proposed instrumentation procedures is stated. Also, an algorithm (Beck, 1978) for the calculation of an instrumentation scheme's efficiency is presented.

The third chapter introduces the reader to the procedure the author is going to use in the analysis. Data regarding the models used in the analysis are described. The chapter ends with the algorithm the author produced for the prediction and selection of instrumentation schemes, described with mathematical equations and geometric figures. The limitations and assumptions of the algorithm are also presented.

The fourth chapter presents the results of the analyses derived from the algorithm. The results constitute of figures that describe which floors should be instrumented and where should the sensors be placed on the floor slab in order to get better prediction. Furthermore, the results are plotted in figures that correlate the schemes' estimation accuracy and the cost of instrumentation. The latter results derived from the application of a number of different seismic events on the algorithm.

The fifth chapter presents the conclusions.

5.2 Conclusions

1. As it is shown by the floor instrumentation schemes, the shape of the building affects the placement of the sensors that calculate the real response of the building. Buildings with non-normal shape, such as Hospital 5 San Bernardino, require the placement of sensors on their far from the center sides in order to better calculate potential torsional motions.
2. All the models require 3 instrumented floors. These floors are the basement floor, the roof and one intermediate floor. By instrumenting three floors and using an algorithm embedded with cubic spline interpolation the real response of the building can be estimated.
3. As it is shown by Figure 4-7 to Figure 4-12 the instrumentation of more floors does not necessarily means that a better accuracy of a building's motion is estimated. The latter can be observed in Figure 4-7 to Figure 4-12 where for increased cost (hence, increase of the sensors placed) the accuracy calculated by the algorithm does not necessarily increases.

4. The selection of the intermediate floor should not be arbitrary. Therefore, the author proposes the use of algorithms in order to propose the exact or approximate position of the sensors.
5. The "Accuracy vs. Cost" figures show that the algorithm produced by the author provides almost the same accuracy of instrumentation in different earthquakes. Therefore, the algorithm can be used to propose instrumentation schemes.
6. The "Accuracy vs. Cost" figures presented can be a sufficient tool for a design engineer which has a specific amount of money to invest on instrumentation. Therefore, engineers can produce plots like the aforementioned using the algorithm proposed by the author or other algorithms in order to select the appropriate instrumentation scheme.

5.3 Limitations

The algorithm and the analyses presented are based on assumptions that limit the application of the algorithm to every building. These limitations are presented in the following bullets.

1. The analyses were conducted considering the models behave elastically. Obviously this is not the case in the real world where structures extend their behavior into the inelastic zone (Naeim, 1989). Therefore, the algorithm is only valid for elastic behavior of the structures.
2. The point of reference on each slab has been the geometric center of the slab. This scheme might not be the most appropriate point of reference since the forces generated by seismic excitation are usually applied in the center of mass of the floor slab (Chopra, 1995).
3. The algorithm considers that the maximum displacement over both horizontal axis coincide in time. This means that a joint on the building model must have at the same time the maximum displacement in the direction of X and Y axis.
4. The algorithm has been produced based on data received from the Northridge earthquake. Although the algorithm's behavior on different earthquakes has been checked; further changes in the code might be needed to make the algorithm "earthquake free".
5. The algorithm calculates the appropriate instrumentation schemes by considering that 5% of difference is the maximum needed for selecting which joints on a floor slab should be instrumented. This means that each proposed instrumentation scheme regarding the estimation of motion on each floor slab is in 5% or less difference of the motion calculated by the scheme that has instruments on each joint.
6. All the above instrumentation schemes are based on calculation of displacements. This might not be the case for an engineer that would like to base his/her instrumentation scheme on accelerations or velocities estimation.
7. The analyses do not take the effects of any soil-structure interaction or the effects that a seismic excitation potentially has on the soil that a structure is founded on.
8. The algorithm proposes optimized schemes with the assistance of the R factor (Eq. 3.18). This R factor correlates the cost of instrumentation with the motion prediction parameter $LS_f(k)$. This correlation might not be valid and therefore the proposed instrumentation schemes might not be optimal.

5.4 Further Investigation

The author proposes the following for further investigation:

1. Check of the validity of the assumptions the algorithm is based.
2. Enhance the algorithm to include vertical motions of slabs, flexible slabs and soil-structure interaction.
3. Expand the algorithm to include inelastic behavior of structures.
4. Lab tests of the results the algorithm proposes in order to estimate its validity quantitatively.
5. Model the buildings in a finite element program with the use of design information derived from the existing buildings' blueprints. Impose the algorithm on the more realistic models and then quantitatively compare the CSMIP-3DV' response with the algorithm's response.
6. Quantitated comparison of the algorithm's proposals with the instrumentation schemes proposed by UBS-1997 and CSMIP.
7. Research on the correlation between motion prediction and cost. This research should show the effect on instrumentation cost of a scheme that does not predicts appropriately the motion.

5.5 Further Thoughts

This dissertation provides an algorithm for the placement of sensors on buildings in order to better estimate a building's behavior under seismic excitation. The initial motivation of the author was to propose an optimization sequence for placing sensors in order to estimate damages under seismic events. Therefore, by using the algorithm of this dissertation or other algorithms derived from it, real time monitoring schemes can be established in buildings in order to estimate with precision and in short time the damage in a building. The knowledge of the damage in buildings may lead to speed up the alerting systems for evacuation after severe earthquakes. Furthermore, accurate prediction might lead to reduction of potential retrofit costs. Finally, the author would like to mention a fact that changed this dissertation's research direction. The author initially wanted to study instrumentation schemes for damage prediction in buildings. In order to check the validity of the proposed schemes real damage data from field investigations after seismic events were needed. Since, the state of California has a significant background in earthquake damage related studies; the author addressed the USGS for damage data in buildings. Although the researchers at USGS were eager to provide help, for which the author is grateful, damage data could not be retrieved for investigation because the damage data are held by the building owners for reasons that the author does not know (but can speculate). Therefore, the author proposes for the sake of academic research (or humankind prosperity) regarding severe and significant events such as earthquakes, data of buildings should be provided without any legal obstacles.

6 Bibliography

1. Anderson, J.C., 2001. Dynamic Response of Structures. The Seismic Design Handbook 185–246.
2. Beck, J.L., 1978. Determining Models of Structures from Earthquake Records. Earthquake Engineering and Structural Dynamics 8, 145–160.
3. Bolt, B.A., 2001. The Nature of Earthquake Ground Motion. The Seismic Design Handbook 1–45.
4. Celebi, M., 2001. Current practice and guidelines for USGS instrumentation of buildings including federal buildings, in: COSMOS Proceedings, Invited Workshop on Strong-Motion Instrumentation of Buildings, Emeryville, Ca.
5. Celebi, M., 2002. Seismic instrumentation of buildings (with emphasis on federal buildings). Special GSA/USGS Project, an administrative report.
6. Chopra, A.K., 1995. Dynamics of Structures: theory and applications to earthquake. Prentice-Hall, Inc.
7. Clough, R.W., Penzien, J., 1964. Dynamics of Structures. McGraw-Hill Book Co., Inc., New York, N.Y.
8. Huang, M., Shakal, A.F., 2002. CSMIP BUILDING INSTRUMENTATION MEASUREMENT OBJECTIVES AND MODELS, in: Invited Workshop on Strong-Motion Instrumentation of Buildings. p. 15.
9. Johansson, J., 2000. Kobe Earthquake, Japan 1995.
10. Kim, D.-H., Feng, M.Q., 2006. Real-time monitoring of structural vibration using a novel fiber optic accelerometer system, in: Diaz, A.A., Wu, H.F., Doctor, S.R., Bar-Cohen, Y. (Eds.), pp. 617801–617801–14.
11. Kircher, C.A., Nassar, A.A., Kustu, O., Holmes, W.T., 1997. Development of Building Damage Functions for Earthquake Loss Estimation. Earthquake Spectra 13, 663–682.
12. Lynch, J.P., Law, K.H., Kiremidjian, A.S., Kenny, T.W., Carryer, E., Partridge, A., 2001. The design of a wireless sensing unit for structural health monitoring, in: Proceedings of the 3rd International Workshop on Structural Health Monitoring. pp. 12–14.
13. McCormick, J., Aburano, H., Ikenaga, M., Nakashima, M., 2008. Permissible residual deformation levels for building structures considering both safety and human elements. 14th WCEE, Beijing, China.
14. McSaveney, E., 2012. Historic earthquakes - The 2011 Christchurch earthquake.
15. Naeim, F., 1989. The Seismic Design Handbook.
16. Naeim, F., 1998. Performance of 20 extensively-instrumented buildings during the 1994 Northridge earthquake. The Structural Design of Tall Buildings 7, 179–194.
17. Naeim, F., 2001. Design for Drift and Lateral Stability. The Seismic Design Handbook 329–372.
18. Naeim, F., Lee, H., Bhatia, H., Hagie, S., Skliros, K., 2004. CSMIP Instrumented Building Response Analysis And 3-D Visualization System (CSMIP-3DV), in: Proceedings of the SMIP-2004 Seminar.
19. Reinoso, E., Miranda, E., 2005. Estimation of floor acceleration demands in high-rise buildings during earthquakes. The Structural Design of Tall and Special Buildings 14, 107–130.

20. Rojahn, C., Matthiesen, R.B., 1977. Earthquake Response and Instrumentation of Buildings. Journal of the Technical Councils of ASCE.
21. Safak, E., 2001. Analysis of Earthquake Records from Structures: An Overview. Strong Motion Instrumentation for Civil Engineering Structures, Series E: Applied Sciences 373, 91–107.
22. Significant Earthquakes of the World, 1994.
23. Uniform Building Code Volume 2 - 1997, 1997.
24. Werner, S.D., Beck, J.L., Levine, M.B., 1987. Seismic Response Evaluation of Meloland Road Overpass using 1979 Imperial Valley Earthquake Records. Earthquake Engineering and Structural Dynamics 15.

Appendix I. Actual instrumentation schemes of the buildings

This Appendix shows the instrumentation scheme which is currently used on the buildings that this dissertation analyzed. The figures have been taken by the database of the CSMIP-3DV program that Dr. Farzad Naeim has produced. Information about the buildings is mentioned on the figures.

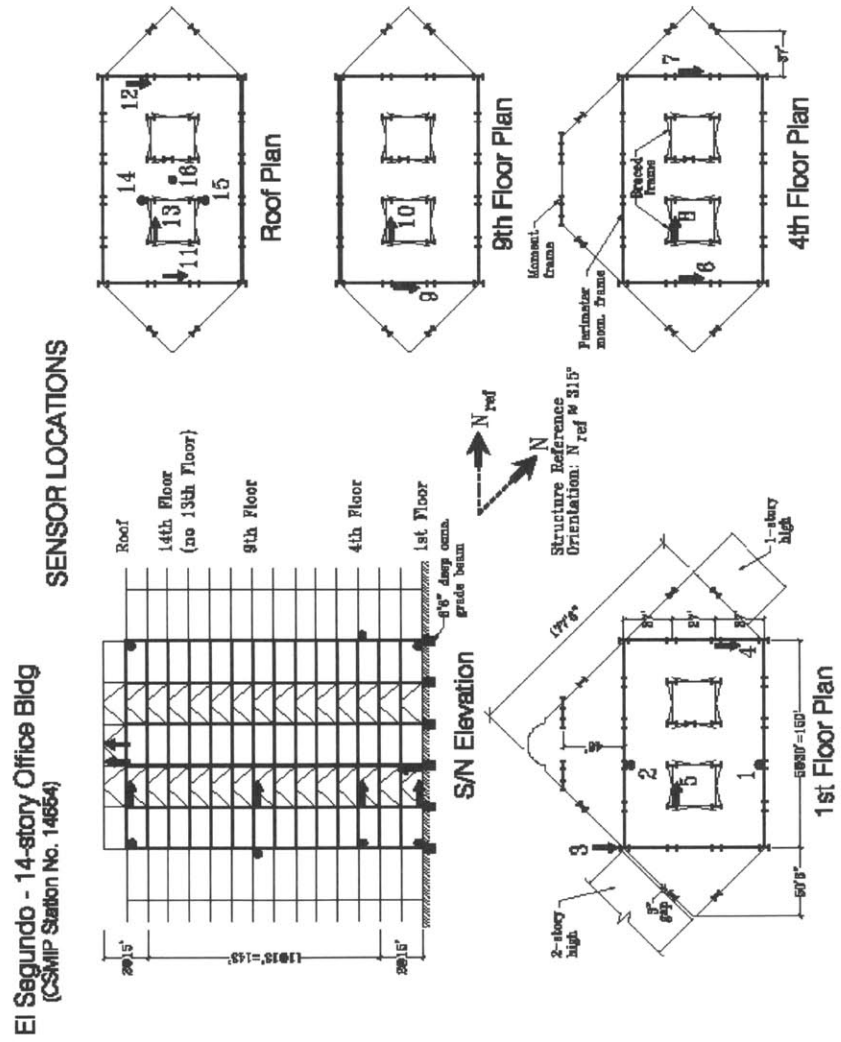

San Bernardino - 5-story Hospital

(CSMIP Station No. 23634)

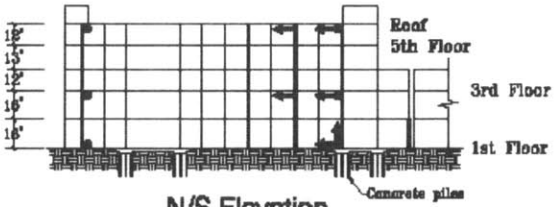

N/S Elevation

SENSOR LOCATIONS

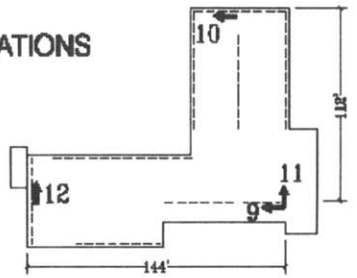

Roof Plan

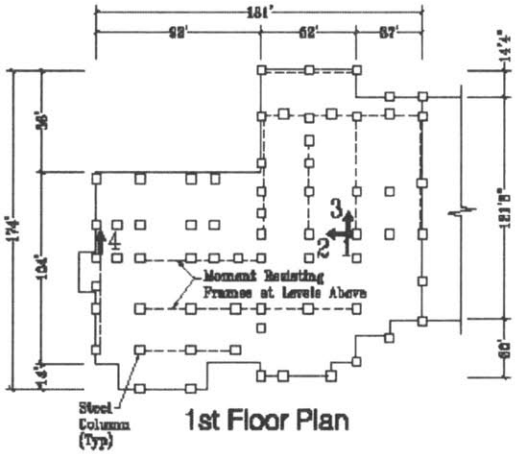

1st Floor Plan

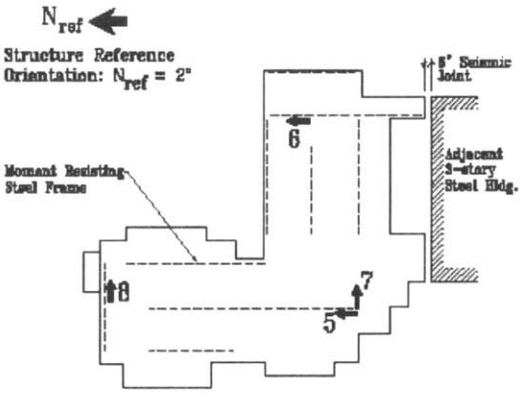

3rd Floor Plan

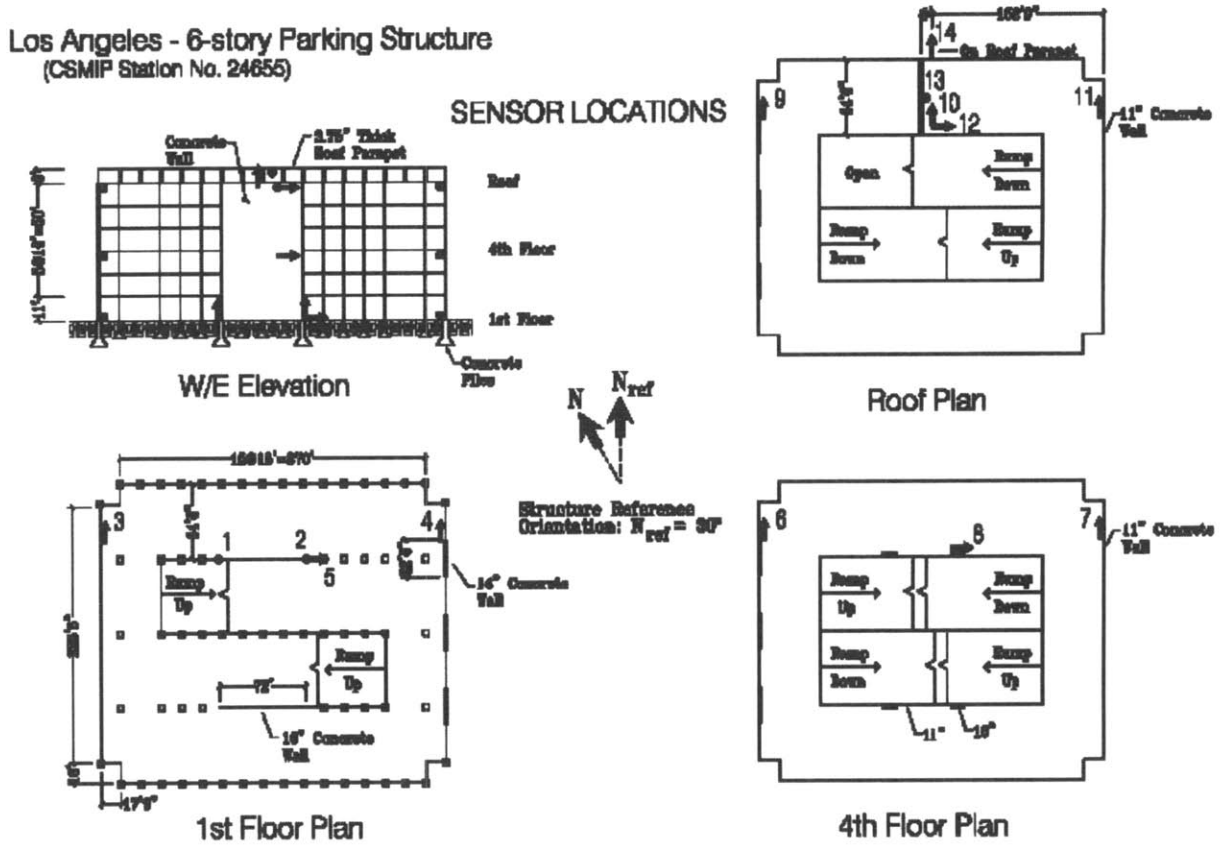
Los Angeles - 6-story Parking Structure
(CSMIP Station No. 24655)
SENSOR LOCATIONS
W/E Elevation
Roof Plan
1st Floor Plan
4th Floor Plan
Structure Reference Orientation: N_ref = 30°

Appendix II. Time History Graphs

This appendix provides information regarding the input acceleration at the base of each building analyzed in this dissertation. The information is given in the form of accelerographs. On the horizontal axis the duration of the recorded is stated in units of seconds. On the vertical axis the ground acceleration is stated in units of g. On the title of each accelerograph the channel that recorded the data is stated. Information on where the sensor embedded with this channel is placed can be found in Appendix I.

Office 14 El Segundo

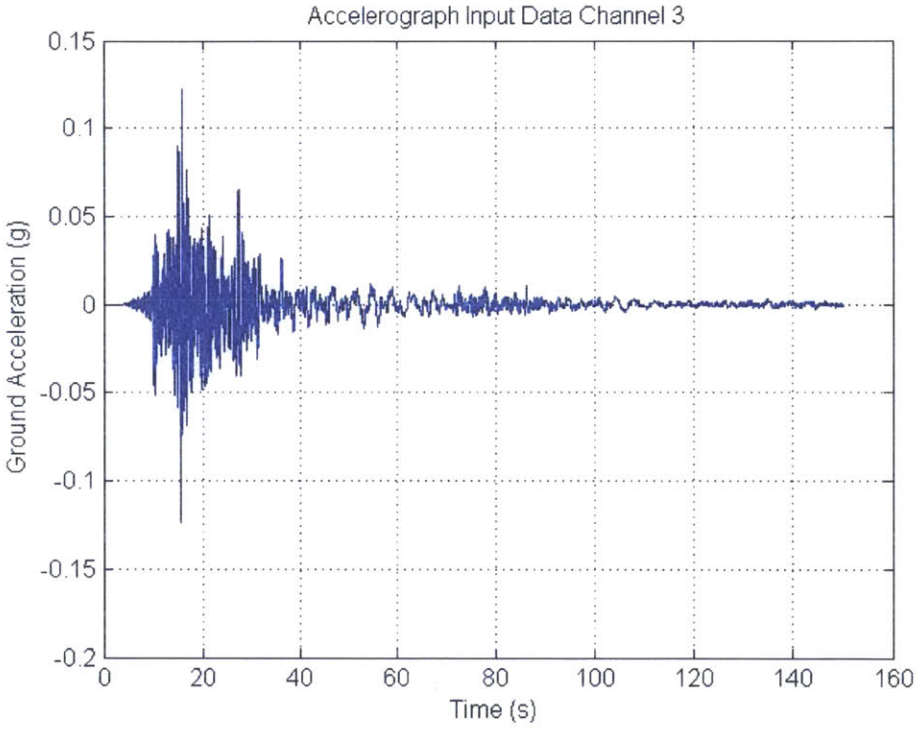

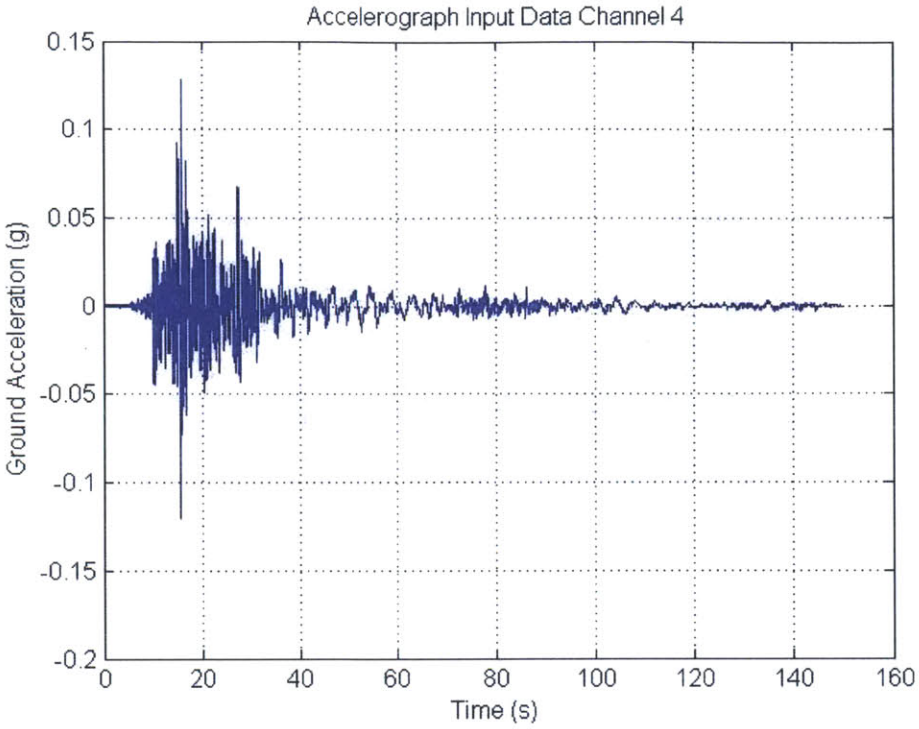
Accelerograph Input Data Channel 4
Ground Acceleration (g)
Time (s)
0.15
0.1
0.05
0
-0.05
-0.1
-0.15
-0.2
0
20
40
60
80
100
120
140
160

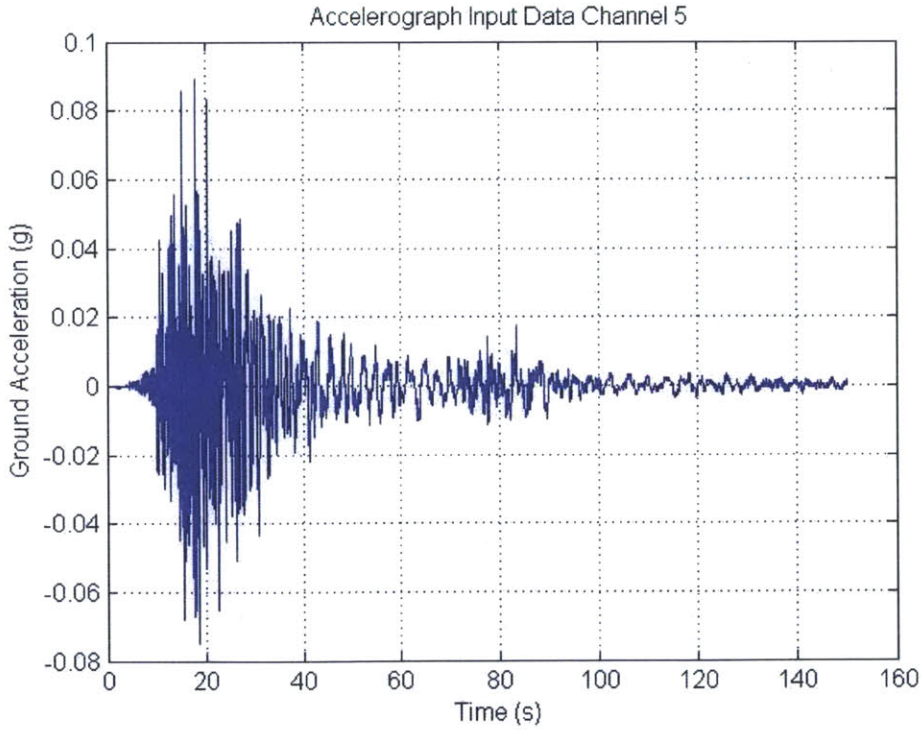
Accelerograph Input Data Channel 5
Ground Acceleration (g)
Time (s)
0.1
0.08
0.06
0.04
0.02
0
-0.02
-0.04
-0.06
-0.08
0
20
40
60
80
100
120
140
160

Hospital 5 San Bernardino

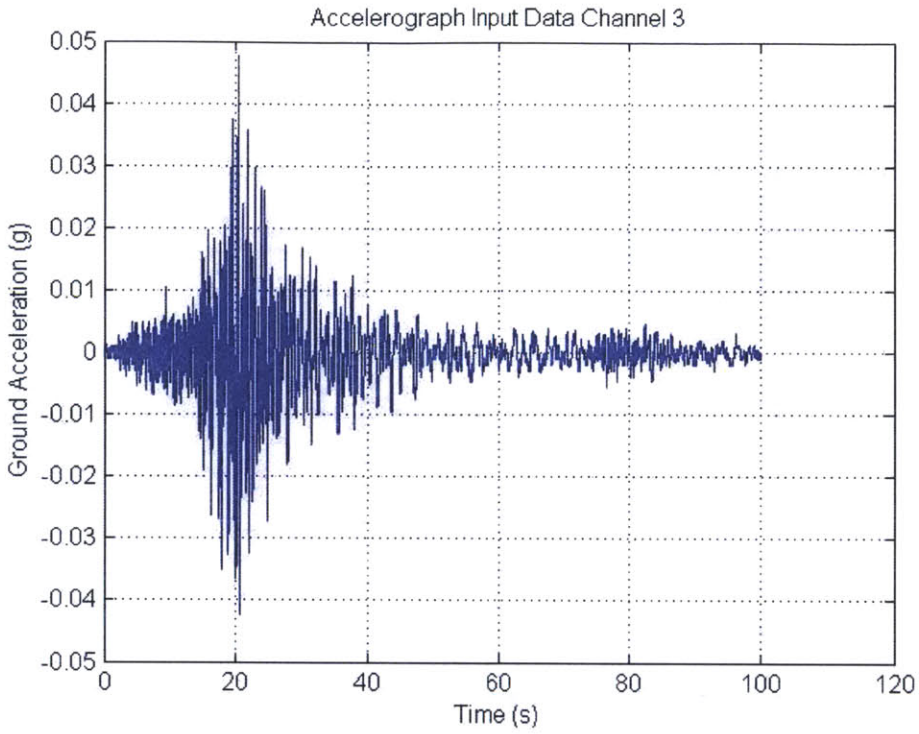

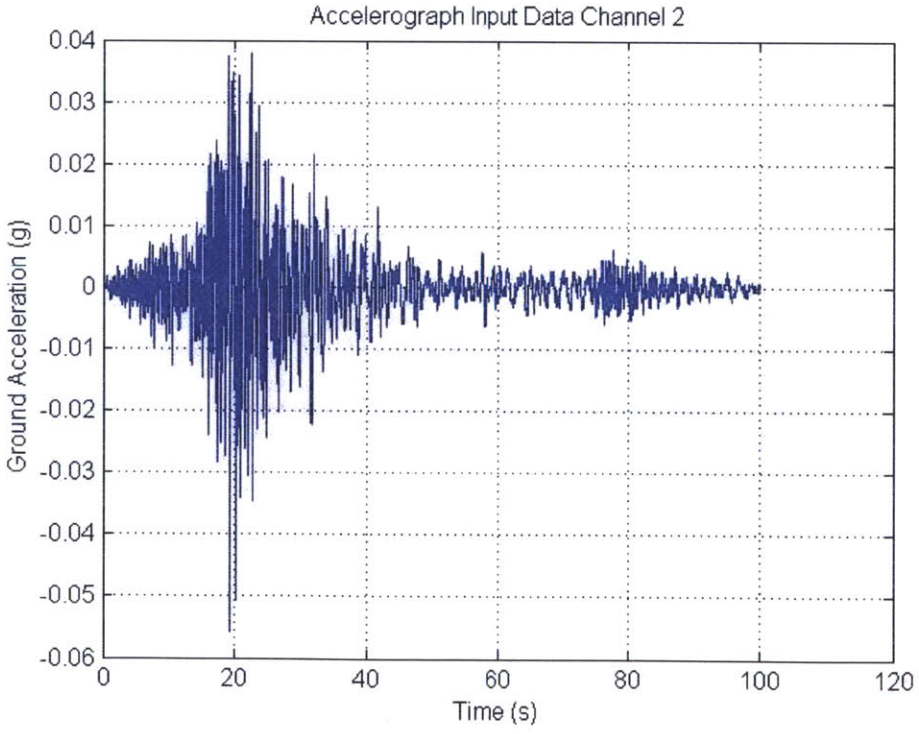

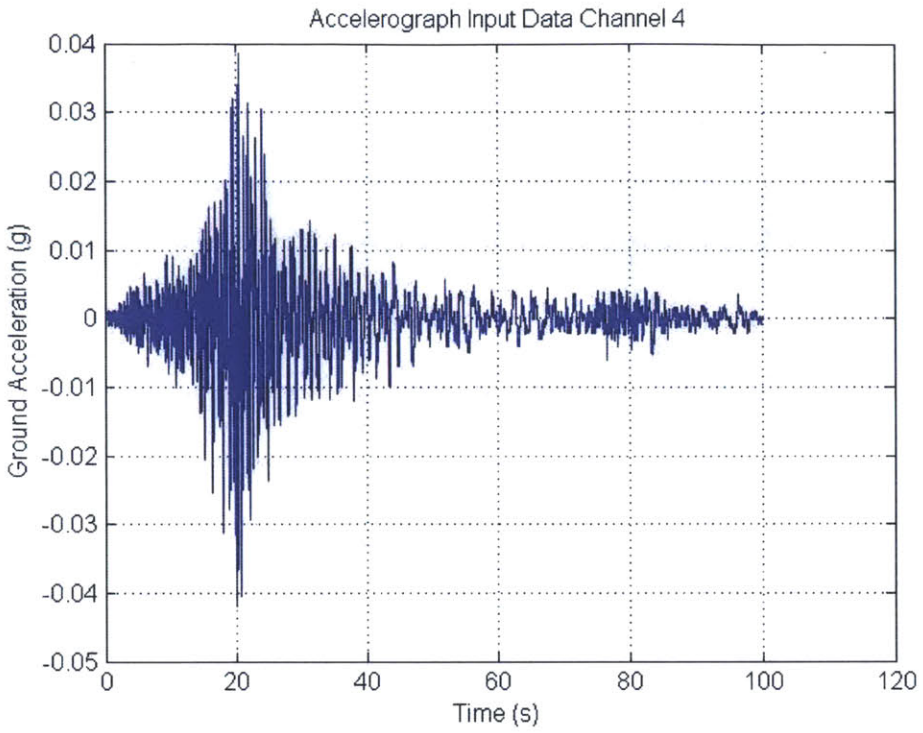

Parking 6 Los Angeles

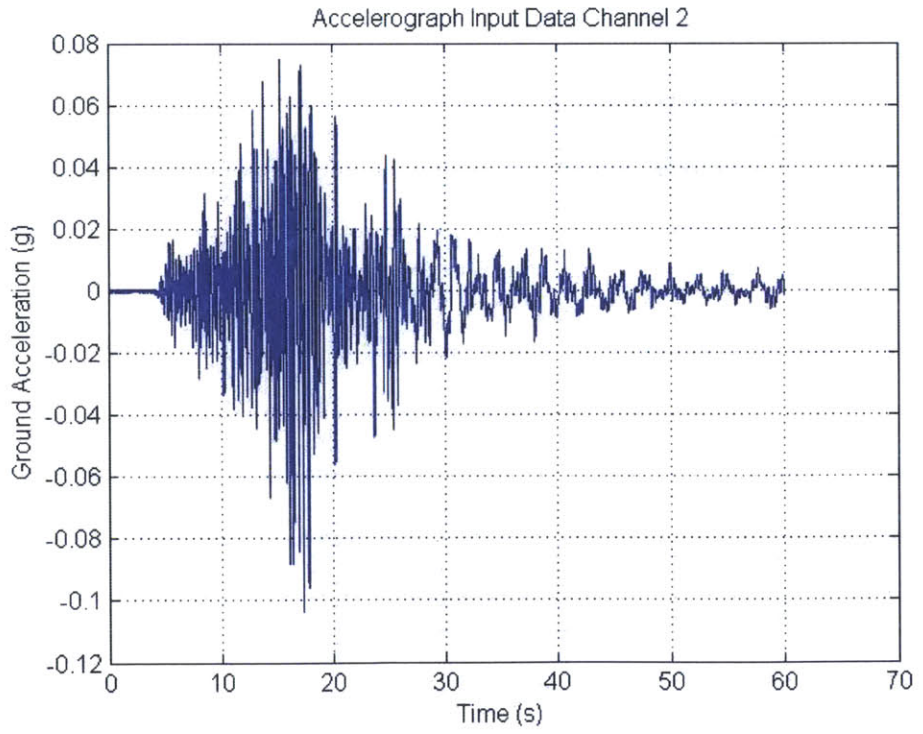

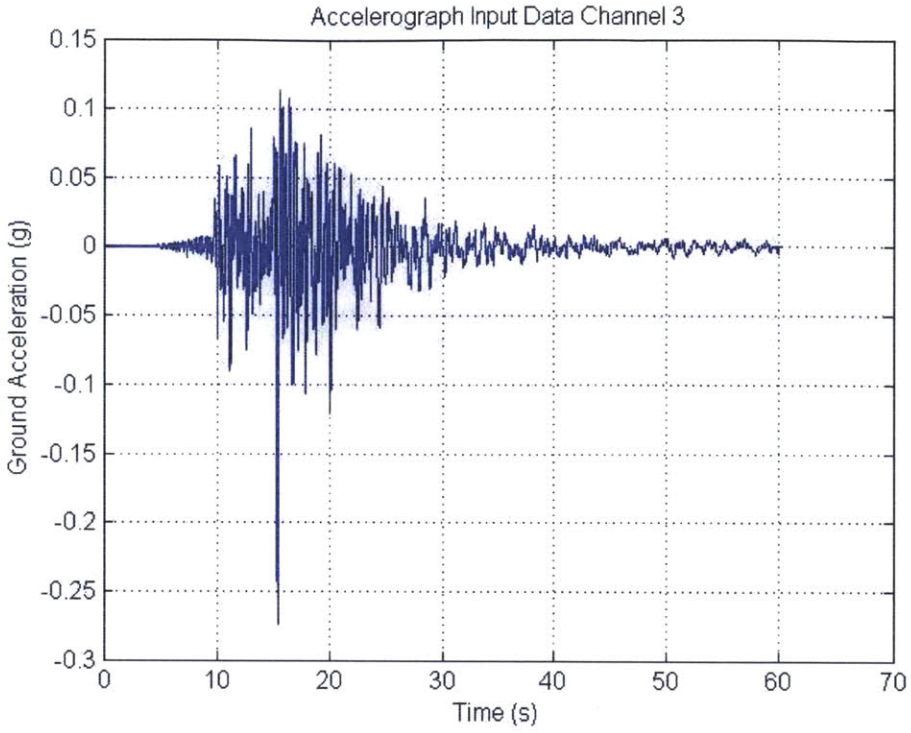
Accelerograph Input Data Channel 3
Ground Acceleration (g)
Time (s)
0.15
0.1
0.05
0
-0.05
-0.1
-0.15
-0.2
-0.25
-0.3
0
10
20
30
40
50
60
70

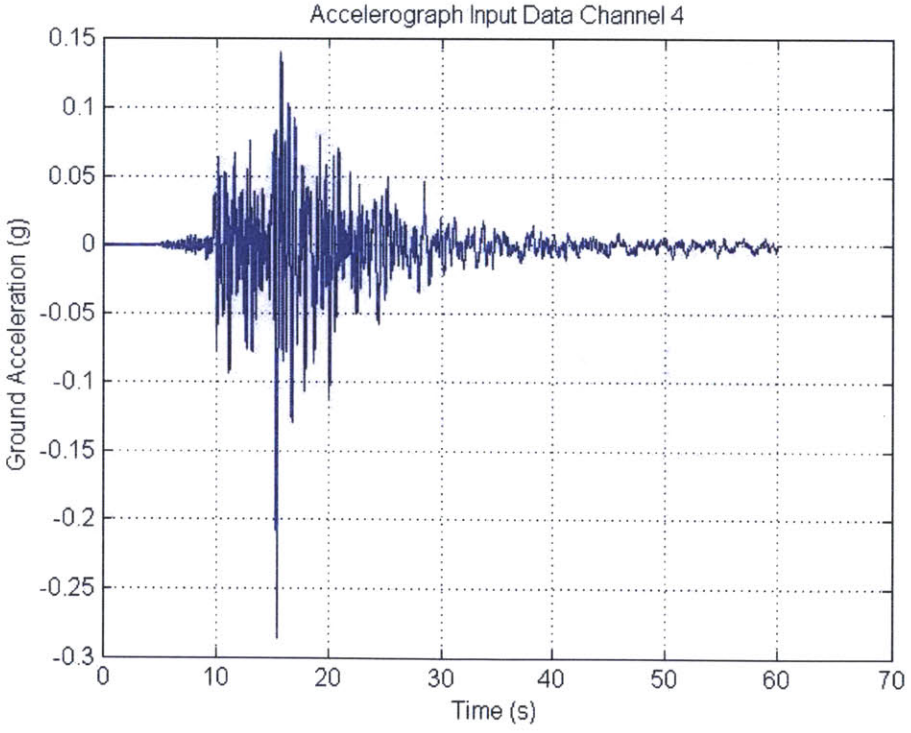
Accelerograph Input Data Channel 4
Ground Acceleration (g)
Time (s)
0.15
0.1
0.05
0
-0.05
-0.1
-0.15
-0.2
-0.25
-0.3
0
10
20
30
40
50
60
70

Appendix III. Results plots

In this Appendix the results plots produced by the algorithm are presented. The figures are organized per model name. Detailed explanation of the figures can be found in section 4.1.

Office 14 El Segundo

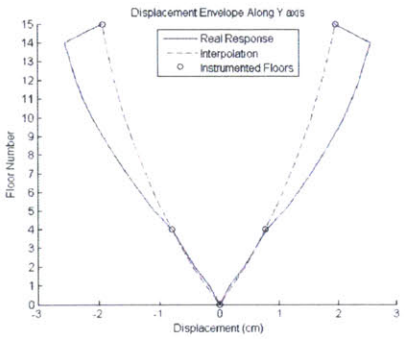

Excitation along the North-South direction

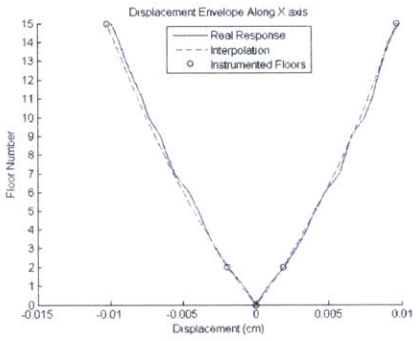

Excitation along the East-West direction

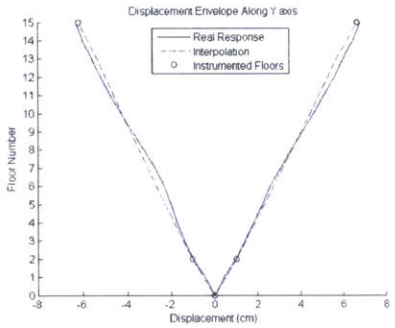

Excitation along the East-West direction

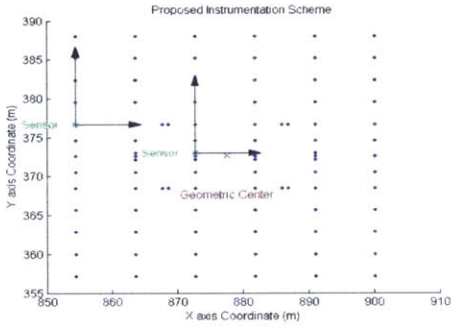

Roof excitation along the N-S direction

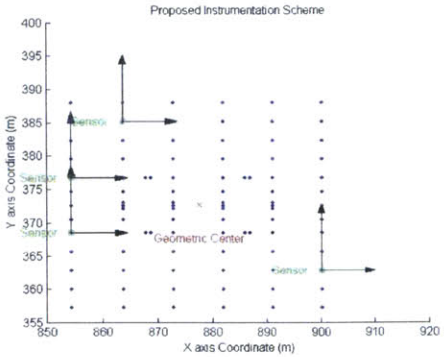

Roof - E-W excitation

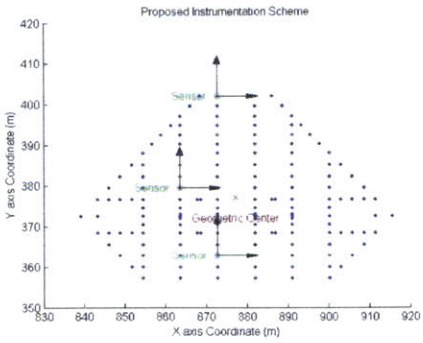

2nd floor - E-W excitation

Hospital 5 San Bernardino

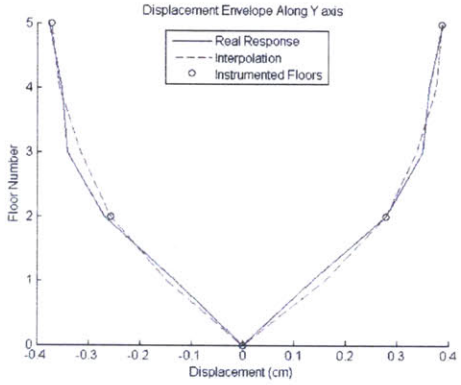

Excitation along the N-S direction

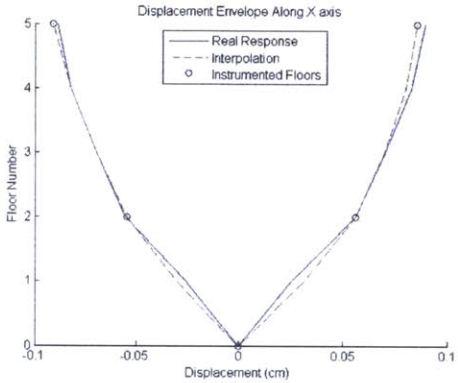

Excitation along the E-W direction

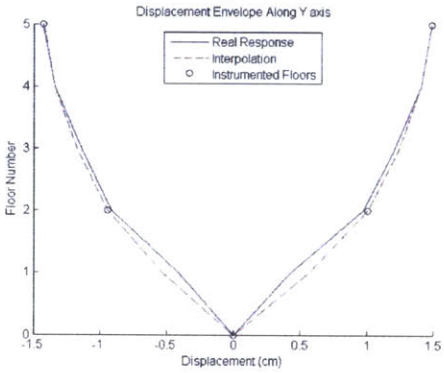

Excitation along the E-W direction

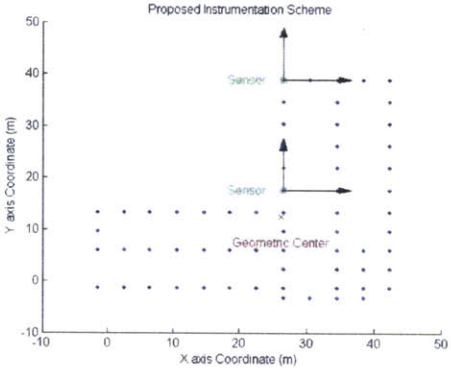

Roof - E-W excitation

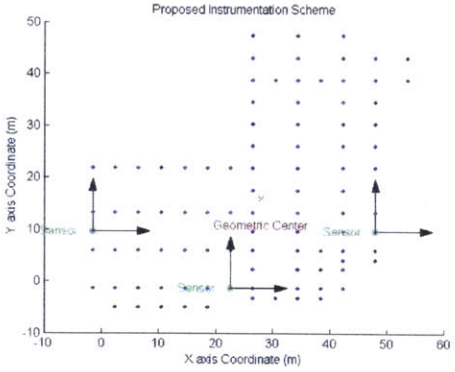

2nd floor - N-S excitation

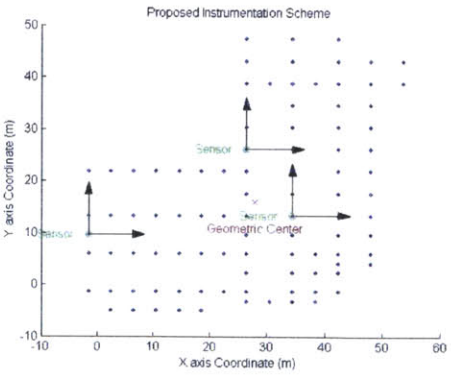

2nd floor - E-W excitation

Parking 6 Los Angeles

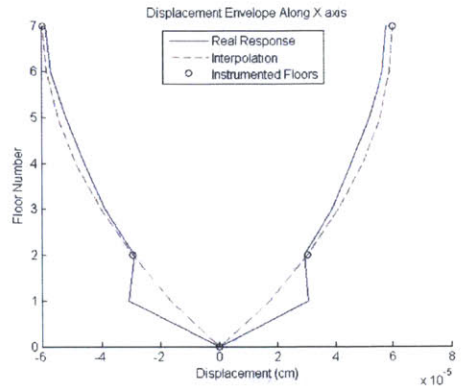

Excitation along the N-S direction

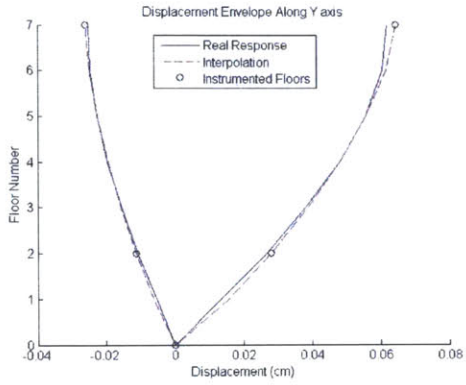

Excitation along the E-W direction

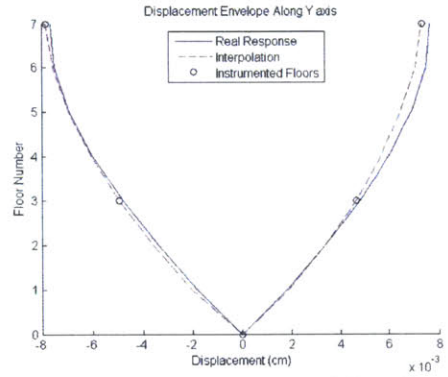

Excitation along the E-W direction

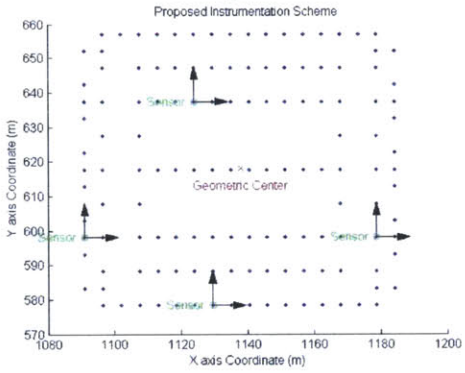

Roof - E-W excitation

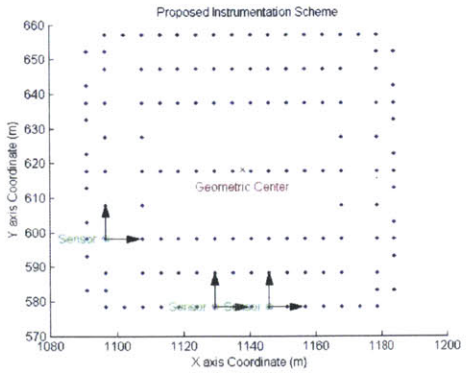

2nd floor - N-S excitation

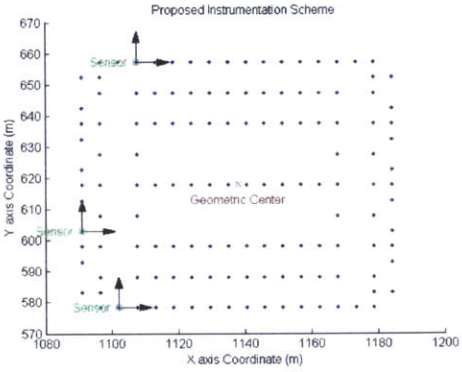

Roof - E-W excitation

Appendix IV. Earthquake Database

This appendix presents information about the earthquake data used for the analyses in the main body of the dissertation. The following table provides all the necessary information regarding the earthquakes used.

Name	Date	Time	Record Number	Station Number	Code Number
Imperial Valley	10/16/1979	06:58	NGA0209	CDMG 11369 Westmorland Fire Station	IPVALL/F-WSM180
Mammoth Lakes	01/07/1983	03:24	NGA0321	CDMG 54099 Convict Creek	MAMMOTH/G-CVK090
Mt. Lewis	03/31/1986	11:55	NGA0502	CDMG 57191 Hall Valley	MTLEWIS/HVR000
Northern California	06/07/1975	08:46	NGA0101	CDMG 89005 Cape Mendocino	NCALIF/D-CPM030
San Fernando	02/09/1971	14:00	NGA0051	USGS 411 2516 Via Tejon PV	SFERN/PVE065
Landers	06/28/1992	04:58	-	CSMIP No. 23481	CDMG QL92A481
Loma Prieta	10/17/1989	17:04	-	CSMIP No. 57355	CDMG QL89A355T

Appendix V. Rojahn and Mathiesen Proposed Schemes

The following appendix shows several instrumentation schemes as they were proposed by Rojahn and Mathiesen in their publication with the title "Earthquake Response and Instrumentation of Buildings". The figures are taken from the aforementioned publication and show:

A. A Three-story building with uniform plan and stiffness along its height.
B. A five-story building with shear walls at the two ends.
C. A seven-story building with uniform plan and stiffness along its height.
D. A nine-story building uniform in plan and stiffness along its height founded on piles.

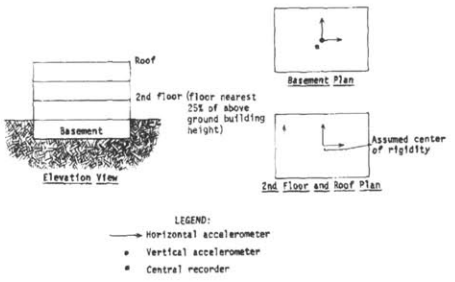

(A)

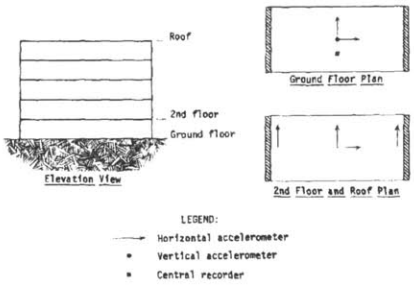

(B)

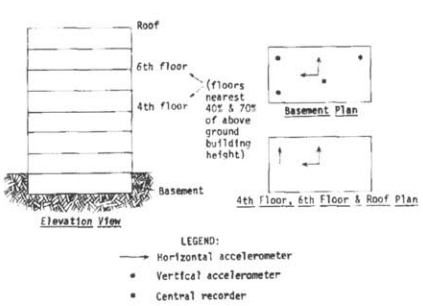

(C)

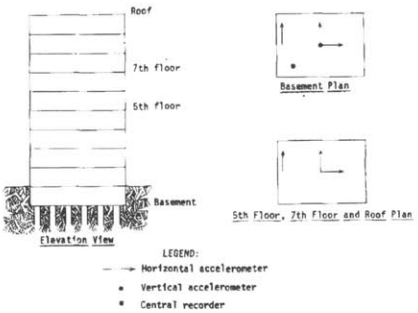

(D)

Appendix VI. Instrumentation Schemes' Comparison

This Appendix contains tables with results pertaining to a quantitative comparison between the instrumentation schemes that are currently implemented in the building and the schemes proposed by the algorithm. The following tables provide the values of the lateral displacements' envelope (in cm) of the buildings as they have been calculated by:

1. The CSMIP-3DV software, produced by Naeim. This software uses recordings from the existing sensors to estimate the lateral motion of the buildings. For the non-instrumented floors the software calculates the displacement using cubic spline interpolation.
2. SAP2000, based on the time history analysis of each model and the implementation of the algorithm on the models described in Chapter 3. The results from SAP2000 are mentioned in the plots of Chapter 4 and Appendix III as *Real Response*.
3. The algorithm's proposed instrumentation schemes and the use of cubic spline interpolation for the estimation of motion of the non-instrumented floors.

Each table provides information for a different excitation direction (North-South and East-West) and for different model (Office 14 El Segundo, Hospital 5 San Bernardino and Parking 6 Los Angeles). The lateral displacements are indicated in centimeters (cm). The X(+) or Y(-) column headings indicate the global axis (X or Y) of the measured displacement and the direction on the horizontal axis (+ or -) with respect to the origin of each floor slab (Geometric Center). The heading CSMIP-3DV refers to the information provided by the CSMIP-3DV software by Naeim, the SAP2000 by the information provided by the finite element software SAP2000 and the Algorithm's Interpolation by the information provided by the algorithm. The "vs." compares the information from the aforementioned sources. The green color indicates which floors of the existing building are instrumented. The yellow color indicates which floors should be instrumented in each excitation direction (North-South or East-West) as proposed by the algorithm. The "n/a" cells indicate that the corresponding floor is not considered in the actual building as a floor. Nevertheless, the finite element model of the buildings considers the "n/a" floors as actual and possible for instrumentation floor slabs. This inconsistency derives from the lack of information provided by the literature related to the buildings' structural elements and design information.

Table 1: Office 14 El Segundo - North-South Excitation

Floor Number	CSMIP-3DV X(+) (cm)	CSMIP-3DV X(-) (cm)	CSMIP-3DV Y(+) (cm)	CSMIP-3DV Y(-) (cm)	SAP2000 X(+) (cm)	SAP2000 X(-) (cm)	SAP2000 Y(+) (cm)	SAP2000 Y(-) (cm)	Algorithm's Interpolation X(+) (cm)	Algorithm's Interpolation X(-) (cm)	Algorithm's Interpolation Y(+) (cm)	Algorithm's Interpolation Y(-) (cm)
0	0.00	0.00	0.00	0.00	0.00	0.00	0.00	0.00	0.00	0.00	0.00	0.00
1	0.87	-0.90	0.62	-0.72	0.68	-0.70	0.17	-0.17	0.75	-0.87	0.22	-0.23
2	1.83	-1.88	1.22	-1.44	1.52	-1.61	0.42	-0.42	1.47	-1.69	0.43	-0.45
3	2.81	-2.85	1.78	-2.06	2.14	-2.34	0.61	-0.61	2.07	-2.36	0.60	-0.63
4	3.96	-4.04	2.36	-2.67	2.70	-3.04	0.79	-0.79	2.66	-3.01	0.77	-0.80
5	5.25	-5.42	2.98	-3.28	3.18	-3.76	1.09	-1.09	3.22	-3.61	0.92	-0.96
6	6.71	-6.91	3.63	-3.90	3.66	-4.47	1.32	-1.32	3.76	-4.19	1.07	-1.10
7	8.21	-8.42	4.29	-4.55	4.13	-5.11	1.54	-1.54	4.29	-4.73	1.20	-1.24
8	9.69	-9.91	4.98	-5.23	4.72	-5.69	1.75	-1.75	4.79	-5.24	1.33	-1.36
9	11.11	-11.32	5.68	-5.94	5.31	-6.18	1.94	-1.94	5.27	-5.72	1.45	-1.47
10	12.45	-12.65	6.39	-6.69	5.86	-6.61	2.11	-2.11	5.74	-6.16	1.55	-1.58
11	13.75	-13.91	7.12	-7.47	6.38	-6.97	2.25	-2.25	6.18	-6.56	1.65	-1.67
12	15.00	-15.13	7.86	-8.27	6.84	-7.28	2.37	-2.37	6.60	-6.94	1.74	-1.75
13	16.23	-16.32	8.60	-9.08	7.25	-7.53	2.47	-2.47	7.01	-7.28	1.82	-1.82
14	17.62	-17.67	9.46	-10.03	7.66	-7.79	2.55	-2.56	7.45	-7.63	1.90	-1.89
15	n/a	n/a	n/a	n/a	7.96	-8.01	1.95	-1.95	7.86	-7.94	1.97	-1.94

Floor Number	CSMIP-3DV vs. SAP2000 X(+) (%)	CSMIP-3DV vs. SAP2000 X(-) (%)	CSMIP-3DV vs. SAP2000 Y(+) (%)	CSMIP-3DV vs. SAP2000 Y(-) (%)	CSMIP-3DV vs. Alg. Interpolation X(+) (%)	CSMIP-3DV vs. Alg. Interpolation X(-) (%)	CSMIP-3DV vs. Alg. Interpolation Y(+) (%)	CSMIP-3DV vs. Alg. Interpolation Y(-) (%)	SAP2000 vs. Alg. Interpolation X(+) (%)	SAP2000 vs. Alg. Interpolation X(-) (%)	SAP2000 vs. Alg. Interpolation Y(+) (%)	SAP2000 vs. Alg. Interpolation Y(-) (%)
0	0	0	0	0	0	0	0	0	0%	0%	0%	0%
1	22%	23%	72%	76%	14%	4%	64%	68%	-10%	-24%	-28%	-34%
2	17%	14%	66%	71%	20%	10%	65%	69%	3%	-5%	-4%	-9%
3	24%	18%	66%	71%	26%	17%	66%	69%	3%	-1%	0%	-4%
4	32%	25%	66%	70%	33%	26%	68%	70%	2%	1%	3%	-1%
5	39%	31%	63%	67%	39%	33%	69%	71%	-1%	4%	15%	12%
6	45%	35%	64%	66%	44%	39%	71%	72%	-3%	6%	19%	17%
7	50%	39%	64%	66%	48%	44%	72%	73%	-4%	7%	22%	20%
8	51%	43%	65%	67%	51%	47%	73%	74%	-1%	8%	24%	22%
9	52%	45%	66%	67%	53%	50%	75%	75%	1%	8%	25%	24%
10	53%	48%	67%	69%	54%	51%	76%	76%	2%	7%	26%	25%
11	54%	50%	68%	70%	55%	53%	77%	78%	3%	6%	27%	26%
12	54%	52%	70%	71%	56%	54%	78%	79%	3%	5%	27%	26%
13	55%	54%	71%	73%	57%	55%	79%	80%	3%	3%	26%	26%
14	57%	56%	73%	75%	58%	57%	80%	81%	3%	2%	26%	26%
15	n/a	n/a	n/a	n/a	n/a	n/a	n/a	n/a	1%	1%	-1%	1%

Table 2: Office 14 El Segundo - East-West Excitation

Floor Number	CSMIP-3DV				SAP2000				Algorithm's Interpolation			
	X(+) (cm)	X(-) (cm)	Y(+) (cm)	Y(-) (cm)	X(+) (cm)	X(-) (cm)	Y(+) (cm)	Y(-) (cm)	X(+) (cm)	X(-) (cm)	Y(+) (cm)	Y(-) (cm)
0	0.00	0.00	0.00	0.00	0.00	0.00	0.00	0.00	0.00	0.00	0.00	0.00
1	0.87	-0.90	0.62	-0.72	0.00	0.00	0.42	-0.43	0.00	0.00	0.51	-0.51
2	1.83	-1.88	1.22	-1.44	0.00	0.00	0.98	-0.97	0.00	0.00	1.01	-1.01
3	2.81	-2.85	1.78	-2.06	0.00	0.00	1.42	-1.37	0.00	0.00	1.45	-1.43
4	3.96	-4.04	2.36	-2.67	0.00	0.00	1.82	-1.72	0.00	0.00	1.88	-1.85
5	5.25	-5.42	2.98	-3.28	0.00	0.00	2.20	-2.01	0.00	0.00	2.32	-2.27
6	6.71	-6.91	3.63	-3.90	0.00	0.00	2.58	-2.31	0.00	0.00	2.74	-2.67
7	8.21	-8.42	4.29	-4.55	0.01	-0.01	3.07	-2.74	0.01	-0.01	3.17	-3.07
8	9.69	-9.91	4.98	-5.23	0.01	-0.01	3.58	-3.25	0.01	-0.01	3.60	-3.47
9	11.11	-11.32	5.68	-5.94	0.01	-0.01	4.10	-3.76	0.01	-0.01	4.02	-3.86
10	12.45	-12.65	6.39	-6.69	0.01	-0.01	4.61	-4.27	0.01	-0.01	4.44	-4.24
11	13.75	-13.91	7.12	-7.47	0.01	-0.01	5.11	-4.75	0.01	-0.01	4.86	-4.62
12	15.00	-15.13	7.86	-8.27	0.01	-0.01	5.58	-5.19	0.01	-0.01	5.27	-4.99
13	16.23	-16.32	8.60	-9.08	0.01	-0.01	6.00	-5.58	0.01	-0.01	5.69	-5.35
14	17.62	-17.67	9.46	-10.03	0.01	-0.01	6.44	-5.99	0.01	-0.01	6.16	-5.76
15	n/a	n/a	n/a	n/a	0.01	-0.01	6.79	-6.32	0.01	-0.01	6.64	-6.17

Floor Number	CSMIP-3DV vs. SAP2000				CSMIP-3DV vs. Alg. Interpolation				SAP2000 vs. Alg. Interpolation			
	X(+) (%)	X(-) (%)	Y(+) (%)	Y(-) (%)	X(+) (%)	X(-) (%)	Y(+) (%)	Y(-) (%)	X(+) (%)	X(-) (%)	Y(+) (%)	Y(-) (%)
0	0	0	0	0	0	0	0	0	0%	0%	0%	0%
1	100%	100%	31%	41%	100%	100%	18%	30%	-19%	-17%	-20%	-18%
2	100%	100%	19%	32%	100%	100%	17%	30%	2%	-1%	-3%	-3%
3	100%	100%	20%	33%	100%	100%	18%	30%	5%	2%	-2%	-4%
4	100%	100%	23%	36%	100%	100%	20%	31%	4%	-2%	-4%	-8%
5	100%	100%	26%	39%	100%	100%	22%	31%	-1%	-7%	-5%	-13%
6	100%	100%	29%	41%	100%	100%	24%	32%	0%	-9%	-6%	-16%
7	100%	100%	28%	40%	100%	100%	26%	32%	6%	-2%	-3%	-12%
8	100%	100%	28%	38%	100%	100%	28%	34%	3%	-4%	-1%	-7%
9	100%	100%	28%	37%	100%	100%	29%	35%	-1%	-6%	2%	-3%
10	100%	100%	28%	36%	100%	100%	31%	37%	4%	-2%	4%	1%
11	100%	100%	28%	36%	100%	100%	32%	38%	4%	-4%	5%	3%
12	100%	100%	29%	37%	100%	100%	33%	40%	2%	-4%	5%	4%
13	100%	100%	30%	39%	100%	100%	34%	41%	1%	-2%	5%	4%
14	100%	100%	32%	40%	100%	100%	35%	43%	-1%	-4%	4%	4%
15	n/a	n/a	n/a	n/a	n/a	n/a	n/a	n/a	2%	-3%	2%	2%

Table 3: Hospital 5 San Bernardino - North-South Excitation

Floor Number	CSMIP-3DV				SAP2000				Algorithm's Interpolation			
	X(+) (cm)	X(-) (cm)	Y(+) (cm)	Y(-) (cm)	X(+) (cm)	X(-) (cm)	Y(+) (cm)	Y(-) (cm)	X(+) (cm)	X(-) (cm)	Y(+) (cm)	Y(-) (cm)
0	0.00	0.00	0.00	0.00	0.00	0.00	0.00	0.00	0.00	0.00	0.00	0.00
1	0.20	-0.22	0.26	-0.25	0.32	-0.37	0.14	-0.13	0.37	-0.46	0.16	-0.15
2	0.37	-0.41	0.51	-0.48	0.75	-0.87	0.28	-0.27	0.72	-0.87	0.28	-0.26
3	0.47	-0.52	0.68	-0.63	0.96	-1.10	0.35	-0.34	0.95	-1.14	0.34	-0.32
4	0.58	-0.64	0.85	-0.79	1.22	-1.42	0.36	-0.35	1.20	-1.39	0.38	-0.36
5	0.67	-0.74	1.01	-0.93	1.34	-1.55	0.39	-0.38	1.40	-1.59	0.39	-0.37

Floor Number	CSMIP-3DV vs. SAP2000				CSMIP-3DV vs. Alg. Interpolation				SAP2000 vs. Alg. Interpolation			
	X(+) (%)	X(-) (%)	Y(+) (%)	Y(-) (%)	X(+) (%)	X(-) (%)	Y(+) (%)	Y(-) (%)	X(+) (%)	X(-) (%)	Y(+) (%)	Y(-) (%)
0	0%	0%	0%	0%	0%	0%	0%	0%	0%	0%	0%	0%
1	-62%	-69%	48%	47%	-88%	-112%	38%	40%	-16%	-25%	-18%	-13%
2	-104%	-112%	45%	44%	-95%	-113%	45%	46%	5%	0%	0%	5%
3	-102%	-110%	48%	46%	-101%	-117%	50%	50%	0%	-3%	4%	7%
4	-111%	-123%	58%	55%	-107%	-118%	56%	55%	2%	2%	-4%	-1%
5	-99%	-110%	62%	59%	-108%	-115%	62%	60%	-5%	-2%	0%	1%

Table 4: Hospital 5 San Bernardino - East-West Excitation

-	CSMIP-3DV				SAP2000				Algorithm's Interpolation			
Floor Number	X(+) (cm)	X(-) (cm)	Y(+) (cm)	Y(-) (cm)	X(+) (cm)	X(-) (cm)	Y(+) (cm)	Y(-) (cm)	X(+) (cm)	X(-) (cm)	Y(+) (cm)	Y(-) (cm)
0	0.00	0.00	0.00	0.00	0.00	0.00	0.00	0.00	0.00	0.00	0.00	0.00
1	0.20	-0.22	0.26	-0.25	0.03	-0.03	0.43	-0.41	0.03	-0.03	0.57	-0.54
2	0.37	-0.41	0.51	-0.48	0.06	-0.06	0.97	-0.91	0.06	-0.05	1.01	-0.95
3	0.47	-0.52	0.68	-0.63	0.07	-0.07	1.21	-1.14	0.07	-0.07	1.24	-1.17
4	0.58	-0.64	0.85	-0.79	0.08	-0.08	1.41	-1.34	0.08	-0.08	1.41	-1.34
5	0.67	-0.74	1.01	-0.93	0.09	-0.09	1.49	-1.43	0.09	-0.09	1.49	-1.43
-	CSMIP-3DV vs. SAP2000				CSMIP-3DV vs. Alg. Interpolation				SAP2000 vs. Alg. Interpolation			
Floor Number	X(+) (%)	X(-) (%)	Y(+) (%)	Y(-) (%)	X(+) (%)	X(-) (%)	Y(+) (%)	Y(-) (%)	X(+) (%)	X(-) (%)	Y(+) (%)	Y(-) (%)
0	0%	0%	0%	0%	0%	0%	0%	0%	0%	0%	0%	0%
1	87%	88%	-68%	-68%	84%	86%	-121%	-118%	-25%	-18%	-31%	-30%
2	85%	87%	-92%	-92%	85%	87%	-99%	-99%	0%	1%	-3%	-3%
3	85%	87%	-78%	-80%	85%	87%	-83%	-86%	1%	0%	-3%	-3%
4	86%	87%	-65%	-70%	86%	87%	-65%	-70%	3%	0%	0%	0%
5	87%	88%	-47%	-54%	87%	88%	-47%	-54%	4%	-2%	0%	0%

Table 5: Parking 6 Los Angeles - North-South Excitation

Floor Number	CSMIP-3DV X(+) (cm)	CSMIP-3DV X(-) (cm)	CSMIP-3DV Y(+) (cm)	CSMIP-3DV Y(-) (cm)	SAP2000 X(+) (cm)	SAP2000 X(-) (cm)	SAP2000 Y(+) (cm)	SAP2000 Y(-) (cm)	Algorithm's Interpolation X(+) (cm)	Algorithm's Interpolation X(-) (cm)	Algorithm's Interpolation Y(+) (cm)	Algorithm's Interpolation Y(-) (cm)
0	0.00	0.00	0.00	0.00	0.0000	0.0000	0.0000	0.0000	0.0000	0.0000	0.0000	0.0000
1	0.24	-0.19	0.42	-0.47	0.0000	0.0000	0.0133	-0.0054	0.0000	0.0000	0.0155	-0.0063
2	0.48	-0.38	0.87	-0.94	0.0000	0.0000	0.0268	-0.0109	0.0000	0.0000	0.0280	-0.0114
3	0.71	-0.58	1.35	-1.42	0.0000	0.0000	0.0383	-0.0155	0.0000	0.0000	0.0388	-0.0157
4	0.91	-0.78	1.88	-1.90	0.0000	0.0000	0.0482	-0.0196	0.0000	0.0000	0.0480	-0.0195
5	1.11	-0.98	2.46	-2.38	0.0001	-0.0001	0.0557	-0.0226	0.0001	-0.0001	0.0556	-0.0226
6	1.30	-1.19	3.05	-2.86	0.0001	-0.0001	0.0606	-0.0246	0.0001	-0.0001	0.0616	-0.0250
7	n/a	n/a	n/a	n/a	0.0001	-0.0001	0.0619	-0.0251	0.0001	-0.0001	0.0645	-0.0262

Floor Number	CSMIP-3DV vs. SAP2000 X(+) (%)	CSMIP-3DV vs. SAP2000 X(-) (%)	CSMIP-3DV vs. SAP2000 Y(+) (%)	CSMIP-3DV vs. SAP2000 Y(-) (%)	CSMIP-3DV vs. Alg. Interpolation X(+) (%)	CSMIP-3DV vs. Alg. Interpolation X(-) (%)	CSMIP-3DV vs. Alg. Interpolation Y(+) (%)	CSMIP-3DV vs. Alg. Interpolation Y(-) (%)	SAP2000 vs. Alg. Interpolation X(+) (%)	SAP2000 vs. Alg. Interpolation X(-) (%)	SAP2000 vs. Alg. Interpolation Y(+) (%)	SAP2000 vs. Alg. Interpolation Y(-) (%)
0	0%	0%	0%	0%	0%	0%	0%	0%	0%	0%	0%	0%
1	100%	100%	97%	99%	100%	100%	96%	99%	44%	46%	-17%	-17%
2	100%	100%	97%	99%	100%	100%	97%	99%	-4%	-2%	-4%	-4%
3	100%	100%	97%	99%	100%	100%	97%	99%	-6%	-3%	-1%	-1%
4	100%	100%	97%	99%	100%	100%	97%	99%	-9%	-6%	0%	0%
5	100%	100%	98%	99%	100%	100%	98%	99%	-7%	-5%	0%	0%
6	100%	100%	98%	99%	100%	100%	98%	99%	-5%	-2%	-2%	-2%
7	n/a	n/a	n/a	n/a	n/a	n/a	n/a	n/a	-4%	-2%	-4%	-4%

Table 6: Parking 6 Los Angeles - East-West Excitation

Floor Number	CSMIP-3DV X(+) (cm)	CSMIP-3DV X(-) (cm)	CSMIP-3DV Y(+) (cm)	CSMIP-3DV Y(-) (cm)	SAP2000 X(+) (cm)	SAP2000 X(-) (cm)	SAP2000 Y(+) (cm)	SAP2000 Y(-) (cm)	Algorithm's Interpolation X(+) (cm)	Algorithm's Interpolation X(-) (cm)	Algorithm's Interpolation Y(+) (cm)	Algorithm's Interpolation Y(-) (cm)
0	0.00	0.00	0.00	0.00	0.0000	0.0000	0.0000	0.0000	0.0000	0.0000	0.0000	0.0000
1	0.24	-0.19	0.42	-0.47	0.0058	-0.0049	0.0018	-0.0018	0.0069	-0.0058	0.0019	-0.0020
2	0.48	-0.38	0.87	-0.94	0.0118	-0.0100	0.0034	-0.0034	0.0124	-0.0104	0.0034	-0.0036
3	0.71	-0.58	1.35	-1.42	0.0170	-0.0144	0.0048	-0.0048	0.0172	-0.0143	0.0046	-0.0049
4	0.91	-0.78	1.88	-1.90	0.0214	-0.0182	0.0060	-0.0060	0.0211	-0.0176	0.0057	-0.0061
5	1.11	-0.98	2.46	-2.38	0.0248	-0.0211	0.0069	-0.0069	0.0244	-0.0203	0.0065	-0.0069
6	1.30	-1.19	3.05	-2.86	0.0269	-0.0229	0.0075	-0.0075	0.0268	-0.0224	0.0071	-0.0076
7	n/a	n/a	n/a	n/a	0.0275	-0.0234	0.0076	-0.0077	0.0279	-0.0233	0.0073	-0.0078

Floor Number	CSMIP-3DV vs. SAP2000 X(+) (%)	CSMIP-3DV vs. SAP2000 X(-) (%)	CSMIP-3DV vs. SAP2000 Y(+) (%)	CSMIP-3DV vs. SAP2000 Y(-) (%)	CSMIP-3DV vs. Alg. Interpolation X(+) (%)	CSMIP-3DV vs. Alg. Interpolation X(-) (%)	CSMIP-3DV vs. Alg. Interpolation Y(+) (%)	CSMIP-3DV vs. Alg. Interpolation Y(-) (%)	SAP2000 vs. Alg. Interpolation X(+) (%)	SAP2000 vs. Alg. Interpolation X(-) (%)	SAP2000 vs. Alg. Interpolation Y(+) (%)	SAP2000 vs. Alg. Interpolation Y(-) (%)
0	0%	0%	0%	0%	0%	0%	0%	0%	0%	0%	0%	0%
1	98%	97%	100%	100%	97%	97%	100%	100%	-20%	-18%	-4%	-11%
2	98%	97%	100%	100%	97%	97%	100%	100%	-5%	-3%	0%	-6%
3	98%	98%	100%	100%	98%	98%	100%	100%	-1%	1%	4%	-3%
4	98%	98%	100%	100%	98%	98%	100%	100%	1%	3%	5%	-1%
5	98%	98%	100%	100%	98%	98%	100%	100%	2%	4%	6%	0%
6	98%	98%	100%	100%	98%	98%	100%	100%	1%	2%	6%	-1%
7	n/a	n/a	n/a	n/a	n/a	n/a	n/a	n/a	-1%	1%	4%	-2%

Appendix VII. MATLAB code

This Appendix presents the algorithm described in Chapter 3 as it was implemented in MATLAB.

Main Program:

```
%Reads from file "Joints.xlsx"
[Results,txt,all]=xlsread('Joints.xlsx','Joint Coordinates');
JC=all((4:end),[1;8;9;10]);
[Results,txt,all]=xlsread('Joints.xlsx','Joint Displacements');
JD=all((4:end),[1;5;6;7]);
%Creating a matrix with the name and coordinates of each joint and
%transform every cell to numerical values
%Form of table:
% Name GlobalX Global Y Global Z
JointCord=zeros(size(JC,1),size(JC,2));
for i=1:size(JC,1)
    temp=str2double(cell2mat(JC(i,1)));
    JointCord(i,1)=temp;
end
for i=1:size(JC,2)-1
    for j=1:size(JC,1)
        temp=cell2mat(JC(j,i+1));
        JointCord(j,i+1)=temp;
    end
end

%Creating a matrix with the name and displacements of each joint and
%transform every cell to numerical values. Also deletion of the zero rows
%Matrix form
%NAME   U1_MAX   U1_MIN   U2_MAX   U2_MIN   U3_MAX   U3_MIN
JointDispl=zeros(size(JD,1),size(JD,2)*2-1);
for i=1:size(JD,1)
    temp=str2double(cell2mat(JD(i,1)));
    JointDispl(i,1)=temp;
end
k=0;
for i=1:size(JD,2)-1%columns
    for j=1:2:size(JD,1)    %rows
        temp=cell2mat(JD(j,i+1));
        JointDispl(j,i+k+1)=temp;
        temp=cell2mat(JD(j+1,i+1));
        JointDispl(j,i+k+1+1)=temp;
    end
    k=k+1;
end
for i=size(JD,1):-1:1
    test=i/2;
    if test-floor(test)==0
        JointDispl(i,:)=[];
    end
end

%JCS has the matrix JointCord sorted by the floor height in an ascending
```

```
%order.
%Form of table
%Name GlobalX Global Y Global Z
JCS=sortrows(JointCord,4);

%FloorNumber is a column vector with the number of floor assigned to each
%joint.
FloorNumber=zeros(size(JCS,1),1);
j=1;
i=1;
while i<size(JCS,1)
    if JCS(i,4)==JCS(i+1,4)
        FloorNumber(i,1)=j;
    end
    if JCS(i,4)~=JCS(i+1,4)
        FloorNumber(i,1)=j;
        j=j+1;
    end
    i=i+1;
end
FloorNumber(i,1)=j;
TotalFloorNumber=j;

%JointNoPF is a vector that has assigned the number of joints on each
floor
B=[JCS,FloorNumber];
j=1;
i=1;
k=0;
JointNoPF=zeros(TotalFloorNumber,1);
while i<=size(B,1)
    if B(i,5)==j
        k=k+1;
        JointNoPF(j)=k;
    end
    if B(i,5)~=j
       i=i-1;
       j=j+1;
       k=0;
    end
    i=i+1;
end

maxNum=0;
minNum=1;
XC=zeros(size(JointNoPF,1),1);
for i=1:size(JointNoPF,1)
    maxNum=maxNum+JointNoPF(i,1);
    k=0;
    for j=minNum:maxNum
        k=k+1;
        SS(k,1)=B(j,2);
    end
    XC(i,1)=mean(SS);
    minNum=maxNum;
    SS=[];
end

%YC is a matrix with the geometric center of each floor on Glogal Y axis
maxNum=0;
minNum=1;
```

```
YC=zeros(size(JointNoPF,1),1);
for i=1:size(JointNoPF,1)
    maxNum=maxNum+JointNoPF(i,1);
    k=0;
    for j=minNum:maxNum
        k=k+1;
        SS(k,1)=B(j,3);
    end
    YC(i,1)=mean(SS);
    minNum=maxNum;
    SS=[];
end
%Z is a vector with the height of each floor
Z=zeros(size(JointNoPF,1),1);
for i=1:size(JointNoPF,1)
    for j=1:size(B,1)
        if i==B(j,5)
            Z(i)=B(j,4);
        end
    end
end

%FloorInfo is matrix with the number of joints representing each floor in
%the first column and the coordinates of the geometric center of each
floor
%along Global X and Global Y axis in the 2nd and 3rd column respectively.
FloorInfo=[JointNoPF,XC,YC,Z];

%FloorDispl is a matrix containing the x displacement, y dipsl and
rotation
%of the geometric center of each floor. The format of the matrix is:
%max_X max_Y max_theta min_X min_Y min_Theta

FloorDispl=zeros(size(FloorInfo,1),6);
for i=2:size(FloorInfo,1)
    height=FloorInfo(i,4);%select floor height
    counter=0;
    maxAngle=0;
    minAngle=0;
    for j=1:size(JCS,1)%uses only the joints assigned on the selected
floor
        if height==JCS(j,4)
            counter=counter+1;
            JointNumber=JCS(j,1);%selects the joint number
            for k=1:size(JointDispl,1)
                if JointNumber==JointDispl(k,1)%finds the displacements
assigned to this joint and calculates the displacemetn of the geometric
center
                    if and(abs(abs((JointCord(k,2))-
abs(FloorInfo(i,2))))>1,abs(abs((JointCord(k,3))-abs(FloorInfo(i,3))))>1)
                        phi=atan((JointCord(k,3)-
FloorInfo(i,3)+JointDispl(k,4))/(JointCord(k,2)-FloorInfo(i,2)))-
atan((JointCord(k,3)-FloorInfo(i,3))/(JointCord(k,2)-FloorInfo(i,2)));
                        theta=atan((JointCord(k,2)-
FloorInfo(i,2)+JointDispl(k,2))/(JointCord(k,3)-FloorInfo(i,3)))-
atan((JointCord(k,2)-FloorInfo(i,2))/(JointCord(k,3)-FloorInfo(i,3)));
                        tempAngleMax=phi-theta;

                        phi=atan((JointCord(k,3)-
FloorInfo(i,3)+JointDispl(k,5))/(JointCord(k,2)-FloorInfo(i,2)))-
atan((JointCord(k,3)-FloorInfo(i,3))/(JointCord(k,2)-FloorInfo(i,2)));
```

```
                        theta=atan((JointCord(k,2)-
FloorInfo(i,2)+JointDispl(k,3))/(JointCord(k,3)-FloorInfo(i,3)))-
atan((JointCord(k,2)-FloorInfo(i,2))/(JointCord(k,3)-FloorInfo(i,3)));
                        tempAngleMin=phi-theta;

                        maxAngle=maxAngle+tempAngleMax;
                        minAngle=minAngle+tempAngleMin;
                    end
                    if or(abs(abs((JointCord(k,2))-
abs(FloorInfo(i,2))))<1,abs(abs((JointCord(k,3))-abs(FloorInfo(i,3))))<1)
                       counter=counter-1;
                    end
                end
            end
        end
    end
    FloorDispl(i,[3 6])=[maxAngle/counter minAngle/counter];
    counter=0;
    for j=1:size(JCS,1)%uses only the joints assigned on the selected
floor
        if height==JCS(j,4)
            counter=counter+1;
            JointNumber=JCS(j,1);%selects the joint number
            for k=1:size(JointDispl,1)
                if JointNumber==JointDispl(k,1)%finds the displacements
assigned to this joint and calculate the displacemetn of the geometric
center
                    xyT=[JointDispl(k,2) FloorInfo(i,3)-JointCord(k,3);
                        JointDispl(k,4) -(FloorInfo(i,2)-
JointCord(k,2))]*[1;FloorDispl(i,3)];
                    temp=xyT';
                   FloorDispl(i,1:2)=FloorDispl(i,1:2)+temp(1,1:2);
                   xyT=[JointDispl(k,3) FloorInfo(i,3)-JointCord(k,3);
                        JointDispl(k,5) -(FloorInfo(i,2)-
JointCord(k,2))]*[1;FloorDispl(i,6)];
                    temp=xyT';
                   FloorDispl(i,4:5)=FloorDispl(i,4:5)+temp(1,1:2);
                end
            end
        end
    end
    tempFloorDispl=FloorDispl(i,[1 2 4 5])/JointNoPF(i,1);
    FloorDispl(i,[1 2 4 5])=tempFloorDispl(1,1:4);
end

%The next two loops are calculating which combination of joints should be
%instrumented in order the calculated displacement at the geometric
%center, is less than 5% of the real displacement that is calculated from
a
%full floor instrumentation.
%SensorSchemeX and SensorSchemeY are functions that produce the above
%results in the X and Y direction respectively. tempRS_ has the number
and
%name of each of joint that is proposed for instrumentation. tempRD_ has
%the calculated displacement at the geometric center due to the proposed
%instrumentation
TempNo=size(FloorDispl,1);
[RoofSensors,RoofDispl]=SensorSchemeX(FloorDispl,JointNoPF,B,JointDispl,F
loorInfo,JointCord,TempNo);
tempRSX=RoofSensors;
tempRDX=RoofDispl;
```

```
[RoofSensors,RoofDispl]=SensorSchemeY(FloorDispl,JointNoPF,B,JointDispl,F
loorInfo,JointCord,TempNo);
tempRSY=RoofSensors;
tempRDY=RoofDispl;

RoofSensors=[tempRSX tempRSY];
RoofDispl=tempRDX+tempRDY;

Estimation=zeros(size(FloorDispl));
Estimation(end,:)=RoofDispl(1,:);
Estimation;

JointsWsensors=zeros(size(FloorInfo,1),max(FloorInfo(:,1)));
for i=2:size(FloorInfo,1)

[FloorSensorsX,FloorDisplCenterX]=SensorSchemeX(FloorDispl,JointNoPF,B,Jo
intDispl,FloorInfo,JointCord,i);

[FloorSensorsY,FloorDisplCenterY]=SensorSchemeY(FloorDispl,JointNoPF,B,Jo
intDispl,FloorInfo,JointCord,i);
    FloorSensors=[FloorSensorsX FloorSensorsY];
    FloorDisplCenter=FloorDisplCenterX+FloorDisplCenterY;
    Estimation(i,:)=FloorDisplCenter(1,:);

JointsWsensors(i,1:size(FloorSensors,2))=JointsWsensors(i,1:size(FloorSen
sors,2))+FloorSensors(1,1:end);
    FloorSensors=[];
    FloorDisplCenter=[];
end%here is the calculation of the instrumentation schemes

%The following commands produce an estimation of the difference between a
%fully instrumented schemed and the proposed schemes using the least
square
%methods
Xmax=R_Instrumented(FloorInfo,Estimation,FloorDispl,JointsWsensors,1);
Xmin=R_Instrumented(FloorInfo,Estimation,FloorDispl,JointsWsensors,4);
Ymax=R_Instrumented(FloorInfo,Estimation,FloorDispl,JointsWsensors,2);
Ymin=R_Instrumented(FloorInfo,Estimation,FloorDispl,JointsWsensors,5);
All=[Xmax;Xmin;Ymax;Ymin];

TempXboundaries=Xmax(1:end,size(Xmax,2))+Xmin(1:end,size(Xmin,2));
Xboundaries=[Xmax TempXboundaries];
sortedX=sortrows(Xboundaries,size(Xboundaries,2));

TempYboundaries=Ymax(1:end,size(Ymax,2))+Ymin(1:end,size(Ymin,2));
Yboundaries=[Ymax TempYboundaries];
sortedY=sortrows(Yboundaries,size(Yboundaries,2));
%Sorting the matrices in an ascending order by using the dummy variable
sortedXmax=sortedX(:,1:size(sortedX,2)-1);
sortedXmin=sortedX(:,1:size(sortedX,2)-1);
sortedYmax=sortedX(:,1:size(sortedY,2)-1);
sortedYmin=sortedX(:,1:size(sortedY,2)-1);
All_new=[sortedXmax;sortedYmax];

%The ProposedFloors matrix has the floors that the previous analysis had
%shown neccessary for instrumentation. The matrix looks like:
%Xmax Xmin Ymax Ymin
%The columns contain the number of the floors and meaningless zeros
temp=[sortedXmax(1,2:size(sortedXmax,2)-2);
```

```
                sortedXmin(1,2:size(sortedXmin,2)-2);
                sortedYmax(1,2:size(sortedYmax,2)-2);
                sortedYmin(1,2:size(sortedYmin,2)-2)];
ProposedFloors=temp';

%This loop is plotting the results. On the X axis is the horizontal
%displacement. On Y axis is the floor number.
for j=1:size(ProposedFloors,2)
        if j==1
            value=1;
        elseif j==2
            value=4;
        elseif j==3
            value=2;
        elseif j==4
            value=5;
        end
    k=0;
    for i=1:size(ProposedFloors,1)
        if ProposedFloors(i,j)~=0
            k=k+1;
            number(k,1)=ProposedFloors(i,j);
            y(k,1)=FloorInfo(number(k,1),4);
        end
    end
    k=0;
    for i=1:size(number,1)
        for h=1:size(Estimation,1)
            if h==number(i,1)
                k=k+1;
                x(k,1)=Estimation(h,value);
            end
        end
    end

    Values=FloorInfo(1:end,4);
    PredictedResponse=csapi(y,x,Values);
    LateralDisplacements(:,j)=PredictedResponse(1:end,1);
    if j==1
        title('Displacement Envelope Along X axis')
        xlabel('Displacement (cm)')
        ylabel('Floor Number')
    end
    if j==3
        hold off
        figure;
        title('Displacement Envelope Along Y axis')
        xlabel('Displacement (cm)')
        ylabel('Floor Number')
    end
    hold on
    plot(FloorDispl(1:end,value),1-1:size(FloorInfo,1)-1)
    plot(PredictedResponse(1:end,1),1-1:size(FloorInfo,1)-1,'--
','color','red')
    plot(x,number-1,'O','color','k')
    legend('Real Response','Interpolation','Instrumented Floors')
    set(gca,'YTick',0:size(FloorInfo,1))
end
hold off
```

```
%This loop plots all the floors as points and the geometric center with
an
%X (red color).
for i=2:size(FloorInfo,1)
    figure;
    hold on
    FLOOR=num2str(i);
    title('Proposed Instrumentation Scheme')
    xlabel('X axis Coordinate (m)')
    ylabel('Y axis Coordinate (m)')
    for j=1:size(B,1)
        if i==B(j,5)
            plot(B(j,2)/100,B(j,3)/100,'.')
        end
    end
    plot(FloorInfo(i,2)/100,FloorInfo(i,3)/100,'X','color','red')
    text(FloorInfo(i,2)/100,FloorInfo(i,3)/100-500/100,'Geometric
Center','HorizontalAlignment','center','Color','red')
    for k=2:size(ProposedFloors,1)
        if i==ProposedFloors(k,1)
            for j=1:size(JointsWsensors,1)
                if JointsWsensors(i,j)~=0

plot(JointCord(JointsWsensors(i,j),2)/100,JointCord(JointsWsensors(i,j),3
)/100,'o','color','g')
                    TEXT1=num2str(JointCord(JointsWsensors(i,j),2)/100);
                    TEXT2=num2str(JointCord(JointsWsensors(i,j),3)/100);
                    text(JointCord(JointsWsensors(i,j),2)/100-
250/100,JointCord(JointsWsensors(i,j),3)/100,'Sensor','HorizontalAlignmen
t','right','color','g')
                    arrow([JointCord(JointsWsensors(i,j),2)/100;
JointCord(JointsWsensors(i,j),3)/100],[JointCord(JointsWsensors(i,j),2)/1
00+1000/100; JointCord(JointsWsensors(i,j),3)/100])
                end
            end
        end
    end
    for k=2:size(ProposedFloors,1)
        if i==ProposedFloors(k,3)
            for j=1:size(JointsWsensors,1)
                if JointsWsensors(i,j)~=0

plot(JointCord(JointsWsensors(i,j),2)/100,JointCord(JointsWsensors(i,j),3
)/100,'o','color','g')
                    arrow([JointCord(JointsWsensors(i,j),2)/100;
JointCord(JointsWsensors(i,j),3)/100],[JointCord(JointsWsensors(i,j),2)/1
00; JointCord(JointsWsensors(i,j),3)/100+1000/100])
                end
            end
        end
    end

    hold off
end

AllRecon=All_new;
temp=sortrows(AllRecon,-1);
AllRecon=[temp(1:end,1) temp(1:end,size(temp,2)-1)];
AllReconXY=AllRecon;
i=size(AllRecon,1);
while i>=2
```

```
    if AllRecon(i-1,2)>AllRecon(i,2)
        AllRecon(i-1,:)=[];
    end
    i=i-1;
end
```

Function "SensorSchemeX"

The same function exists for the Y axis. This section presents only the function regarding the X axis.

```
function
[SensorJoints,tempSensors]=SensorSchemeX(FloorDispl,JointNoPF,B,JointDisp
l,FloorInfo,JointCord,TempNo)
TempJoints=JointsOnFloor(JointNoPF,B,TempNo);

%This loop has the purpose of checking all the possible combinations of
%sensor placement on the selected floor in order the displacement
provided
%by the proposed scheme has less than 1% difference with the "real"
%displacement.
%Sensors is an matrix with just one row that has the displacements
%calculated by the proposed placement scheme.
%SensorsScheme has the names of joints that are proposed by the scheme
for
%the selected floor
%The next loop calculates the scheme ONLY FOR THE ROOF
%DisplCenter is an outside function to calculate the displacement at the
%center of geometry
value=0;
Sensors=zeros(1,6);
for i=1:size(TempJoints,1)
    combos=combntns(TempJoints,i);

    for j=1:size(combos,1)
        SensorJoints=combos(j,:);
        counter=0;
        for h=1:size(SensorJoints,2)
            for k=1:size(JointDispl,1)
                if JointDispl(k,1)==SensorJoints(h)
                    if and(abs(abs((JointCord(k,2))-
abs(FloorInfo(TempNo,2))))>1,abs(abs((JointCord(k,3))-
abs(FloorInfo(TempNo,3))))>1)
                        counter=counter+1;

[tempAngleMax,tempAngleMin]=Angles(k,TempNo,JointDispl,JointCord,FloorInf
o);
                    end
                end
            end
            Sensors(1,[3 6])=[tempAngleMax/counter tempAngleMin/counter];



            for k=1:size(JointDispl,1)
                if JointDispl(k,1)==SensorJoints(h)



tempSensors1=DisplCenter(k,1,Sensors,JointDispl,JointCord,FloorInfo);
                    Sensors(1,[1 4])=Sensors(1,[1 4])+tempSensors1(1,[1
3]);
                end
            end
            tempSensors=Sensors/size(SensorJoints,2);
```

```
            maxXcheck=abs(FloorDispl(TempNo,1)-
tempSensors(1))/abs(FloorDispl(TempNo,1));
            minXcheck=abs(FloorDispl(TempNo,4)-
tempSensors(4))/abs(FloorDispl(TempNo,4));
            limit=5/100;
            if and(maxXcheck<limit,minXcheck<limit)
                value=1;
                break
            end
        end
        Sensors=zeros(1,6);
        if value==1
            break
        end
    end
    if value==1
    break
    end
end

end
```

Function "R_Instrumented"

```
function
R_I=R_Instrumented(FloorInfo,Estimation,FloorDispl,JointsWsensors,UV)
TempFloors=[2:size(FloorInfo,1)-1];
    k=1;
    for i=1:size(TempFloors,2)
        combos=combntns(TempFloors,i);
        for j=1:size(combos,1)
            y=FloorInfo([1 combos(j,1:end) size(FloorInfo,1)],4);
            x=Estimation([1 combos(j,1:end) size(FloorInfo,1)],UV);
            Values=FloorInfo(1:end,4);
            Ass=csapi(y,x,Values);
            FloorDispl(1:end,UV);
            Ass(1:end,1);
            SS=(FloorDispl(1:end,UV)-Ass(1:end,1)).^2;

            tempcost=0;
            temp=[1 combos(j,:) size(FloorInfo,1)];
            for n=1:size(temp,2)
                for h=1:size(JointsWsensors,1)
                    if temp(1,n)==h
                        for m=1:size(JointsWsensors,2)
                            if JointsWsensors(h,m)~=0
                                tempcost=tempcost+3000;
                            end
                        end
                    end
                end
            end
            InstrumentedFloors(k,1:size(temp,2))=temp(1,1:end);
            R(k,1)=sum(SS);
            cost(k,1)=tempcost;
            Dummy(k,1)=R(k,1)*1+cost(k,1);%I changed this today (Apr. 30)
from 10000 to 1
            k=k+1;
        end
    end
    R_I=[R InstrumentedFloors cost Dummy];
end
```